CONTRIBUTIONS IN STATISTICAL PROCESS CONTROL
FOR HIGH QUALITY PRODUCTS

CHEONG WEE TAT

NATIONAL UNIVERSITY OF SINGAPORE

2005

CONTRIBUTIONS IN STATISTICAL PROCESS CONTROL FOR HIGH QUALITY PRODUCTS

CHEONG WEE TAT

(B.Eng.(Hons), University of Technology, Malaysia)

A THESIS SUBMITTED

FOR THE DEGREE OF DOCTOR OF PHILOSOPHY

DEPARTMENT OF INDUSTRIAL AND SYSTEMS ENGINEERING

NATIONAL UNIVERSITY OF SINGAPORE

2005

Acknowledgments

Many people have inspired and contributed significantly to this work. It would be impossible for me to mention each and everyone without the risk of overlooking some. The following is only a partial list of some of those more notable ones.

I would like to express my sincerest appreciation and gratitude towards my research supervisor, Associate Professor Tang Loon Ching for his excellent guidance, invaluable suggestions and constant encouragement. Special gratitude goes to all other faculty members of the Department of Industrial and Systems Engineering, from whom I have learnt a lot through coursework, research seminars and discussions. Special thanks to staff members of the department, especially Ms Ow Lai Chun and Mr Victor Cheo who are very helpful in all the administrative procedures during my studies.

I want to extend my hearties thanks to Ms Low Pei Chin, Mr Lau Yew Loon, Dr Adam Ng Tsan Sheng and all other fellow graduate students in the department and who have provided much needed help and made my stay in NUS an enjoyable and memorable one. I especially cherish the stimulating environment for conducting research provided by the Department of Industrial and Systems Engineering.

Cheong Wee Tat

Summary

This dissertation is mainly focused on the study of Statistical Process Control (SPC) techniques for high yield processes, and includes some topics on high reliability systems. It deals with the statistical aspects of establishing SPC in high yield processing, and providing insight and promising opportunity for future research on high reliability systems.

The objective is to study the theory and practice of SPC for its use in the modern manufacturing environment, and establish a new research area on the topic of high reliability systems.

Chapter 1 is an introduction to the background and the motivations of this research. It presents some basics of control charting, including the development and operation of the control chart and the assessments of the control chart performance. Brief introductions on control charts for high yield processes, particularly based on Cumulative Conformance Count (CCC) and high performance systems are presented. This chapter also defines the scope of the study of this dissertation. Chapter 2 gives a literature review on the topics of high yield process monitoring, including the statistical properties and the recent studies of CCC chart. In addi-

tion, the use of p-chart in monitoring the high yield processes is studied and the high performance system is defined.

The second part of the dissertation 'Some New Results in CCC Analyses' contains 2 chapters. Chapter 3 presents the CCC chart with sequentially estimated parameters. The effects of parameter estimation in implementing CCC chart are substantially investigated. The parameter estimation is presented and the run length distributions of the CCC Charts with sequentially estimated parameter are derived in order to assess the performances of the charts together with the proposed scheme for Phase I CCC Chart. Chapter 4 compliments the results from Chapter 3. The guidelines in establishing the CCC charts for both cases where process parameters are known or estimated are presented.

In the third part of this dissertation, the high yield process with sampling inspection is considered. The statistical properties for the sampling inspection are studied, considering the correlation between items within a sample. A chain control scheme is proposed in order to monitor the process fraction nonconforming.

In Part IV of this dissertation 'Studies of High Performance Systems,' the term High Performance System (HPmS) is defined and the role of reliability tests in reliability improvement programs are highlighted. Besides, quality and reliability issues for high performance systems are discussed, paving the way for future research. Chapter 7 presents a screening scheme for high performance systems, with the computer hard disk drive (HDD) as the application example.

Nomenclature

α	type I error
β	type II error
γ	adjustment factor
ρ	correlation coefficient
σ	population standard deviation
$\hat{(\cdot)}$	estimate of $\hat{(\cdot)}$
ADT	accelerated degradation test
AFR	average failure rate
ALT	accelerated life test
ANOM	analysis of mean
ARL	average run length
ARL_m	ARL of sequentially estimated parameter CCC chart given m
ARL_n	ARL for different n under the binomial scheme
ARL_0	in-control ARL
AT	Accelerated tests
CCI	consecutive conformance items
CCC	Cumulative Conformance Count

CCCS   Cumulative Chain Conforming Sample

CDF   cumulative distribution function

CL   center line

CRL   cumulative run length

CUSUM   cumulative sum

dpmo   defects per million opportunities

E the event when the ith plotting point is either above UCL or below LCL

ESS   environment stress screening

EWMA   exponentially weighted moving average

F the event when a point on is either above $\widehat{UCL}$ or below $\widehat{LCL}$

FA   failure analysis

HDD   Hard disk drive

HPmS   high performance systems

i.i.d.   independently identical distributed

LCL   Lower Control Limit

LDL   Lower Decision Line

m the number of nonconforming items to be observed in sequential estimation

M_n the nonconforming count in conventional binomial estimate

n sample size used for conventional binomial estimation

NDF   Not Defect-free

NPF   No Problem Found

N_m the total number of samples to be inspected in sequential estimation

OC	operating characteristic
OOBA	out-of-box audit
p	fraction nonconforming
p_0	in-control fraction nonconforming
$\bar{p}$	estimated p using sequential estimator
pmf	probability mass function
ppm	parts per million
RDE	robust-design experiment
R_m	run length of the sequentially estimated parameter CCC chart given m
S^2	sample variance
SDRL	standard deviation of a run length
$SDRL_m$	standard deviation of R_m
$SDRL_n$	standard deviation of run length under binomial scheme
SPC	statistical process control
U	the number of points plotted until an out-of-control signal is given
UCL	Upper Control Limit
UDL	Upper Decision Line
UMVU	uniform minimum variance unbiased
x_α	the maximum number of nonconformities allowable during the test
$Y_{i:r}$	the i-th occurrence of the r nonconforming items

Contents

List of Tables

List of Figures

PART I

PRELIMINARIES

Chapter 1

Introduction

The quest for solutions to problems plaguing the Western industries in the 80s has brought renewed interest in quality and productivity. As a result, a large amount of research work in almost all aspects of quality, reliability, and productivity improvement had been produced during that period. One of the major topics that elicited great attention was statistical process control (SPC) introduced in the 1930s by Dr. Walter A. Shewhart.

It is well-known that one cannot inspect or test quality into a product; the product must be built right at the first time. This implies that the manufacturing process must be stable and that all individuals involved with the process must continuously seek to improve process performance and reduce variability on key parameters. On-line SPC is a primary tool for achieving this objective. Control charts are the simplest type of on-line SPC procedure. As a fundamental SPC tool, control charts are widely used for maintaining stability of the process, establishing

process capability, and estimating process parameters. Deming [21] stressed that the control chart is a useful tool for discriminating the effects of assignable causes versus the effects of chance causes. The chance causes of variation are defined as the cumulative effect of many small, essentially unavoidable causes, whereas the assignable causes are generally large compared to the chance causes, and usually representing the unacceptable level of process performance. The general theory of control chart was first proposed by Dr. Walter A. Shewhart [79]. Shewhart's idea is based on the postulate that there exists a constant system of chance causes. This is supported by the result of Brown's experiment concerning the behaviour of suspended particles (now popularly known as the Brownian motion). Brown's experiment shows that as long as the ambient temperature remains constant, there will not be any change in the particles's behaviour which is in accordance with the normal law. Shewhart [79] observed that this result applies to many production systems; as long as the common cause system remains, the process will continue producing products with characteristics forming independent and identical distributions (i.i.d.) over time. When an external factor (i.e., a special cause) starts to affect the process, one can expect deviation from i.i.d. behaviour of the sequence of process measurements $\{y_t, t = 1, 2, \ldots\}$. This leads to the idea of tracking down special causes by observing changes in the i.i.d. behaviour of $\{y_t\}$ and thus, the control chart is introduced. The control charts developed according to this idea are often called Shewhart control charts.
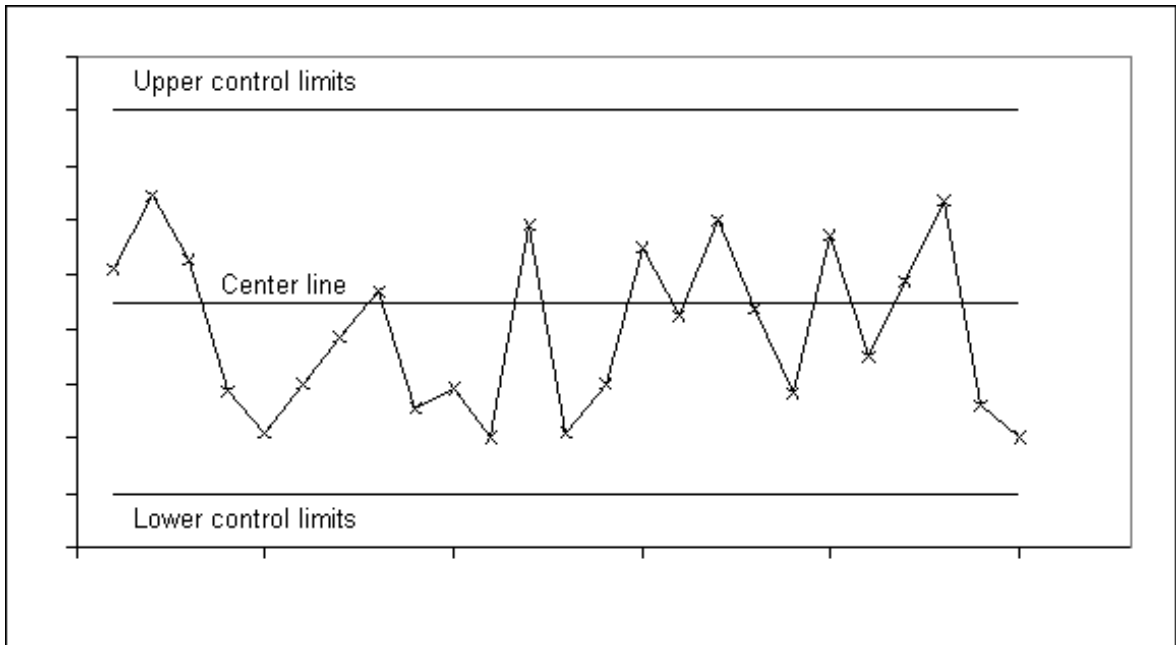
Figure 1.1: The typical control chart

A typical control chart as shown in Figure 1.1 is a graphical display of a quality characteristic that has been measured or computed from a sample versus the sample number or time. The chart normally contains a center line (CL) that represents the average value of the quality characteristic corresponding to the in-control state, i.e., only chance causes are present. The other two horizontal lines, namely upper control limit (UCL) and lower control limit (LCL) are also shown in the chart. These control limits are used so that if the process is in control, nearly all of the sample points will fall between them. As long as the points plotted are within the control limits, the process is said to be in statistical control, and no action is necessary. However, if a point is plotted outside the control limits, it is interpreted as an evidence that the process is out of control, and investigation and corrective

4

actions are required to find and eliminate the assignable cause or causes responsible for this behaviour. It is a common practice to connect the sample points on the control chart with straight-line segments, so that it is easier to visualize how the sequence of points has evolved over time.

Control charts can be used to determine if a process (e.g., a manufacturing process) has been in a state of statistical control. There are two distinct phases of control chart usage. In Phase I, we plot a group of points all at once in a retrospective analysis, constructing trial control limits to determine if the process has been in control over the period of time where the data were collected, and to see if reliable control limits can be established to monitor future production. In other words, besides checking the statistical control state, one estimates the process parameters which are to be used to determine the control limits for process monitoring phase (Phase II). In Phase II, we use the control limits to monitor the process by comparing the sample statistic for each sample as it is drawn from the process to the control limits. Thus, the recent data can be used to determine control limits that would apply to future data obtained from a process. (Note: Some writers have referred to these two phases as Stage 1 and Stage 2, respectively.) The details of Phase I will be discussed in the following Chapter.

1.1 Control Charts for Variable and Attribute

Control charts can be generally classified into variable control charts and attribute control charts. The former ones require quality characteristics that can be measured and expressed in a continuous scale. Thus, these control charts are limited only to a small fraction of the quality characteristics specified to products and services. The typical example for variable control charts are $\bar{X}$ charts and R charts, one for the measure of process central tendency and another for process variability. Both of the charts are powerful tools for diagnosis of quality problems, and serve as a mean of routine detection of sources of trouble.

The other type of chart, namely attribute control charts are constructed to monitor the process level by plotting the attribute data (also often referred to as *count data*), as many quality characteristics are not measured on a continuous scale or even a quantitative scale. In these cases, each unit of product can only be categorized as either conforming or nonconforming based on the attributes possessed or the number of nonconformities (defects) appearing on a unit.

The attribute data are used where, for example, the number of nonconforming parts for a given time period may be charted instead of the measurements being charted for one or more quality characteristics. Although automation has greatly simplified the measurement process, it is still often easier to classify a unit of production as conforming or nonconforming than to obtain the measurement for each of many quality characteristics. Furthermore, attribute control charts can be used in many applications, such as clerical operations, for which count data occur

naturally, not measurement data. The most frequently used attribute control charts are:

1. p chart, the chart for monitoring the fraction nonconforming of the sample;

2. np chart, the chart for monitoring the number of nonconforming items in the sample;

3. c chart, the chart for monitoring the number of nonconformities of the sample; and

4. u chart, the chart for monitoring the number of nonconformities per unit sample.

1.1.1 Development and Operation of Control Charts

A control chart plots the data collected and then compare with the control limits. When the process is operating at a desired level, the plotted statistics are within the control limits. When an unexpected process change occurs, some plotted points will be plotted outside the control limits and thus, the alarm signal is issued. In the control charting process, the control chart can indicate whether or not statistical control is being maintained and provide users with other signals from the data.

The conventional Shewhart control charting techniques have been widely used in the process control, these techniques work best if the data are at least approximately normally distributed and there are enough data available for parameter estimation.

For variable control charts, let w be a quality characteristic of interest, and suppose that the mean of w is μ_w and the standard deviation of w is σ_w. Then the center line, the upper control limit, and the lower control limit become

$$UCL = \mu_w + k\sigma_w$$
$$CL = \mu_w \tag{1.1}$$
$$LCL = \mu_w - k\sigma_w$$

where k is the "distance" of the control limits from the center line, which is called the control limit coefficient, expressed in standard deviation units. Conventionally, k is set at 3, and the limits are called 3-sigma (3 σ) limits.

By making some normality approximations, the control limits for the attribute control charts can be obtained similarly. For example, the control limits for the p and np chart can be derived in the following manner. It is well known that the number of nonconforming items in a subgroup of size n follows the binomial distribution with parameter p. The mean of such numbers is np and the variance is $np(1-p)$. Hence the control chart for p can be constructed from Equation (1.1) with

$$UCL = p + k\sqrt{p(1-p)/n}$$
$$CL = p \tag{1.2}$$
$$LCL = p - k\sqrt{p(1-p)/n}$$

where the adequacy of the normal approximation to the binomial distribution is assumed. Only when the normal approximation is satisfied, the Shewhart attribute control chart can then be used. Otherwise, the analysis based on the assumption

8

of normal distribution will not be able to provide correct information for decision making in process monitoring. The details will be discussed in the following sections.

1.1.2 Assessments of the Control Chart Performance

In order to evaluate the performance of control charts, some assessments can be used. The effectiveness of a control chart can usually be evaluated by the following criteria:

1. average run length (ARL),

2. type I (α) and type II (β) errors, and

3. operating characteristic (OC).

These criteria are highly related to each other and will be discussed accordingly in the following.

1.1.2.1 Average Run Length (ARL)

The performance of control charts can be measured in terms of how fast it can detect changes in distributional characteristics (i.e., in an applied sense, how fast it can detect the onset of assignable causes). Quantitatively, it is usually measured in terms of the average run length (ARL), which is defined as the average number of points that must be plotted before a point indicates an out-of-control condition

(from the starting point of previous out-of-control state). There are two different ARL being used to evaluate the control chart performance.

- *In-control ARL*, ARL_0, the expected number of points plotted before a point indicates an out-of-control signal while the process is in the state of statistical control.

- *Out-of-control ARL*, the expected number of points plotted before a point indicates an out-of-control signal when the process is out of control.

It is desirable for the ARL to be reasonably large when the process is in control, so that false alarm will rarely occur. On the other hand, when the process is out of control, early detection is preferable, thus the ARL of the control chart should be as low as possible. A good control charting scheme must provide high in-control ARL and low out-of-control ARL. With 3-sigma limits, the in-control ARL (of the $\bar{X}$ chart) has the value of 370.

1.1.2.2   Type I and Type II Errors

The concept of type I (α) and type II (β) errors in control chart is very similar to the types of errors defined in hypothesis testing. The type I error of the control chart is defined as the chart indicates an out-of-control signal when it is really in control. On the other hand, the type II error of the control chart is defined as the chart fails to issue an out-of-control signal when it is really out of control.

For an effective control chart, both type I and type II errors are expected to be reasonably small. Small type I error means that the process is seldom interrupted

by unpleasant false alarm; the popular 3-sigma limits have the type I error as low as 0.0027. While small type II error means that the control chart is sensitive enough to unusual changes in the process.

1.1.2.3 Operating characteristic (OC)

The operating characteristic (OC) function of the control chart is the probability of incorrectly accepting the hypothesis of statistical control (i.e., a type II error) against the quality characteristic of interest. The OC curve, which is a graphical display of the probability, provides a measure of the sensitivity of the control chart, that is, its ability to detect a change in the process from the desired state to the out-of-control state.
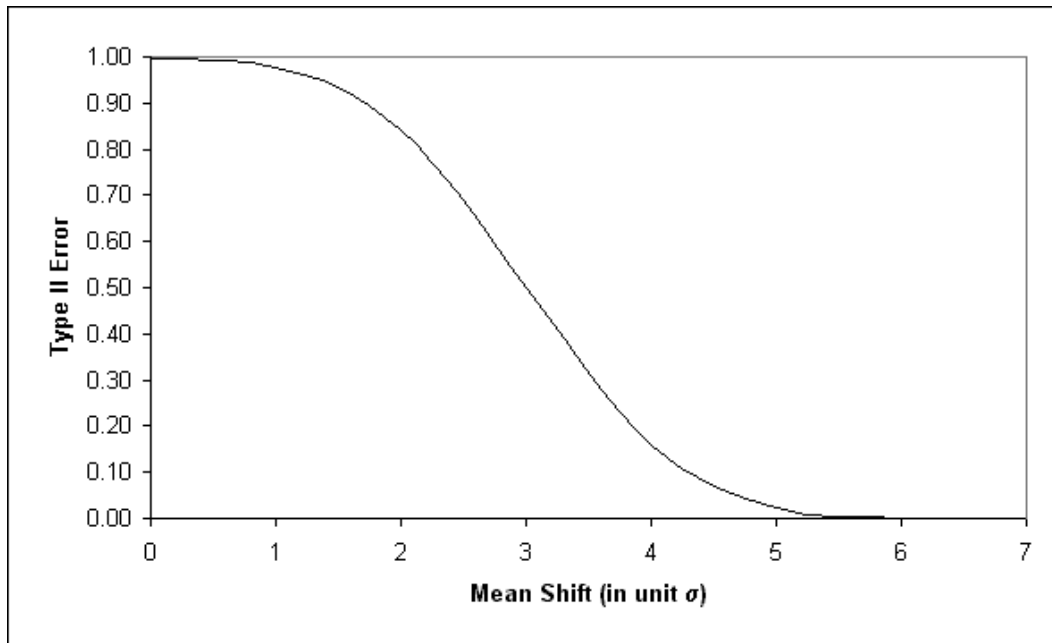
Figure 1.2: OC Curve for an $\bar{x}$ chart

Figure 1.2 is the OC curve for a typical $\bar{x}$ chart. In general, it is desirable for the OC function to have a large value when the shift is zero, and to have small OC function when the shift is non zero, as shown in the figure.

1.2 Control Charts for High Yield Processes

Just as its name implies, a high yield process means that the quality level of the process is very high, i.e., the probability of observing nonconforming products is very small. The fraction of nonconforming items, p, for such process is usually on the order of parts-per-million (ppm). (Note: Some authors have referred to such process as High Quality Process.) Here, the high yield process is be defined as:

Definition 1 High Yield Process *is the process with in-control fraction non-conforming, p_0, of at most 0.001, or 1000 ppm.*

1.2.1 Problems with Traditional Control Charts

Due to the increasing effort of process improvement and rapidly improving technology, more and more industrial processes have been improved to high yield processes where many traditional control charts would face practical problems. The situation is more serious with attribute control charts which, at the same time, are of increasing importance because of the possibility of obtaining count data quickly enabling processes to be monitored at a low cost.

Goh [28] showed that the use of p chart for high yield processes results in high false alarm rates and inability to detect process improvement by illustrating the following example. Consider a production process that has been improved to such an extent that there is only an average of 400 ppm nonconforming, and suppose that each inspection sample contains 200 items. Then, from Equations (1.2) with $k = 3$, the control limits used are

$$UCL = \bar{p} + 3\sqrt{\frac{\bar{p}(1 - \bar{p})}{n}}$$

$$= 0.0046$$

$$CL = \bar{p}$$

$$= 0.0004$$

$$LCL = \bar{p} - 3\sqrt{\frac{\bar{p}(1 - \bar{p})}{n}}$$

$$= 0.0004 - 0.0042$$

$$= -0.0038.$$

Since a negative value has no physical meaning, LCL is set equal to 0.

The application of the p chart for this very low p process is awkward in several respects. First, as stated before, the zero LCL is meaningless, as it is impossible to detect any process improvement. Process improvement detection is also important so that the reasons for process improvement can be further studied and the quality improvement can then be sustained. As the continuous improvement is the cornerstone of modern quality management, such meaningless LCL should be avoided in practice. Secondly, the control chart will give an out-of-control signal as long as a single nonconforming item is observed, from the example, one nonconforming item

in a sample will raise p to 0.0050, which exceeds the UCL. This is tantamount to an absolutely zero nonconformity requirement which not only is virtually impossible to meet in practice but also contradicts the concept of statistical control, namely elimination of systematic shifts, but tolerance of random fluctuations. A control chart like this does not provide much information and is far from useful.

For high yield processes, in order for the traditional p-chart or np-chart to perform effectively, the sample size used has to be relatively large. To overcome these deficiencies, it can be shown that the sample size, n should be large enough such that np is at least 8.9. Table 1.1 gives the values of sample sizes for different in-control fraction nonconforming, p_0, such that $np = 8.9$. It can be seen that for $p_0 < 0.0005$, n is prohibitively large and thus other control scheme is needed.

Table 1.1: Values of n such that $np = 8.9$ for different p_0, type I risks for np-charts with different p_0.

n	p_0	$P(X > UCL)$	$P(X < LCL)$
8900	0.001	0.00092	0.00135
9889	0.0009	0.00092	0.00135
11125	0.0008	0.00092	0.00135
12714	0.0007	0.00092	0.00135
14833	0.0006	0.00092	0.00135
17800	0.0005	0.00092	0.00135
22250	0.0004	0.00092	0.00135
29667	0.0003	0.00092	0.00135
44500	0.0002	0.00093	0.00135
89000	0.0001	0.00093	0.00135

Setting the sum of probability of type I risks for both control limits as close to 0.0027 as possible, the corresponding LCLs and the UCLs for the np-charts above are 1 and 19 respectively. Other details and examples of the inadequacies of the p-chart or np-chart can be found in Goh [28] and Goh and Xie [29].

14

1.2.2 Control Charts based on Cumulative Conformance Count (CCC)

The cumulative conformance count (CCC) chart, which has gained much attention in the industry, was first introduced by Calvin [6] and popularized by Goh [28], is primarily designed for processes with sequential inspection carried out automatically one at a time. This chart, instead of counting the nonconforming ones, tracks the number of conforming items produced between successive nonconforming ones. It has been hailed for its ability in detecting improvement under high yield production while overcoming the problem of possible false alarm experienced by Shewhart chart when a defective item sporadically occurs. In addition, this chart has being introduced as a Six Sigma tool in dealing with high yield processes (see Goh and Xie [29]). The use of CCC chart was further studied by Xie and Goh [103], [104]; Glushkovsky [26]; Xie, *et al.* [105]; and Ohta *et al.* [67]. The detailed statistical properties of CCC chart will be presented in the following chapter.

1.3 High Performance Systems

Besides having high quality outputs, for many mission-critical systems, building in redundancies has become a standard practice in ensuring the system performance during the design phase. For some products, redundancies are also used to cater for process variation and to maintain high process yield. The concept of redundancy in reliability engineering can be found in most of the reliability engineering

books such as those by Elsayed [23], and Tobias and Trindade [92]. Built-in redundancies improve not only process yield and system reliability but also their overall performance. Thus, systems having this feature with low defects per million opportunities (dpmo) quality level can be termed as *high performance systems* (HPmS). This is because their intended functions will not be compromised even if there exists nonconformities within each item; as long as the number of such nonconformities is below a critical threshold.

For example, a simple telecommunications component such as copper transmission line or optical cable, the occurrence of failure in transmitting signal is extremely low, as there are numerous small wires in pair or quad within the core of the cable (see Thorsen [91]). Minor breakage within a pair or quad would definitely not affect the effectiveness of the current or signal transmission of the cable. Consequently, these systems are still conforming when the number of nonconformities within an item is below the critical threshold. Another example of high performance system is computer hard disk. The occurrence of nonconformities within the system is sporadic and rare (see Hughes *et al.* [43]), and a reasonable amount of faulty bits, bad sectors or bad tracks are acceptable and can be marked resulting in usable drives. A small number of sectors are reserved as substitutes for any bad sectors discovered in the main data storage area. During testing, any bad sectors that are found on the disk are programmed into the controller. When the controller receives a read or write for one of these sectors, it uses its designated substitute instead, taken from the pool of extra reserves. This spare sectoring process will

16

replace the amount of 'lost' capacity. Thus, as long as the occurrence of faulty bits is not too frequent, the performance and the total capacity of the disk drive will not be affected.

A high performance system is considered to be failure-prone when the number of nonconformities exceeds a critical threshold. In order to ensure the number of nonconformities does not exceed the threshold, some screening tests are needed to eliminate products that are out-of-specifications and/or failure-prone.

1.4 Scope of the Research / Organization of the Dissertation

This dissertation focuses mainly on the problems related to statistical analysis of high yield processes and also high performance systems. As shown in Figure 1.3, this dissertation addresses several problems related to high yield process monitoring and high performance systems. Part I contains the Introduction (Chapter 1) and Literature Review (Chapter 2), the statistical properties and the recent developments of the high yield (CCC) chart are reviewed, and some problems in monitoring the high yield processes as well as topics on high reliability systems are highlighted. The second part of the dissertation, 'Some New Results in CCC Analyses,' presents the guidelines in establishing the CCC charts. A sequential sampling scheme for CCC chart is first examined and the performance of the chart constructed using an unbiased estimator of the fraction nonconforming, p is investigated. The run

length distributions of the CCC Charts are then derived in order to assess the performances of the charts and the parameter estimation is presented together with the proposed scheme for Phase I CCC Chart. A systematic treatment for establishing the chart particularly when the parameter is estimated will be provided, so the users are able to construct the CCC chart under different sampling and estimation conditions. New insights on the behaviours of CCC chart when the parameter is estimated will be given and some procedures for constructing the CCC chart when the process fraction nonconforming is given, when it is estimated sequentially, and when it is estimated with a fixed sample size are presented. Part III - High Yield Process with Sampling Inspection - deals with high yield process under sampling inspection. The statistical properties for the sampling inspection are studied. A control scheme that is effective in detecting changes in fraction nonconforming for high yield processes with correlation within each inspection group is presented. A Markov model is used to analyze the characteristics of the proposed scheme. In Part IV, the high performance system is coined to pave the way for future research in this area. The importance of reliability tests in reliability improvement programs are highlighted. In addition, a screening scheme for such system is presented.

```
┌─────────────────────────────────────────┐
│ Part II : Some New Results In CCC         │
│              Analyses                     │
│                                           │
│            Chapter 3                      │
│      CCC Chart with Sequentially          │
│         Estimated Parameters              │
│                                           │
│            Chapter 4                      │
│      Establishing CCC Charts              │
└─────────────────────────────────────────┘

┌─────────────────────────────────────────┐
│ Part III : High Yield Processes With      │
│            Sampling Inspection            │
│                                           │
│            Chapter 5                      │
│   Control Scheme for High Yield Correlated│
│      Production with Sampling Inspection  │
└─────────────────────────────────────────┘

┌─────────────────────────────────────────┐
│ Part IV : Studies Of High Performance     │
│              Systems                      │
│                                           │
│            Chapter 6                      │
│      High Performance Systems             │
│                                           │
│            Chapter 7                      │
│  Screen Scheme for High Performance Systems│
└─────────────────────────────────────────┘

┌──────────────────────┐
│ Part I : Preliminaries│
│                       │
│      Chapter 1        │
│     Introduction      │
│                       │
│      Chapter 2        │
│  Literature Review    │
└──────────────────────┘

┌──────────────────────┐
│      Chapter 8        │
│    Conclusions and    │
│   Recommendations     │
└──────────────────────┘
```

Figure 1.3: Organization of this dissertation.

Chapter 2

Literature Review

As stated in previous chapter (see Section 1.2.1), the traditional control techniques are not adequate in a high yield manufacturing environment. It is necessary to use some new techniques to monitor the high yield processes, which are very common in modern electronics industries. This area of research has attracted increasing interest recently with numerous publications have appeared and several alternative of control schemes designated for high yield processes have been proposed. In the following sections, we first review the phase I control charts together with the statistical properties of CCC charts as well as some recent studies on the related issues. In addition, we also investigate some of the issues regarding high performance systems. These high performance systems not only have a very high quality level, but are also highly reliable under normal usage.

2.1 Phase I Control Charts

The usual approach in setting up a control chart entails collecting m subgroups of size n (preliminary samples) and using these values to obtain the estimate of the process mean and process variability. The control limits are constructed based on these estimated process parameters. When preliminary samples are used to construct limits for control charts, these limits are customarily treated as trial control limis. Therefore, the m trial values should be plotted on the appropriate chart, and any points that exceed the trial control limits should be investigated. On the other hand, if assignable causes for these points are discovered, they should be eliminated and new limits for the control chart is determined. If all the trial values obtained from the m subgroups are plotted within the control limits, the process is said to be in control and these control limits will be used in Phase II. In this way, the process may be eventually brought into statistical control.

Typical approach to the phase I problem of a control chart is to address two pertinent issues:

One is to investigate the performance of the control chart in terms of its run length distribution and false alarm rate when the control limits are derived from the estimates of the parameters involved; such as those of Ghosh *et al.* [24], Quesenberry [71], Del Castillo [19], [20], Chen [15], and more recently Chakraborti [8], and Champ and Jones [9] for $\bar{X}$ chart; Chen [16] for R, s, and s^2 charts, Braun [5] for c and p charts and Jones *et al.* [45] for EWMA chart. Such study will help determine the appropriate number of subgroups and the corresponding subgroup size

for the desired level of performance. This guideline for the sampling scheme should be independent of the parameters involved. For example, the number of subgroups needed to establish an $\bar{X}$ chart should not depend on the mean or variance of the quality characteristic.

The other issue is to examine homogeneity of the samples such as the analysis of mean (ANOM) for $\bar{X}$ chart to ensure that the estimates are obtained from samples of the same population.

2.2   Basic Properties of CCC Charts

The CCC chart is a powerful technique for process control when a large number of consecutive conforming items are observed between two nonconforming ones. CCC chart is set up to monitor the CCC and decisions are made based on whether this number is too large or too small. The chart is very useful for one-at-a-time sequential inspections or tests which are common in automated manufacturing process. It is generally a technique for high yield processes when nonconforming items are rarely observed.

2.2.1   Control Limits

In CCC chart, the control limits are determined based on the probability limits (see Xie and Goh [104]). During the inspection, the probability of the nth item

being the first nonconforming item to be discovered is given by

$$P\{X = n\} = (1 - p)^{n-1}p \qquad \text{where } n = 1, 2, \ldots \tag{2.1}$$

which is a geometric distribution with parameter p. Tacitly, it is envisaged that inspections are carried out sequentially and the above random variables (CCC) are independently and identically distributed (i.i.d.). The cumulative distribution function (CDF) of Equation (2.1) is given by

$$\begin{aligned} P\{X < k\} &= p\sum_{i=1}^{k}(1 - p)^{i-1} \\ &= 1 - (1 - p)^{k-1}. \end{aligned} \tag{2.2}$$

Thus,

$$\begin{aligned} P\{X > UCL\} &= p_0 \sum_{i=UCL+1}^{\infty}(1 - p_0)^{i-1} \\ &= \frac{p_0(1 - p_0)^{UCL}}{1 - (1 - p_0)} \\ &= (1 - p_0)^{UCL} \end{aligned} \tag{2.3}$$

and from Equation (2.2),

$$P\{X < LCL\} = 1 - (1 - p_0)^{LCL-1} \tag{2.4}$$

where p_0 is the in-control fraction nonconforming.

Given a type I error, α, and p_0, from the above equations, the upper control limit (UCL) and the lower control limit (LCL) are respectively,

$$UCL = \frac{\ln \alpha/2}{\ln(1 - p_0)} \tag{2.5}$$

$$LCL = \frac{\ln(1 - \alpha/2)}{\ln(1 - p_0)} + 1. \tag{2.6}$$

Unlike the control limits we normally see in Shewhart charts, it is clear that the control limits for CCC chart are highly asymmetric. Hence, it is recommenced that the log-scale be used on Y-axis for the plotting. A typical CCC chart is shown in Figure 2.1.
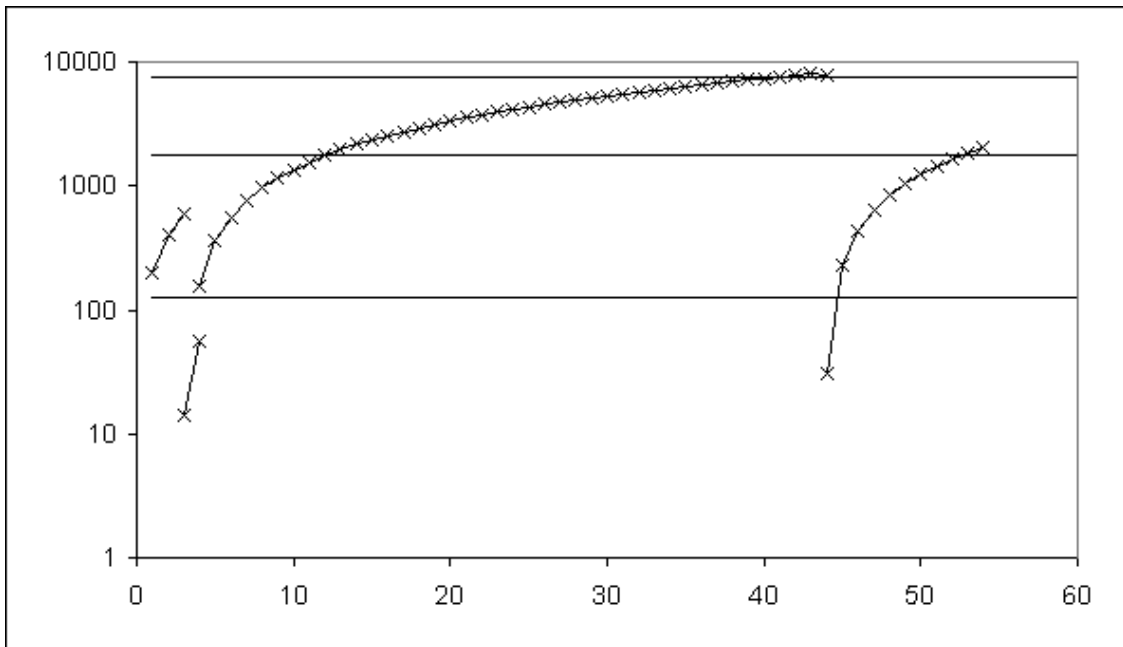
Figure 2.1: The typical CCC chart

2.2.2 Decision Making Related to CCC Charts

Decision making based on a CCC chart is very straightforward. When the chart shows an out-of-control signal in form of a value smaller than the LCL, the process has probably deteriorated. Process improvement should be signaled at values that are larger than the UCL, this is different from p chart, where value larger than the UCL is concluded as process deterioration (increase in p). Therefore, the CCC

24

chart can detect not only process deterioration but also process improvement of high yield processes.

The CCC chart has been devised much along the same line as the traditional Shewhart control charts. It assumes a fairly reliable knowledge of the steady-state fraction nonconforming p_0, and the control limits are associated with a predetermined α.

2.3 Review of Recent Studies

Here, some of the recent works related to high yield process control chart, particularly CCC chart, are investigated. Besides CCC chart, other high yield process control charts are studied and presented in the following sections.

2.3.1 Developments and Refinements for CCC Charts

Xie and Goh [103] presented that when p is extremely low, the p and α would be sensitive to short term drifts in process parameters, it is better to focus more on the current p value in determining whether the process is out of control. Thus, α need not be fixed, since it is in fact a confidence level parameter. A reference graph is developed in judging the state of control of a process via the $p - \alpha$ relationship. In order to hitherto gather information about the process as far as possible, a non-zero restarting point procedure is developed. Thus, fuller use is made of the information contained in the observed data during the application of the CCC control chart.

Similar to the traditional implementation of Shewhart chart, a decision when

using the typical CCC chart is based on a single count value. This could be relatively insensitive in detecting small process shift. Kuralmani *et al.* [49] proposed a conditional procedure to improve the sensitivity in detecting the moderate to large process shifts in either direction. The idea of a conditional procedure is to incorporate some run rules into the regular CCC control scheme.

Besides, some economic studies were done on the CCC charts such as those by Xie *et al.* [111], [113]. Xie *et al.* [113] developed an economic model for CCC chart; a simplified algorithm was used to search the optimal setting of the sampling and control parameters.

2.3.1.1 Shewhart-like CCC Charts

The layout of the original CCC Chart which is shown in Figure 2.1 can be difficult to interpret and confusing to non-statisticians who are used to the format of Shewhart control chart. Xie *et al.* [114] proposed a Shewhart-like CCC charting technique which has a more traditional layout as other Shewhart charts. The proposed layout which is also recommended by Xie *et al.* [106] (see Xie *et al.* [106], Chapter 3, page 55-57) is shown in Figure 2.2 (Note: Some writers preferred naming this Shewhart-like CCC as conforming run length (CRL) control chart).
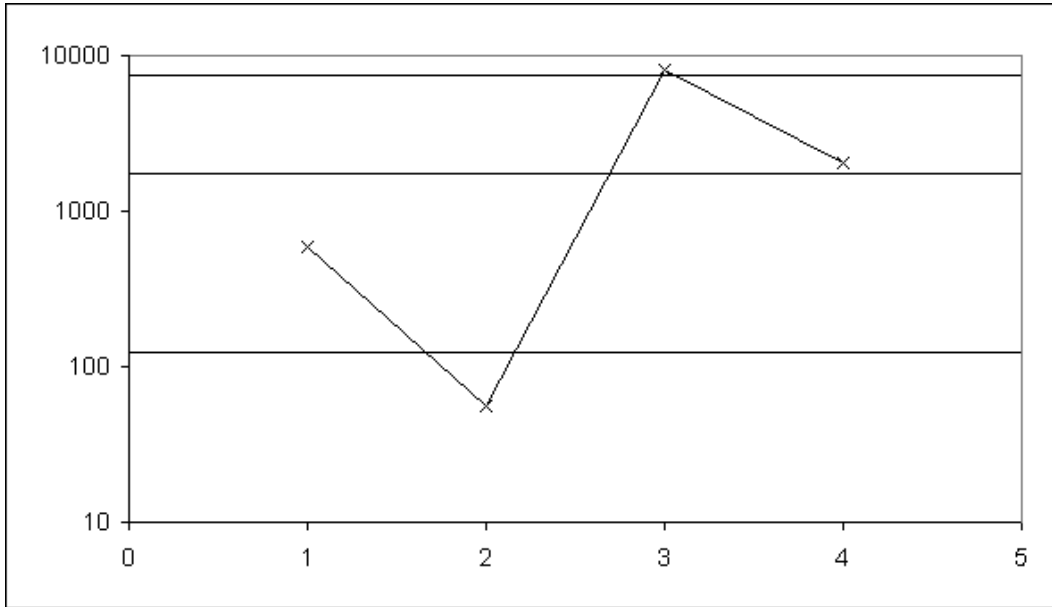
Figure 2.2: The Shewhart-like CCC chart

2.3.1.2 Control Limits Based on Probability Limits

Xie and Goh [104] studied the use of probability limits instead of the traditional limit based on mean $\pm$ 3 σ. They pointed out the use of 3 σ limits for geometric distribution should not be used due to the distribution is always skewed and normal approximation is not valid. They also showed that for geometric distribution, the control limits based on k times standard deviation which has been used traditionally will cause a frequent false alarm and cannot provide any reasonable lower control limits for further process improvement detection without introducing complicated run rules.

2.3.1.3 Adjusted Control Limits for CCC Charts

As discussed in Section 1.1.2.1, the ARL of a control chart should have relatively large in-control ARL compared to the out-of-control ARL, i.e., the in-control ARL,

ARL_0, should have the maximum value compared to the out-of-control ones. However, in CCC chart, the ARL will initially increase when the process is deteriorated (p increased), which is in fact a common problem for data having a skewed distribution (see Xie and Goh [104] and Xie *et al.* [105]), it renders the CCC chart rather insensitive in detecting minor increase in p and may lead to the misinterpretation that the process is well in control, or has improved.

Table 2.1: ARL values at in-control $p_0 = 100$ ppm for various α.

p	$\alpha = 0.0027$	$\alpha = 0.005$	$\alpha = 0.01$
1	1.07	1.06	1.05
10	1.94	1.82	1.70
20	3.75	3.31	2.88
30	7.24	6.01	4.87
40	13.95	10.87	8.19
50	26.72	19.51	13.66
60	50.54	34.52	22.40
70	93.06	59.39	35.70
80	162.82	97.21	54.26
90	261.16	147.02	76.96
100	**370.37**	**200.00**	**100.00**
110	458.27	242.55	118.45
120	505.09	266.42	129.37
130	515.30	272.99	133.06
140	503.64	268.40	131.69
150	482.17	258.22	127.48
160	457.71	245.96	122.01
170	433.42	233.42	116.17
180	410.57	221.42	110.44
190	389.55	210.25	105.03
200	370.35	199.99	100.00
210	352.86	190.60	95.36
220	336.90	182.02	91.11

For illustration, Table 2.1 shows some ARL values for $p_0 = 100$ ppm and $\alpha = 0.0027, 0.005$ and 0.01. From the table, the ARLs are clearly lower at $p = 100$ ppm irrespective of false alarm probabilities. However, the highest ARL values

are not at p_0, this is undesirable. Figure 2.3 is the graphical representation of the ARL values. From the graph, this can also be seen that at p_0, the ARL for different values of α are not at the peak of the curve. Such behaviour will affect the sensitivity of the control chart in detecting minor increase in p.

In addressing this problem, Xie *et al.* [105] developed a new procedure for determination of control limits for geometric distribution and derived the control limits which provides maximum ARL when the process is in control by introducing an adjustment factor.
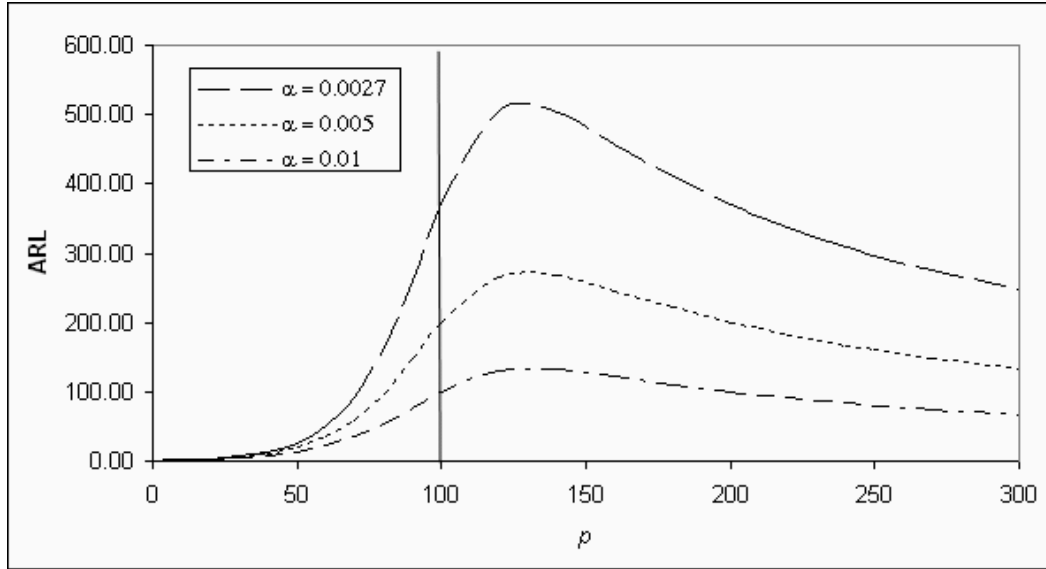
Figure 2.3: ARL curves at in-control $p_0 = 100$ ppm for various α.

For CCC chart, the ARL is given in Equation (3.8) and the maximum ARL at $p = p_0$ can be obtained by differentiating them and then solve for p, which is,

$$(1 - p_0)^{LCL-1} \ln(1 - p_0)\frac{dLCL}{dp} - (1 - p_0)^{UCL-1} \ln(1 - p_0)\frac{dUCL}{dp} = 0. \quad (2.7)$$

Solving this equation, the p value, where ARL reaches the maximum, is given as

$$p = 1 - \exp\left(\frac{\ln(1-p_0)\ln\left[\frac{(\alpha/2)}{(1-\alpha/2)}\right]}{\ln\left[\frac{\ln(1-\alpha/2)}{\ln(\alpha/2)}\right]}\right).$$

(2.8)

Substituting this function into Equations (2.3) and (2.4) (by replacing p_0 by p), the new control limits can be obtained as

$$UCL = \frac{\ln(\alpha/2)\ln\left[\frac{\ln(1-\alpha/2)}{\ln(\alpha/2)}\right]}{\ln(1-p_0)\ln\left[\frac{(\alpha/2)}{(1-\alpha/2)}\right]}$$

(2.9)

$$LCL = \frac{\ln(1-\alpha/2)\ln\left[\frac{\ln(1-\alpha/2)}{\ln(\alpha/2)}\right]}{\ln(1-p_0)\ln\left[\frac{(\alpha/2)}{(1-\alpha/2)}\right]} + 1$$

(2.10)

Xie *et al.* [105] presented that, for a given p_0 and specified α, by using the control limits derived using Equations (2.9) and (2.10), the ARL is maximized at $p = p_0$.

The control limits above (Equations (2.9) and (2.10)) do not have a direct probability interpretation. However, these control limits can be derived by multiplying the probability limits (control limits derived based on probability limits and shown in Equations (2.5) and (2.6)) with a constant. This constant is called adjustment factor by Xie *et al.* [105] and denoted by γ_α. By comparing Equations (2.5) and (2.6) with Equations (2.9) and (2.10), it can be seen that the adjustment factor is given by

$$\gamma_\alpha = \frac{\ln\left[\frac{\ln(1-\alpha/2)}{\ln(\alpha/2)}\right]}{\ln\left[\frac{(\alpha/2)}{(1-\alpha/2)}\right]}.$$

(2.11)

Notably, this adjustment simply shifts the existing control limits by a factor of γ_α.

The advantage of using the adjustment factor is that the ARL of the chart will always decrease when the process is shifted from the in-control value. The false alarm probability is thus, further reduced. Figure 2.4 is the ARL curves at $p_0 = 100$ ppm for $\alpha = 0.0027$ with non-adjusted and adjusted control limits. From the ARL curves, it is clear that with the adjustment factor, the performance of the CCC chart is much satisfactory as the ARL peaks at in-control p.
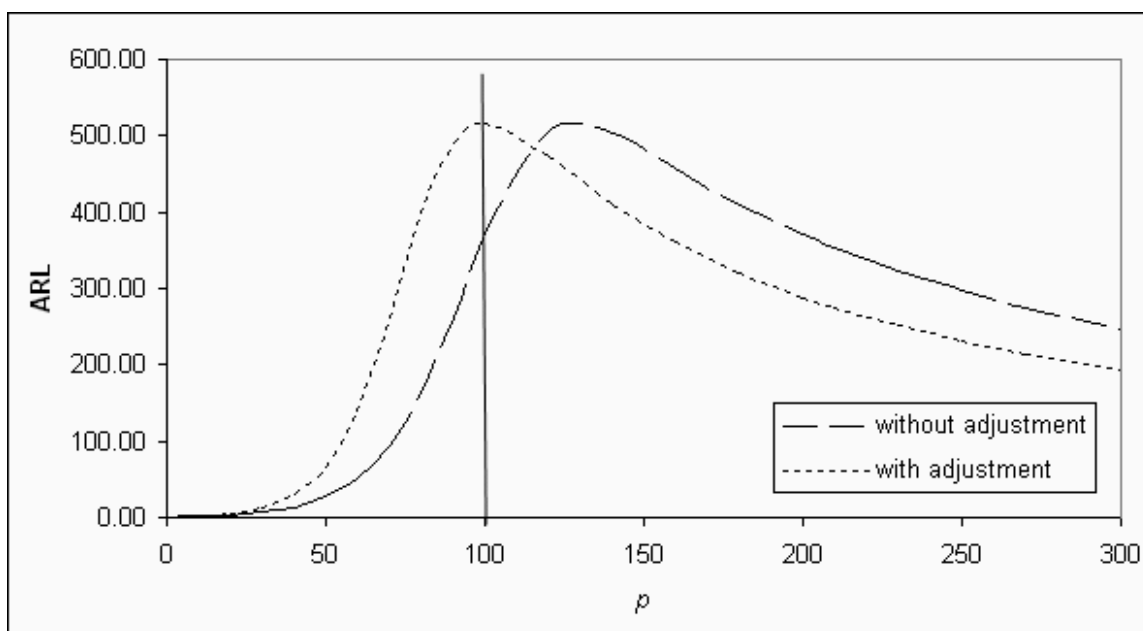
Figure 2.4: ARL curves at $p_0 = 100$ ppm for $\alpha = 0.0027$ with non-adjusted and adjusted control limits.

Recently, Zhang $et\ al.$ [119] defined a nearly ARL-unbiased design by setting the in-control ARL as near as possible to the peak of the ARL curve. However, their

proposed procedure involve several iterations in choosing different sets of control limits, and the results are similar to those using the adjustment factor.

2.3.2 Some Extensions to the CCC Model

The idea of CCC chart is extended to process monitoring by considering the number of items inspected until a fixed number of nonconforming items are observed by several writers. The control chart based on this count of items inspected until r nonconforming items are called CCC-r chart. The idea of CCC-r control chart is presented by Xie *et al.* [107], [112] and further discussed in Sun and Zhang [82] and Ohta *et al.* [67].

Lai *et al.* [51] investigated the Markov model for a serially dependent process in the context of CCC related data. Lai *et al.* [50], on the other hand, studied the effects of correlation of the CCC chart. They shown that the process control procedures based on the conforming run lengths or based on random samples taken from the production processes are seriously affected if the production processes exhibit a serial correlation. They derived the control limits using a correlation binomial model.

2.3.3 Other High Yield Process Monitoring Methods

Besides the CCC chart, which popularized by Goh [28] and has being introduced as a Six Sigma tool (see Goh and Xie [29]), there are other control chart techniques being developed for monitoring high yield processes.

2.3.3.1 Pattern Recognition Approach

An alternative charting technique given by Thomas *et al.* [89] which is based on exact probability calculations had not been commonly understood or adopted. Goh [27] explained in detail the rationale and procedures of this alternative 'pattern recognition' charting technique. This method has been found appropriate for controlling processes producing less than 1% defective and is more reliable than the conventional p chart because there is no loss of reaction to out-of-control situations, yet there is no overreaction to very short runs of defectives. This 'pattern recognition' approach is similar to the Western Electric decision rules.

2.3.3.2 G-charts

The use of c and u charts are based upon the underlying assumption that the Poisson distribution is an appropriate model for the outcomes. But some of the processes are best described by a geometric distribution. If the process is best described by a geometric distributed events, wrong management is commonly made if the traditional c charts are used. A shifted geometric distribution is used by Kaminsky *et al.* [46] as the basic model for the number of occurrences of a given event per unit of process output. They developed the Geometric charts (G-charts) for monitoring the total number of occurrences and the average numbers of the occurrences found in a fixed number of units of process output. However, probability of false alarm is higher than expected and the lower control limits will often be meaningless. Glushkovsky [26] studied the G-charts and described the use

of the control-charts, besides high yield processes, G-charts can be also used for monitoring low volume manufacturing, short runs and 'stepped' processes.

2.3.3.3 Data Transformation Methods

Most of the charts in monitoring high yield processes are based on geometric counts/transformed geometric counts, the main argument for using a transformation of geometric counts is to obtain an approximate normal distribution. Nelson [63] proposed a Shewhart chart based on $X^{\frac{1}{3.6}}$ where X is a geometric count. Quensenberry [72] proposed the geometric Q Charts for high yield processes, the Q charts are based on transforming the data into standard normal random variable. This Q-statistics is based on the geometric distribution, which can be used for high yield processes. The proposed geometric Q charts are for both the cases when p is assumed known or unknown. However, for the p unknown case which the estimate is based on the uniform minimum variance unbiased (UMVU) estimator, the calculations are complicated and not straightforward. McCool and Motley [56] considered Shewhart and exponentially weighted moving average (EWMA) chart based on $Y = X^{\frac{1}{3.6}}$ and $Z = \ln(X)$. Xie et $al.$ [110] proposed a double square root transformation where $Y = X^{\frac{1}{4}}$.

However, the disadvantage in implementing a chart based on transformed measurements is the difficulty in interpretation as some transformations involve complicated calculations which are not easily done without the use of a computer.

2.3.3.4 Cumulative Sum Charts

Cumulative sum (CUSUM) chart is well-known to be sensitive in detecting small and moderate parameter changes. Lucas [54] and Bourke [3] investigate the use of CUSUM in high yield processes, in particular, Bourke [3] presented a design procedures for the geometric CUSUM charts, but it is only meant for an in-control p_0 of at least 0.002. Bourke [3] noted that for very small in-control p_0, the use of Markov chain approach in determining ARL results in a very large matrix for inversion and is computationally prohibited.

Chang and Gan [14] proposed the CUSUM chart for monitoring a high yield process. They introduced the procedures for designing optimal CUSUM charts for monitoring a high yield process and CUSUM charts based on non-transformed geometric and Bernoulli counts were developed. Although the CUSUM is more sensitive in detecting the process shift, the implementation and the physical interpretation of the chart is rather complicated.

2.4   Use of p-chart in Monitoring High Yield Processes

The implicit assumption in using p-chart (or np-chart) is that the inspection is carried out in sample (normally with constant sample size). As stated in Section 1.2.1, for high yield processes with sampling inspection, in order for the traditional p-chart or np-chart to perform effectively, the sample size has to be relatively large (at least $np > 8.9$). Otherwise, as the UCL of the np-chart is less than 1, once

a nonconforming item is detected, the np-chart will raise an out-of-control signal. This often results in unnecessary disruptions. Moreover, the corresponding LCL is zero and often results in loss of opportunity in identifying process improvement.

Figure 2.5 shows the ARL curve for the np-chart with in-control $p_0 = 0.0005$, $n = 17800$, and $\alpha = 0.0027$ (from Table 1.1). From the ARL curve, it is clear that with np set to be at least 8.9, the np-chart and p-chart could raise an out-of-control signal when the fraction nonconforming deviates from the initial in-control value.

Thus, for high yield processes with sample inspection, if Shewhart p-chart or np-chart with probability limits were to be used to monitor the process, the batch size should be large enough such that np is at least 8.9. However, if np is less than 8.9, which is common for high yield processes, other control scheme is needed.
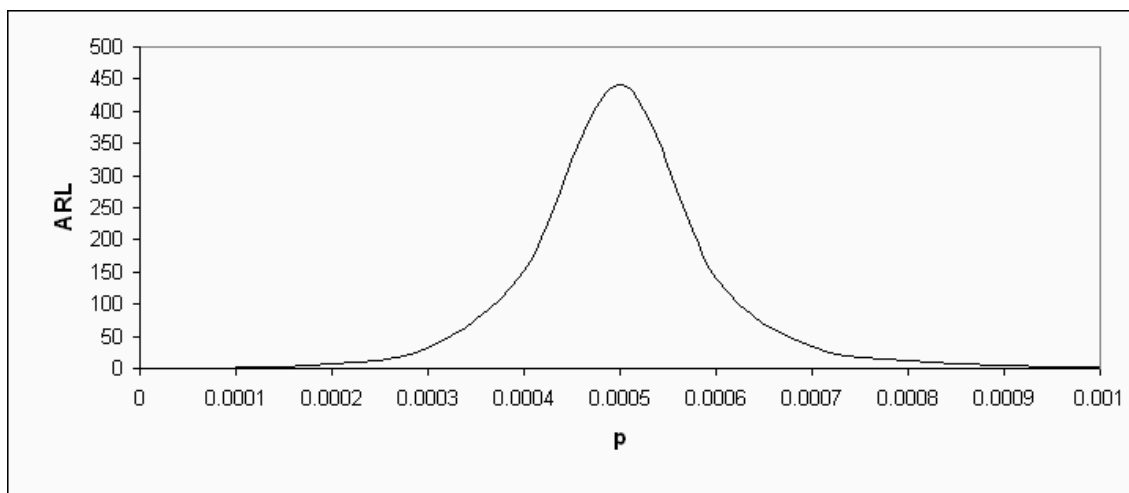
Figure 2.5: ARL curve for np-chart with in-control $p_0 = 0.0005$, $\alpha = 0.0027$

2.5 High Reliability Systems

Due to the rapid advances in technology and increasing consumer expectations, continuous improvement of a product's quality or reliability has become necessary for manufacturers to compete with others. In achieving such task, more and more highly reliable products have been introduced to the market.

For a highly reliable product, it is difficult or nearly impossible to assess it's reliability by using traditional life tests or accelerated life tests (ALT). If there exist some product characteristics whose degradation over time can be related to reliability, then conducting a degradation test or an accelerated degradation test (ADT) to collect the degradation data of whose characteristics can provide information about the product's reliability. As the degradation measurements contain credible, accurate, and useful information about product reliability, thus, the studies of performance degradation have attracted many interests and efforts. For example, Yu and Tseng [118] investigate the optimal design for a fractional factorial experiment with a degradation model of a highly reliable product; and Whitmore and Schenkelberg [97] model the degradation paths using Wiener diffusion. However, as stated before, degradation models can only be used for the systems or product whose degradation data can be measured and related to reliability.

Besides degradation models, some writers focus on other aspects of high reliable systems such as Sentler [77] studies particularly on the reliability of the high performance fibre reinforced plastics; and Tseng *et. al.* [93] propose a decision rule for classifying a unit as normal or weak, and give an economic model for determin-

ing the optimal termination time and other parameters of a burn-in test for highly reliable products.

As stated in Section 1.3, in order to maintain the high performance of a system, some of the manufacturers employ the built-in redundancy. Redundant structure named Daniels System has frequently been used as a demonstration example in structural system reliability studies. Gollwitzer and Rackwitz [30] review the theoretical results on time-invariant and time-variant Daniels systems with emphasis on asymptotic solutions. Grigoriu [31], [32], [33], [34], [35] contributes greatly in the area of reliability of Daniels systems by investigating the reliability of Daniels systems subject to quasistatic and dynamic nonstationary Gaussian load processes, analyzing the reliability of dynamic Daniels systems with local load-sharing rule and with applications of diffusion models. On the other hand, some other researchers such as Taylor [88], Sentler [77], and Phoenix [68], [69], [70] study the reliability of the fiber bundle, which is one of the Daniel systems. However, the studies mentioned above are restricted to structural system reliability, redundancy on other systems reliability is still not well-covered.

PART II

SOME NEW RESULTS IN CCC ANALYSES

Chapter 3

CCC Chart with Sequentially Updated Parameters

In this chapter, a sequential sampling scheme is introduced to provide an almost "self-starting" version of the CCC chart. The proposed scheme uses the actual sequence of observations, i.e., every successive observation accumulated to date, adaptively updates the estimate and revises the control limits, at the same time, the results are used for monitoring the process. This means that it is not necessary to assemble a huge number of initial samples before the control begins. Nevertheless, the scheme can only start after two nonconforming items have been observed and a substantial sample size is still expected for small p. This adaptive operation ensures that the control chart incorporates more and more data into the estimation of process parameter, so that the estimate of p_0 would get closer and closer to the true value. As a result, the performance of the CCC chart improves steadily as more

data become available. To prevent using data from a drifted process in updating the estimate of p_0, some decision rules could be implemented, this issue will be dealt with in the following chapter.

Here, we propose a sequential sampling scheme for CCC chart, in which both issues of the phase I problem discussed in previous chapter can be addressed simultaneously. Moreover, unlike the binomial sampling scheme considered in Yang *et al.* [115], the performance of the chart under the sequential sampling scheme is independent of the parameter, p.

In the following, the phase I problem of CCC charts is first presented, followed by a sequential sampling scheme and the estimate of p_0 under this scheme. The expressions for the alarm rate and the distribution of the run length are shown. This is followed by computing the average and standard deviation of the run length and detailed comparison with those of Yang *et al.* [115]. Then a description of the construction of the proposed CCC chart with estimated parameter is given.

3.1 Phase I Problem of CCC Charts

As stated in Section 2.2, CCC chart is very useful for one-at-a-time sequential inspections. However, while much has been done in enhancing the applicability of the CCC chart, the important phase I problem of the chart (See Woodall and Montgomery [100]) has not been fully addressed. If there is no previous/past data available for estimating the process fraction nonconforming, p, estimation using the current/future data has to be done. However, the common problem faced by

practitioners when doing so is that the initial data set from a sample for estimating p may not contain any nonconforming items. As a result, there are instances where sample size needs to be increased without a specific guideline. A logical solution is to specify the number of nonconforming items to be observed as this is the key parameter in determining the accuracy of the estimate for p. This provides the motivation on our studies in investigating different inspection schemes for high yield processes. Recently, Yang *et al.* [115] investigated the sample size effect when the proportion nonconforming p is estimated using the conventional estimate. In their recent work on Phase I problem of the CCC chart, the implicit assumption was that the inspection is carried out in large samples, which might not be the case for some processes. Furthermore, the performance of the chart under their proposed scheme is not independent of the parameter, p.

3.2   Sequential Sampling Scheme

Consider an industry setting where, in order to estimate the parameter p for establishing a CCC chart, a prescribed value for the number of nonconforming items to be observed is given, say, m. The total number of samples to be inspected is then a random variable, N_m, such that

$$N_m = \sum_{i=1}^{m} X_i$$

where X_i are independently and identically distributed (i.i.d.) geometric random variables with parameter p. It then follows that N_m is a negative binomial random

variate with parameter (m, p); i.e.

$$P(N_m = n) = p^m(1 - p)^{n-m}\binom{n - 1}{m - 1} \quad n = m, m + 1, \ldots$$

Usually p is estimated by its maximum likelihood estimate (see Yang *et al.* [115])

$$\hat{p} = \frac{m}{N_m} \tag{3.1}$$

However, this estimate is biased under sequential sampling (see Girshick *et al.* [25]) and this problem can be quite serious for small m, which is always the case during the establishment of CCC chart. Here, the unbiased estimate $\bar{p}$ given by Haldane [37] is used:

$$\bar{p} = \frac{m - 1}{N_m - 1} \tag{3.2}$$

This bias-correction is crucial as it is well known that CCC chart is less sensitive in picking up process deterioration (see Section 3.4). This problem is further aggravated by the use of the conventional estimate given in Equation (3.1) which tends to over-estimate p, giving a higher in-control p, especially for small m; making it harder to detect process deterioration. Table 3.1 gives the comparison of the two estimates using 1000 simulation runs with $p = 0.0005$. From the table, it can be seen that for small m, while $\bar{p}$ is unbiased, $\hat{p}$ tends to over-estimate p.

From Equation (3.2), it is clear that the minimum value for m is 2 such that p could be estimated. If there is no previous data or history on the similar process and the process parameter has to be estimated using the current observations, a

simple way to start using the CCC chart is to establish the chart with $m = 2$. As long as the cumulative number of conforming items for the next occurrence of nonconforming is within the control limits, the estimate and the control limits are updated. In this way, two problems are simultaneously solved. First, the homogeneity of samples is ensured. Second, the chart can be put in place within a reasonable time frame without the usual problem that a random sample may not consist of any nonconforming items. Details of the proposed scheme for setting up CCC chart will be presented in the following sections.

Table 3.1: The Comparisons of the estimates using $\bar{p}$ and $\hat{p}$ on 1000 simulation runs with $p = 0.0005$ for different m.

m	$\bar{p}$	$\hat{p}$
2	0.000498	0.000911
3	0.000505	0.000742
4	0.000501	0.000661
5	0.000497	0.000616
6	0.000494	0.000590
7	0.000496	0.000576
8	0.000499	0.000568

3.3   Run Length Distribution

A control chart may indicate an out-of-control condition either when one point falls beyond the control limits or when the plotted points exhibit some nonrandom pattern of behaviours. When the chart signals an out-of-control alarm, this indicates that a shift has occured and actions will be taken to diagnose the shift. Generally, the control charting will then be restarted. The whole sequence going from the

starting point to the plotting point going beyond the control limits is called a *run*. The number of observations from the starting point up to the point which is beyond the control limits is called the *run length*. The run length is a random variable, having a mean, a variance and a distribution. Its mean is called the *average run length* (ARL), which had been described in Section 1.1.2.1, and is usually used to measure the performance of the control chart.

3.3.1 Run Length Distribution of CCC Chart with Known Parameter (Phase II)

When the process parameter, p_0 is known, i.e., Phase II on the implementation of a control chart. The run length distribution of the CCC chart can be obtained easily.

Let E be the signaling event, i.e., the event when the ith plotting point is either above UCL or below LCL. This event can be expressed as

$$E = \{X_i > UCL \quad \text{or} \quad X_i < LCL\} \tag{3.3}$$

where X_i is the geometric random variable with parameter p when this event occurs. Then, $P(E)$ is the alarm rate for a CCC chart

$$
\begin{aligned}
P(E) &= P(X_i > UCL) + P(X_i < LCL) \\
&= (1-p)^{UCL} + 1 - (1-p)^{LCL-1} \\
&= 1 - \{(1-p)^{LCL-1} - (1-p)^{UCL}\}.
\end{aligned}
\tag{3.4}
$$

When the process is in control, $p = p_0$, the probability of a signal or the false alarm

rate is equal to

$$1 - \{(1 - p_0)^{LCL-1} - (1 - p_0)^{UCL}\} = \alpha \qquad (3.5)$$

where $\{(1 - p)^{LCL-1} - (1 - p)^{UCL}\}$ denoted as β is the operating characteristic (OC) function, which defined as the probability that the count will fall within the control limits. For different value of p, the OC curve provides a measure of the sensitivity of the control chart, as stated in Chapter 1, that is, its ability to detect process shift.

As X is geometrically distributed, X_i and X_j are independent for $i \neq j$, the sequence of trials of determining if X exceeds the known constant control limits would be a sequence of Bernoulli trials. Thus, the events E are independent. If U is defined as the number of points plotted until an out-of-control signal is given, i.e., until the first E occurs, then U is known as the run length of the chart and comes from another geometric distribution with parameter $\mathbf{p} = P(E)$. Therefore, the mean of the distribution of E or the ARL is given by

$$ARL = \frac{1}{1 - \beta} \qquad (3.6)$$

and the standard deviation, SDRL, is given by

$$SDRL = \frac{\sqrt{\beta}}{1 - \beta}$$
$$= \sqrt{ARL(ARL - 1)} \qquad (3.7)$$

For the CCC chart, the ARL for a given fraction nonconforming p is

$$ARL = \frac{1}{1 - \beta} = \frac{1}{1 - (\{(1 - p)^{LCL-1} - (1 - p)^{UCL}\})} \qquad (3.8)$$

3.4 Performance of CCC chart with $\bar{p}$

Using $\bar{p}$ as the estimate of p, it follows from Equations (2.5), (2.6) and (3.2) that the estimated control limits are:

$$\widehat{UCL} = \frac{\ln(\alpha/2)}{\ln(1 - (m-1)/(N_m - 1))} \tag{3.9}$$

$$\widehat{LCL} = \frac{\ln(1 - \alpha/2)}{\ln(1 - (m-1)/(N_m - 1))} + 1 \tag{3.10}$$

Analogously to what had been presented in Section 3.3, define F to be the event that a particular point on the CCC chart constructed with $\bar{p}$, plots above $\widehat{UCL}$ or below $\widehat{LCL}$. This event can be expressed as

$$F = \{X > \widehat{UCL} \quad \text{or} \quad X < \widehat{LCL}\}$$

where X is the geometric random variable with parameter p when this event occurs. Then, $P(F|m)$ is the alarm rate for a CCC chart constructed given a prescribed value for m. For large $m(\to \infty)$, this would become the true false alarm rate as $\bar{p} \to p_0$. From the law of total probability, $P(F|m)$ can be written as

$$
\begin{aligned}
P(F|m) &= \sum_{n=m}^{\infty} P(F|m, N_m) P(N_m = n|m) \\
&= \sum_{n=m}^{\infty} \left(P\{X > \widehat{UCL}|m, N_m = n\} + P\{X < \widehat{LCL}|m, N_m = n\} \right) \\
&\qquad \binom{n-1}{m-1} p_0^m (1-p_0)^{n-m} \\
&= \sum_{n=m}^{\infty} \left((1-p)^{\frac{\ln(\alpha/2)}{\ln(1-(m-1)/(n-1))}} - (1-p)^{\frac{\ln(1-\alpha/2)}{\ln(1-(m-1)/(n-1))}} + 1 \right) \binom{n-1}{m-1} p_0^m (1-p_0)^{n-m}
\end{aligned}
$$

$$\tag{3.11}$$

The equation above gives the alarm rate under the sequential sampling scheme.

Note that when $p = p_0$, Equation (3.11) gives the false alarm probability, which would have the value of $\alpha/2$, for two-sided chart.

Since p_0 is a small number as the high yield manufacturing process involves only with very low percent nonconforming level, from Equation (3.11), both the conditional probability and the negative binomial probability for very large values of n are negligible. Hence, to simplify the computation, a truncation procedure is used. Based on Chebyshev's Inequality, the truncation is applied in Equation (3.11) such that

$$P(F|m) \le \sum_{n=m}^{c'} \left(\left(P\{X > \widehat{UCL}|m, N_m = n\} + P\{X < \widehat{LCL}|m, N_m = n\} \right) \binom{n-1}{m-1} p_0^m (1-p_0)^{n-m} \right) + \sum_{m \ge c'} \binom{n-1}{m-1} p_0^m (1-p_0)^{n-m}$$

where $c' = \dfrac{cm}{p_0}$. The second term is bounded using the Chebyshev's Inequality, where

$$P\{|X - \mu| \ge c' - \mu\} \le \frac{\sigma^2}{(c' - \mu)^2}$$
$$= \frac{m(1-p_0)/p_0^2}{(c' - \frac{m}{p_0})^2}$$
$$= \frac{m(1-p_0)}{p_0^2(c' - \frac{m}{p_0})^2}$$

Thus, the probability mass beyond c' is bounded by

$$\frac{m(1-p_0)}{p_0^2 \big((c-1)(m/p_0) \big)^2}.$$

The values of c can be chosen so that this bound is arbitrary small. Here, in this study, the c value is used so that the bound is smaller than 10^{-3}.

Table 3.2 provides the values of false alarm rate for different combinations of p_0 and m, ranging from $p_0 = 0.0001$ to 0.001 and $m = 2(1)15$, to 350 with $\alpha = 0.0027$.

From this table, it is noted that the actual false alarm rate deviates significantly from its desired value, α, when the chart is constructed using the estimated value of p_0. The false alarm rate decreases and approaches α as m increases, regardless of p_0; in other words, the probability of false signal is not affected by the in-control percent nonconforming, p_0, but it does depend on the number of nonconforming items, m, and in turns, N_m, the total number of samples.

Table 3.2: The false alarm rates with estimated control limits, $\alpha = 0.0027$.

$m \setminus p_0$	0.00005	0.0001	0.0002	0.0003	0.0004	0.0005	0.0006	0.0007	0.0008	0.0009	0.001
2	0.01998	0.01998	0.0200	0.01999	0.02000	0.02000	0.02000	0.02001	0.02001	0.02002	0.02002
3	0.01457	0.01457	0.01458	0.01457	0.01458	0.01458	0.01458	0.01458	0.01458	0.01458	0.01458
4	0.01131	0.01131	0.01131	0.01131	0.01131	0.01131	0.01131	0.01131	0.01131	0.01131	0.01132
5	0.00931	0.00931	0.00931	0.00931	0.00931	0.00931	0.00931	0.00931	0.00931	0.00931	0.00931
6	0.00801	0.00801	0.00801	0.00801	0.00801	0.00801	0.00801	0.00801	0.00801	0.00801	0.00801
7	0.00710	0.00710	0.0071	0.00710	0.00710	0.00710	0.00710	0.00710	0.00711	0.00711	0.00711
8	0.00645	0.00645	0.00645	0.00645	0.00645	0.00645	0.00645	0.00645	0.00645	0.00645	0.00645
9	0.00595	0.00595	0.00595	0.00595	0.00595	0.00595	0.00595	0.00595	0.00595	0.00595	0.00595
10	0.00556	0.00556	0.00557	0.00557	0.00557	0.00557	0.00557	0.00557	0.00557	0.00557	0.00557
11	0.00526	0.00526	0.00526	0.00526	0.00526	0.00526	0.00526	0.00526	0.00526	0.00526	0.00526
12	0.00501	0.00501	0.00501	0.00501	0.00501	0.00501	0.00501	0.00501	0.00501	0.00501	0.00501
13	0.00480	0.00480	0.0048	0.00480	0.00480	0.00480	0.00480	0.00480	0.00480	0.00480	0.00480
14	0.00463	0.00463	0.00463	0.00463	0.00463	0.00463	0.00463	0.00463	0.00463	0.00463	0.00463
15	0.00448	0.00448	0.00448	0.00448	0.00448	0.00448	0.00448	0.00448	0.00448	0.00448	0.00448
20	0.00398	0.00398	0.00398	0.00398	0.00398	0.00398	0.00398	0.00398	0.00398	0.00398	0.00398
25	0.00369	0.00369	0.00369	0.00369	0.00369	0.00369	0.00369	0.00369	0.00369	0.00369	0.00369
30	0.00351	0.00351	0.00351	0.00351	0.00351	0.00351	0.00351	0.00351	0.00351	0.00351	0.00351
35	0.00339	0.00339	0.00339	0.00339	0.00339	0.00339	0.00339	0.00339	0.00339	0.00339	0.00339
40	0.00329	0.00329	0.00329	0.00329	0.00329	0.00329	0.00329	0.00329	0.00329	0.00329	0.00329
50	0.00317	0.00317	0.00317	0.00317	0.00317	0.00317	0.00317	0.00317	0.00317	0.00317	0.00317
60	0.00309	0.00309	0.00309	0.00309	0.00309	0.00309	0.00309	0.00309	0.00309	0.00309	0.00309
70	0.00303	0.00303	0.00303	0.00303	0.00303	0.00303	0.00303	0.00303	0.00303	0.00303	0.00303
80	0.00299	0.00299	0.00299	0.00299	0.00299	0.00299	0.00299	0.00299	0.00299	0.00299	0.00299
90	0.00295	0.00295	0.00295	0.00295	0.00295	0.00295	0.00295	0.00295	0.00295	0.00295	0.00295
100	0.00293	0.00293	0.00293	0.00293	0.00293	0.00293	0.00293	0.00293	0.00293	0.00293	0.00293
150	0.00285	0.00285	0.00285	0.00285	0.00285	0.00285	0.00285	0.00285	0.00285	0.00285	0.00285
200	0.00281	0.00281	0.00281	0.00281	0.00281	0.00281	0.00281	0.00281	0.00281	0.00281	0.00281
250	0.00279	0.00279	0.00279	0.00279	0.00279	0.00279	0.00279	0.00279	0.00279	0.00279	0.00279
300	0.00277	0.00277	0.00277	0.00277	0.00277	0.00277	0.00277	0.00277	0.00277	0.00277	0.00277
350	0.00276	0.00276	0.00276	0.00276	0.00276	0.00276	0.00276	0.00276	0.00276	0.00276	0.00276

3.4.1 The Run Length Distribution with $\bar{p}$

Denote $P(F|m, N_m = n)$ by $p_{m,n}$, and the run length of the constructed chart with a given m by R_m. That is,

$$P(F|m, N_m = n) = P\{X > \widehat{UCL}|m, N_m = n\} + P\{X < \widehat{LCL}|m, N_m = n\}$$

$$= (1 - p)^{\frac{\ln(\alpha/2)}{\ln(1-(m-1)/(n-1))}} - (1 - p)^{\frac{\ln(1-\alpha/2)}{\ln(1-(m-1)/(n-1))}} + 1$$

$$= p_{m,n}$$

The conditional distribution of R_m, given $N_m = n$ is geometric with parameter $p_{m,n}$ as

$$P_{R_m|N_m}(r|N_m = n) = (1 - p_{m,n})^{r-1} p_{m,n} \tag{3.12}$$

The expectation of R_m for a given m can be expressed as

$$E(R_m) = E[E(R_m|N_m)]$$

From Equation (3.12), we have $E(R_m) = E[1/p_{m,n}]$. Thus, the ARL_m, which is the expectation of R_m, would be

$$\text{ARL}_m = E[1/p_{m,n}]$$
$$= \sum_{n=m}^{\infty} \frac{1}{p_{m,n}} \binom{n-1}{m-1} p_0^m (1 - p_0)^{n-m} \tag{3.13}$$

Hence, the unconditional distribution of R_m, which is the run length distribution, is given by

$$P_{R_m}(r; p_0, p) = \sum_{n=m}^{\infty} (1 - p_{m,n})^{r-1} p_{m,n} P(N_m = n|m)$$
$$= \sum_{n=m}^{\infty} (1 - p_{m,n})^{r-1} p_{m,n} \binom{n-1}{m-1} p_0^m (1 - p_0)^{n-m} \tag{3.14}$$

50

From the usual conditional expectation property,

$$E\big[\mathrm{var}[R_m|N]\big] = E\big[E[R_m^2|N]\big] - E\big[(E[R_m|N])^2\big]$$

$$= E[R_m^2] - (E[R_m])^2 - E\big[(E[R_m|N])^2\big] + (E[R_m])^2 \tag{3.15}$$

$$= \mathrm{var}[R_m] - E\big[(E[R_m|N])^2\big] + \big(E\big[E[R_m|N]\big]\big)^2$$

$$= \mathrm{var}[R_m] - \mathrm{var}\big[E[R_m|N]\big]$$

It follows that, the variance of R_m is

$$\mathrm{var}[R_m] = E\big[\mathrm{var}[R_m|N]\big] + \mathrm{var}\big[E[R_m|N]\big]$$

$$= E\big[(1 - p_{m,n})/(p_{m,n})^2\big] + \mathrm{var}[1/p_{m,n}]$$

$$= \sum_{n=m}^{\infty} \left(\frac{1 - p_{m,n}}{(p_{m,n})^2}\right)\binom{n-1}{m-1}p_0^m(1-p_0)^{n-m}$$

$$+ \left(\sum_{n=m}^{\infty}\left(\frac{1}{p_{m,n}}\right)^2\binom{n-1}{m-1}p_0^m(1-p_0)^{n-m}\right) \tag{3.16}$$

$$- \left(\sum_{n=m}^{\infty}\left(\frac{1}{p_{m,n}}\right)\binom{n-1}{m-1}p_0^m(1-p_0)^{n-m}\right)^2$$

$$= \sum_{n=m}^{\infty}\left(\frac{2 - p_{m,n}}{(p_{m,n})^2}\right)\binom{n-1}{m-1}p_0^m(1-p_0)^{n-m}$$

$$- \left(\sum_{n=m}^{\infty}\frac{1}{p_{m,n}}\binom{n-1}{m-1}p_0^m(1-p_0)^{n-m}\right)^2$$

The standard deviation of the run length, R_m, SDRL_m is then given by the square

root of Equation (3.16) as

$$\mathrm{SDRL}_m = \sqrt{E\big[(1 - p_{m,n})/(p_{m,n})^2\big] + \mathrm{var}[1/p_{m,n}]}$$

$$= \left(\sum_{n=m}^{\infty}\left(\frac{2 - p_{m,n}}{(p_{m,n})^2}\right)\binom{n-1}{m-1}p_0^m(1-p_0)^{n-m}\right.$$

$$\left. - \left(\sum_{n=m}^{\infty}\frac{1}{p_{m,n}}\binom{n-1}{m-1}p_0^m(1-p_0)^{n-m}\right)^2\right)^{1/2} \tag{3.17}$$

Values of ARL_m and SDRL_m are computed from Equations (3.13) and (3.17)

for a range of m and p with $p_0 = 0.0005$ and tabulated in Table 3.3. For each

combination of m and p, the first value shown is the ARL_m and the second is the SDRL_m, followed by the coefficient of variation of the run length, the values in bracket under each value of m are the expected number of samples with m nonconforming items when $p = p_0$, $E(N_m)$; the ARL and SDRL of the CCC chart using the known p_0 are given in the last row.

It is noted that, as m gets larger, ARL_m and SDRL_m approach to those of the known parameter. It is also noted that, as p decreases, both ARL_m and SDRL_m decrease, and when p increases, both ARL_m and SDRL_m first increase then decrease. This implies that CCC chart is better in detecting quality improvement and is not effective in detecting process deterioration unless the amount of increase in p is large. This is in fact a common problem for data having a skewed distribution, regardless of whether the parameter is known or estimated (see discussions in Section 2.3.1.3). This problem will be addressed in the proposed scheme given in the next section. Figure 3.1 shows the ARLs for known p_0 and the ARLs using $\bar{p}$ for different m. It can be seen that, as m increases, the behavior of the chart is getting closer to the known value chart.

3.4.2   Comparison with CCC chart under $\hat{p}$

The conventional estimate of p, given in Equation (3.1), is obtained by sampling a large number of items so that there are at least one nonconforming item. In this case, the nonconforming count, M_n is a binomial random variable with parameter

Table 3.3: The Average Run Length (ARL$_m$), Standard Deviation Run Length (SDRL$_m$) and the coefficient of variation of the run length with estimated control limits, $\alpha = 0.0027$, $p_0 = 0.0005$. The number in the parenthesis below each m is the expected sample size.

$m \setminus p$	0.0001	0.0002	0.0003	0.0004	**0.0005**	0.0006	0.0007	0.0008	0.0009	0.001
2	49.83	178.82	250.09	275.68	**279.16**	272.74	262.16	250.11	237.86	226.02
(4000)	154.92	321.57	363.61	365.99	**356.70**	344.06	330.76	317.78	305.45	293.89
	3.11	1.80	1.45	1.33	**1.28**	1.26	1.26	1.27	1.28	1.30
3	16.36	112.95	220.04	282.83	**309.57**	315.24	309.86	299.07	285.95	272.12
(6000)	56.85	246.16	349.15	382.50	**386.53**	379.08	367.16	353.63	339.76	326.13
	3.48	2.18	1.59	1.35	**1.25**	1.20	1.18	1.18	1.19	1.20
4	9.55	78.60	193.41	279.22	**323.55**	338.82	337.37	327.23	313.04	297.34
(8000)	26.44	187.90	324.30	383.21	**399.53**	397.11	386.67	372.82	357.70	342.34
	2.77	2.39	1.68	1.37	**1.23**	1.17	1.15	1.14	1.14	1.15
5	7.28	59.33	172.59	273.66	**331.97**	355.09	356.63	346.64	331.18	313.66
(10000)	15.49	146.57	299.69	379.19	**406.54**	408.77	399.69	385.55	369.29	352.38
	2.13	2.47	1.74	1.39	**1.22**	1.15	1.12	1.11	1.12	1.12
6	6.20	47.51	156.19	267.82	**337.67**	367.42	371.27	361.09	344.29	325.04
(12000)	10.19	116.67	277.26	373.44	**373.44**	417.19	409.35	394.91	377.56	359.21
	1.64	2.46	1.78	1.39	**1.11**	1.14	1.10	1.09	1.10	1.11
7	5.66	40.09	143.29	262.38	**341.94**	377.38	383.05	372.45	354.28	333.42
(14000)	8.36	95.77	257.44	367.04	**413.22**	423.64	416.92	402.15	383.76	364.07
	1.48	2.39	1.80	1.40	**1.21**	1.12	1.09	1.08	1.08	1.09
8	5.30	35.03	132.83	257.31	**345.22**	385.65	392.77	381.61	362.09	339.75
(16000)	7.22	80.37	239.97	360.51	**414.77**	428.83	423.12	408.01	388.60	367.66
	1.36	2.29	1.81	1.40	**1.20**	1.11	1.08	1.07	1.07	1.08
9	5.06	31.43	124.24	252.64	**347.83**	392.68	400.97	389.16	368.34	344.65
(18000)	6.46	68.81	224.60	354.07	**415.70**	433.13	428.35	412.86	392.48	370.37
	1.28	2.19	1.81	1.40	**1.20**	1.10	1.07	1.06	1.07	1.07
10	4.88	28.78	117.08	248.36	**349.96**	398.77	408.01	395.50	373.44	348.51
(20000)	5.93	59.99	211.03	347.83	**416.20**	436.80	432.84	416.96	395.65	372.44
	1.22	2.08	1.80	1.40	**1.19**	1.10	1.06	1.05	1.06	1.07
15	4.42	22.12	94.35	231.66	**356.66**	420.53	432.43	416.19	388.89	359.33
(30000)	4.69	37.18	162.81	320.65	**415.66**	449.48	448.68	430.70	405.19	377.53
	1.06	1.68	1.73	1.38	**1.17**	1.07	1.04	1.03	1.04	1.05
20	4.22	19.45	82.50	220.20	**360.14**	434.25	447.03	427.38	396.26	363.83
(40000)	4.21	28.19	134.12	299.58	**413.38**	457.37	458.61	438.49	409.59	378.82
	1.00	1.45	1.63	1.36	**1.15**	1.05	1.03	1.03	1.03	1.04
50	3.92	15.81	62.18	191.36	**366.79**	468.33	479.09	447.61	407.02	369.13
(100000)	3.55	17.86	80.20	236.94	**400.49**	477.70	482.54	452.96	413.98	376.49
	0.91	1.13	1.29	1.24	**1.09**	1.02	1.01	1.01	1.02	1.02
60	3.89	15.47	60.09	187.22	**367.50**	473.32	483.12	449.63	407.84	369.43
(120000)	3.49	17.01	74.54	226.82	**397.60**	480.95	485.89	454.34	413.90	375.73
	0.90	1.10	1.24	1.21	**1.08**	1.02	1.01	1.01	1.01	1.02
70	3.87	15.23	58.62	184.11	**368.00**	477.10	486.05	451.00	408.36	369.62
(140000)	3.45	16.43	70.63	219.07	**395.21**	483.49	488.37	455.24	413.74	375.14
	0.89	1.08	1.20	1.19	**1.07**	1.01	1.00	1.01	1.01	1.01
80	3.85	15.06	57.55	181.70	**368.36**	480.07	488.26	451.99	408.73	369.74
(160000)	3.42	16.01	67.78	212.94	**393.20**	485.54	490.28	455.85	413.56	374.66
	0.89	1.06	1.18	1.17	**1.07**	1.01	1.00	1.01	1.01	1.01
90	3.84	14.93	56.72	179.78	**368.63**	482.47	489.99	452.74	408.99	369.83
(180000)	3.39	15.69	65.61	207.99	**391.49**	487.23	491.79	456.29	413.39	374.27
	0.88	1.05	1.16	1.16	**1.06**	1.01	1.00	1.01	1.01	1.01
100	3.83	14.83	56.07	178.21	**368.85**	484.44	491.37	453.31	409.19	369.89
(200000)	3.37	15.45	63.91	203.91	**390.01**	488.65	493.02	456.62	413.23	373.95
	0.88	1.04	1.14	1.14	**1.06**	1.01	1.00	1.01	1.01	1.01
150	3.80	14.52	54.15	173.32	**369.45**	490.71	495.53	454.94	409.72	370.06
(300000)	3.32	14.74	58.99	191.01	**384.93**	493.34	496.74	457.42	412.64	372.95
	0.87	1.01	1.09	1.10	**1.04**	1.01	1.00	1.01	1.01	1.01
200	3.79	14.37	53.22	170.78	**369.72**	494.06	497.59	455.69	409.95	370.12
(400000)	3.29	14.40	56.64	184.20	**381.94**	495.97	498.61	457.72	412.29	372.42
	0.87	1.00	1.06	1.08	**1.03**	1.00	1.00	1.00	1.01	1.01
250	3.78	14.29	52.67	169.23	**369.88**	496.14	498.82	456.12	410.07	370.16
(500000)	3.27	14.20	55.27	180.00	**379.97**	497.66	499.73	457.87	412.06	372.10
	0.87	0.99	1.05	1.06	**1.03**	1.00	1.00	1.00	1.00	1.01
-	3.74	13.94	50.52	162.79	**370.37**	505.10	503.62	457.66	410.51	370.28
	3.21	13.44	50.02	162.29	**369.87**	504.60	503.12	457.16	410.01	369.78

Figure 3.1: ARL for the exact value, and $m = 3, 5,$ and 10, with $p_0 = 0.0005$.

(n, p). Recently, Yang *et al.* [115] presented the performance of this chart using this binomial sampling scheme.

For comparison, corresponding results to those in Tables 3.2 and 3.3 are reproduced in Tables 3.4 and 3.5. It can be seen that the false alarm rate for the binomial sampling scheme is dependent on the true percent nonconforming p_0. This is undesirable in practice as p_0 needs to be estimated and there may be no defective / nonconforming item in the initial sample. As a result, practitioners / engineers cannot be sure of the risk when they need to decide on the sample size n. In practice, this often leads to a situation where n is increased incrementally until some arbitrary number of defective / nonconforming items are observed which, in turn, induces bias in the estimate of p.

From Table 3.5, it is clear that the values of ARL for different n under the

Table 3.4: Values of false alarm rate with estimated control limits, under binomial sampling scheme, $\alpha = 0.0027$ (from Yang *et al.* [115] Table 1).

$n \setminus p_0$	0.0001	0.0002	0.0003	0.0004	0.0005	0.0006	0.0007	0.0008	0.0009	0.001
10000	0.38651	0.14718	0.05911	0.02623	0.01371	0.00878	0.00671	0.00575	0.00524	0.00492
20000	0.14719	0.02623	0.00878	0.00575	0.00492	0.00452	0.00425	0.00406	0.00391	0.00379
50000	0.01372	0.00492	0.00415	0.00379	0.00357	0.00343	0.00332	0.00325	0.00319	0.00314
100000	0.00492	0.00379	0.00343	0.00325	0.00314	0.00306	0.00301	0.00297	0.00294	0.00292
200000	0.00378	0.00324	0.00306	0.00297	0.00291	0.00288	0.00286	0.00283	0.00282	0.00281
300000	0.00343	0.00306	0.00294	0.00288	0.00284	0.00282	0.00281	0.00279	0.00278	0.00277
400000	0.00324	0.00297	0.00288	0.00283	0.00281	0.00279	0.00278	0.00277	0.00276	0.00276
500000	0.00314	0.00292	0.00285	0.00281	0.00279	0.00277	0.00276	0.00276	0.00275	0.00275
600000	0.00306	0.00288	0.00282	0.00279	0.00279	0.00277	0.00276	0.00275	0.00274	0.00274
700000	0.00301	0.00286	0.0028	0.00278	0.00276	0.00275	0.00275	0.00274	0.00274	0.00273
800000	0.00297	0.00284	0.00279	0.00277	0.00276	0.00275	0.00274	0.00274	0.00273	0.00273
900000	0.00294	0.00282	0.00278	0.00276	0.00274	0.00274	0.00274	0.00273	0.00273	0.00273
1000000	0.00292	0.00281	0.00277	0.00276	0.00274	0.00273	0.00273	0.00273	0.00273	0.00272
2000000	0.00281	0.00276	0.00274	0.00273	0.00272	0.00272	0.00272	0.00272	0.00271	0.00271
∞	0.0027	0.0027	0.0027	0.0027	0.0027	0.0027	0.0027	0.0027	0.0027	0.0027

binomial scheme, ARL_n, are larger than the exact value (370.37) when the process is in control. This is counter-intuitive, as the performance of the estimated chart is normally weaker than the known parameters chart. This could be due to the positive biased in estimating p and the inherent problem of CCC chart having a larger ARL when the true proportion nonconforming is larger than the in-control value. The performance of the chart using the unbiased estimate, as shown in Table 3.3, shows that the in-control ARL_m, is smaller than the exact value; and as m increases, the ARL_m increases towards the exact ARL.

3.5 The Proposed Scheme for CCC Chart with Sequentially Estimated p

From the previous section, it is noted that the ARL for CCC chart behaves differently from the conventional chart in that the ARL is larger when process begins to deteriorate. Moreover, due to the use of an estimated p, the in-control ARL, ARL_0 is dependent on m and is smaller than the nominal value with known p. In

Table 3.5: Values of ARL_n and SDRL_n with estimated control limits, under binomial sampling scheme, $\alpha = 0.0027$, $p_0 = 0.0005$ (from Yang *et al.* [115] Table 3).

$n \setminus p_0$	0.0001	0.0002	0.0003	0.0004	**0.0005**	0.0006	0.0007	0.0008	0.0009	0.001
10000	95.05	173.62	262.73	331.30	**374.10**	397.50	406.90	406.00	397.1	382.70
	18.55	64.10	138.51	221.40	**291.80**	339.10	362.30	366.00	356.7	340.10
20000	29.42	108.72	221.54	323.80	**391.60**	426.20	436.40	429.00	410.1	385.40
	6.56	37.08	114.24	224.10	**326.20**	391.00	414.40	408.40	386.7	359.50
50000	4.50	34.67	134.84	281.30	**398.80**	457.40	467.60	447.90	415.1	380.20
	4.18	19.38	78.43	206.80	**353.00**	442.00	460.80	439.00	403.6	367.90
100000	3.61	19.18	87.26	239.50	**394.80**	474.90	483.40	454.00	414.0	375.80
	3.93	16.02	63.25	190.40	**362.90**	467.80	480.90	449.10	407.8	369.40
200000	3.38	15.65	65.55	205.60	**387.60**	487.10	492.80	456.20	412.4	373.00
	3.83	14.87	56.33	178.10	**367.50**	484.30	492.00	453.70	409.3	370.00
300000	3.32	14.81	59.63	191.90	**383.40**	492.20	496.20	456.70	411.7	372.00
	3.80	14.54	54.26	173.30	**368.70**	490.70	495.80	455.10	409.8	370.10
400000	3.29	14.43	56.96	184.70	**380.80**	494.90	497.90	456.90	411.3	371.40
	3.79	14.38	53.27	170.80	**369.20**	494.00	497.80	455.80	410.0	370.10
500000	3.27	14.22	55.45	180.30	**379.00**	496.70	498.90	457.00	411.1	371.30
	3.78	14.29	52.70	169.20	**369.50**	496.10	498.90	456.20	410.1	370.20
600000	3.26	14.08	54.47	177.30	**377.70**	497.90	499.60	457.00	410.9	370.90
	3.77	14.23	52.32	168.20	**369.70**	497.50	499.70	456.40	410.2	370.20
700000	3.25	13.98	53.79	175.10	**376.70**	498.80	500.10	457.10	410.8	370.70
	3.77	14.19	52.05	167.40	**369.80**	498.60	500.30	456.60	410.2	370.20
800000	3.25	13.91	53.29	173.50	**376.00**	499.50	500.50	457.10	410.7	370.60
	3.77	14.16	51.85	166.80	**369.90**	499.30	500.70	456.70	410.3	370.20
900000	3.24	13.86	52.91	172.30	**375.40**	500.00	500.80	457.10	410.6	370.50
	3.76	14.13	51.70	166.40	**369.90**	500.00	501.00	456.90	410.3	370.20
1000000	3.24	13.81	52.61	171.30	**374.90**	500.40	501.00	457.10	410.6	370.50
	3.76	14.11	51.58	166.00	**370.00**	500.40	501.30	456.90	410.3	370.20
2000000	3.75	14.03	51.04	164.40	**370.20**	502.70	502.40	457.30	410.4	370.30
	3.22	13.62	51.28	166.80	**372.50**	502.40	502.10	457.10	410.3	370.10
∞	3.74	13.95	50.52	162.80	**370.40**	505.10	503.10	457.70	410.5	370.30
	3.21	13.44	50.02	162.30	**369.90**	504.60	503.10	457.20	410.0	369.80

the following, a construction scheme of CCC chart is proposed, this scheme results in a consistently large τ which is also the maximum point on the ARL curve.

To ensure that the ARL of the CCC chart will always decrease whenever there is a process shift, the adjustment factor, γ given in Equation (2.11) which discussed in Section 2.3.1.3 is used.

In order to maintain a consistently large τ for each m, the parameter ϕ_m, satisfying

$$\sum_{n=m}^{\infty} \left((1-\bar{p})^{\frac{\ln(\phi_m/2)\gamma_{\phi_m}}{\ln(1-\bar{p})}} - (1-\bar{p})^{\frac{\ln(1-\phi_m/2)\gamma_{\phi_m}}{\ln(1-\bar{p})}} + 1 \right)^{-1} \binom{n-1}{m-1} \bar{p}^m (1-\bar{p})^{n-m} = \tau. \quad (3.18)$$

should be used for computing the adjustment factor and the corresponding control

limits; where τ is the desired ARL_0. Given an estimate, $\bar{p}$, and m with the desired

ARL_0, τ, the value of ϕ_m could be obtained from Equation (3.18). Note that due

to random N_m, $\bar{p}$ varies from run to run even when m is fixed. Table 3.6 shows the

values of ϕ_m for different m and for $\bar{p}$ ranging from 0.0001 to 0.001 with the desired

in-control ARL, τ set at 370. Not only that $\bar{p}$ has no effect on ϕ_m, ϕ_m converges to

that of the known value chart as m increases; which takes place for m more than

50. Figure 3.2 is the graphical representation of ϕ_m. The exact value, ϕ_∞, could

be obtained by solving

$$\frac{1}{\tau} = 1 + (1 - p_0)^{\frac{\ln \phi/2}{\ln(1-p_0)} \cdot \frac{\ln\left[\frac{\ln(1-\phi_\infty/2)}{\ln(\phi_\infty/2)}\right]}{\ln\left[\frac{(\phi_\infty/2)}{(1-\phi_\infty/2)}\right]}} - (1 - p_0)^{\frac{\ln(1-\phi/2)}{\ln(1-p_0)} \cdot \frac{\ln\left[\frac{\ln(1-\phi_\infty/2)}{\ln(\phi_\infty/2)}\right]}{\ln\left[\frac{(\phi_\infty/2)}{(1-\phi_\infty/2)}\right]}}. \quad (3.19)$$

The details of the above equation will be discussed in the following chapter.

Table 3.6: The parameter ϕ_m with different m, $\bar{p}$, and $\tau = 370$.

$m \setminus \bar{p}$	0.0001	0.0002	0.0003	0.0004	0.0005	0.0006	0.0007	0.0008	0.0009	0.0010
2	0.00196	0.00196	0.00196	0.00196	0.00196	0.00196	0.00196	0.00196	0.00196	0.00196
3	0.00229	0.00229	0.00229	0.00229	0.00229	0.00229	0.00229	0.00229	0.00229	0.00229
4	0.00248	0.00248	0.00248	0.00248	0.00248	0.00248	0.00248	0.00248	0.00248	0.00248
5	0.00261	0.00261	0.00261	0.00261	0.00261	0.00261	0.00261	0.00261	0.00261	0.00261
6	0.00271	0.00271	0.00271	0.00271	0.00271	0.00271	0.00271	0.00271	0.00271	0.00271
7	0.00279	0.00279	0.00279	0.00279	0.00279	0.00279	0.00279	0.00279	0.00279	0.00279
8	0.00286	0.00286	0.00286	0.00286	0.00286	0.00286	0.00286	0.00286	0.00286	0.00286
9	0.00292	0.00292	0.00292	0.00292	0.00292	0.00292	0.00292	0.00292	0.00292	0.00292
10	0.00296	0.00296	0.00296	0.00296	0.00296	0.00296	0.00296	0.00296	0.00296	0.00296
15	0.00314	0.00314	0.00314	0.00314	0.00314	0.00314	0.00314	0.00314	0.00314	0.00314
20	0.00324	0.00324	0.00324	0.00324	0.00324	0.00324	0.00324	0.00324	0.00324	0.00324
50	0.00350	0.00350	0.00350	0.00350	0.00350	0.00350	0.00350	0.00350	0.00350	0.00350

As shown in previous section, the false alarm rate using $\bar{p}$ as the estimate is

independent of p_0; this implies that ϕ_m obtained from the above equation should

also be independent of $\bar{p}$ and can be used for any high yield processes. The control
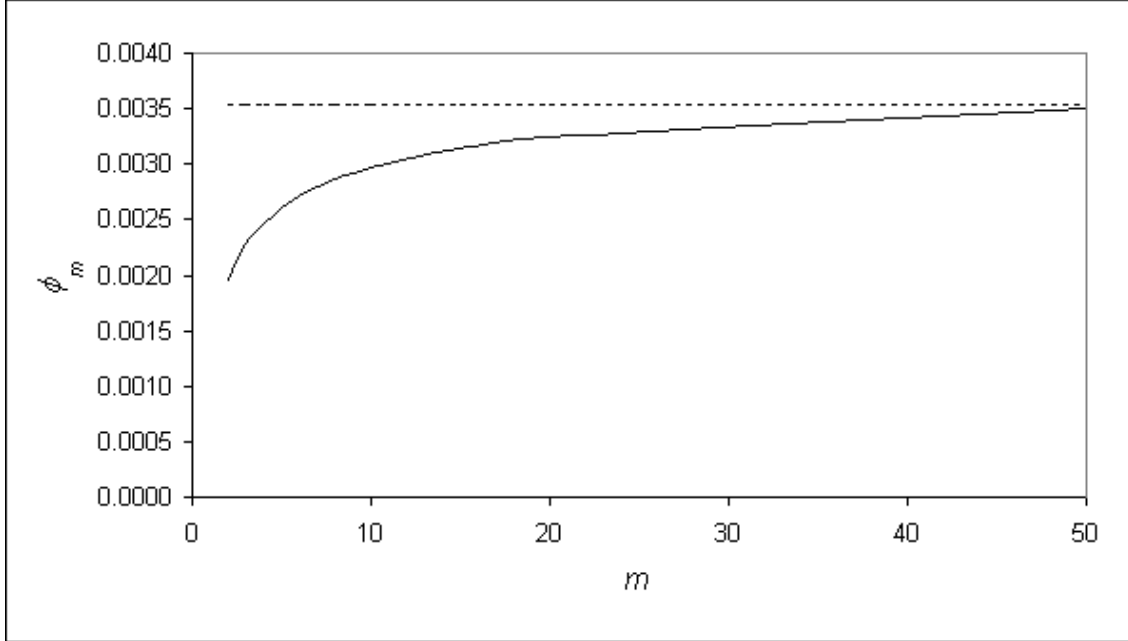
Figure 3.2: Values of ϕ_m for $\tau = 370$.

limits are thus given by

$$UCL_{\phi_m} \quad = \quad \frac{\ln(\phi_m/2)}{\ln(1 - (m-1)/(N_m-1))} \times \gamma_{\phi_m} \tag{3.20}$$

$$LCL_{\phi_m} \quad = \quad \left(\frac{\ln(1-\phi_m/2)}{\ln(1 - (m-1)/(N_m-1))}\right)\gamma_{\phi_m} + 1 \tag{3.21}$$

By using the proposed adaptive adjustment factor, the CCC scheme becomes more effective in detecting the shift in p. To obtain the ARL curves for different m using this proposed sequential estimation scheme, the Equation (3.18) can be re-written as

$$\sum_{n=m}^{\infty} \left((1-\bar{p})^{\frac{\ln(\phi_m/2)\gamma_{\phi_m}}{\ln(1-\bar{p})}} - (1-\bar{p})^{\frac{\ln(1-\phi_m/2)\gamma_{\phi_m}}{\ln(1-\bar{p})}} + 1\right)^{-1} \binom{n-1}{m-1} p^m (1-p)^{n-m} = \tau_m \tag{3.22}$$

where τ_m is the desired in-control ARL with $\bar{p}$ estimated after observing m non-conforming items.

Table 3.7 shows the ARL as well as the SDRL of the CCC chart with the adjustment factor for m ranging from $m = 2$ to 10, $p_0 = 0.0005$, and the in-control ARL $= 370$. For ease of comparison, the last row of the table gives the ARL and SDRL with known parameter. The general behaviour of ARL is depicted in Figure 3.3 for $m = 3$, 5, and 10, with $p_0 = 0.0005$.
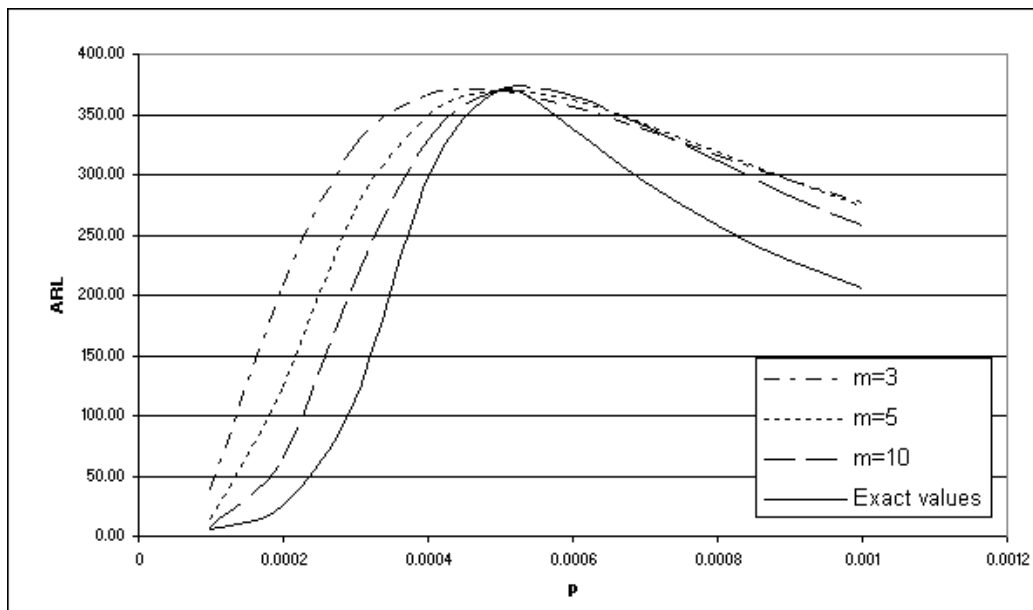
Figure 3.3: ARL for the exact value, and $m = 3, 5$, and 10, using ϕ_m with $p_0 = 0.0005$.

Table 3.7: The Average Run Length, Standard Deviation Run Length and the coefficient of variation of the run length with estimated control limits and ϕ_m, constant $\tau = 370$, and $p_0 = 0.0005$.

$m \setminus p$	0.0001	0.0002	0.0003	0.0004	**0.0005**	0.0006	0.0007	0.0008	0.0009	0.001
2	117.34	309.28	375.61	383.36	**369.93**	349.70	328.17	307.44	288.24	270.75
	304.91	489.09	507.74	491.55	**468.41**	444.90	422.72	402.29	383.62	366.58
	2.60	1.58	1.35	1.28	**1.27**	1.27	1.29	1.31	1.33	1.35
3	39.84	208.47	324.63	366.62	**370.04**	356.87	337.50	316.61	296.24	277.19
	129.88	373.76	449.40	456.33	**442.54**	422.72	401.62	380.98	361.44	343.22
	3.26	1.79	1.38	1.24	**1.20**	1.18	1.19	1.20	1.22	1.24
4	21.14	156.33	292.76	355.88	**369.80**	360.19	341.04	319.03	297.13	276.57
	66.46	301.06	412.24	436.12	**428.79**	411.00	389.96	368.47	347.70	328.15
	3.14	1.93	1.41	1.23	**1.16**	1.14	1.14	1.15	1.17	1.19
5	14.54	124.99	270.41	348.59	**370.05**	362.41	342.71	319.31	295.94	274.09
	39.41	250.30	384.83	422.28	**420.03**	403.58	382.23	359.72	337.71	316.93
	2.71	2.00	1.42	1.21	**1.14**	1.11	1.12	1.13	1.14	1.16
6	11.54	104.32	253.31	342.89	**370.12**	363.60	343.03	318.26	293.60	270.75
	26.42	212.68	362.71	411.43	**413.41**	397.92	376.11	352.59	329.43	307.60
	2.29	2.04	1.43	1.20	**1.12**	1.09	1.10	1.11	1.12	1.14
7	9.92	89.91	239.74	338.38	**370.22**	364.29	342.71	316.65	290.91	267.29
	19.56	183.98	344.36	402.67	**408.29**	393.51	371.15	346.63	322.45	299.73
	1.97	2.05	1.44	1.19	**1.10**	1.08	1.08	1.09	1.11	1.12
8	8.93	79.35	228.37	334.24	**369.83**	364.17	341.56	314.36	287.76	263.58
	15.60	161.33	328.32	394.83	**403.64**	389.40	366.48	341.05	315.98	292.56
	1.75	2.03	1.44	1.18	**1.09**	1.07	1.07	1.08	1.10	1.11
9	8.26	71.40	218.85	330.71	**369.43**	363.82	340.19	311.98	284.67	260.08
	13.14	143.30	314.42	388.09	**399.73**	385.91	362.39	336.11	310.27	286.29
	1.59	2.01	1.44	1.17	**1.08**	1.06	1.07	1.08	1.09	1.10
10	7.80	65.46	211.54	328.99	**370.59**	364.85	340.15	310.92	282.91	257.93
	11.54	129.19	303.48	383.83	**398.07**	384.50	360.29	333.09	306.47	281.93
	1.48	1.97	1.43	1.17	**1.07**	1.05	1.06	1.07	1.08	1.09
-	5.12	25.77	113.48	296.72	**370.03**	337.51	293.82	257.80	229.30	206.42
	4.60	25.26	112.98	296.22	**369.53**	337.01	293.32	257.30	228.80	205.92

3.6   Numerical Examples

Here, two examples are presented to demonstrate the usage and efficiency of the proposed charting technique. A set of 60 simulated process observations with percent nonconforming, $p = 0.0005$, i.e., 500 parts-per-million (ppm), is shown in Table 3.8. Besides the simulated data, Table 3.8 also shows the updates of the cumulative conformance counts, x, the estimates, $\bar{p}$ and the control limits for m ranging from 2 to 60.

From Table 3.8, the 60 observations are listed and the control limits are computed with the proposed scheme. The results are depicted in Figure 3.4 where the

60

Table 3.8: The simulated data from geometric distribution for $m = 60$ with $p = 0.0005$.

m	x	$\sum x$	$\bar{p}$	$LCL_{\phi m}$	$UCL_{\phi m}$	m	x	$\sum x$	$\bar{p}$	$LCL_{\phi m}$	$UCL_{\phi m}$
1	3779	3779	-	-	-	31	261	67290	0.00045	6	18579
2	1885	5664	0.00018	9	50196	32	4099	71389	0.00043	7	19075
3	494	6158	0.00032	6	26735	33	2428	73817	0.00043	7	19108
4	3591	9749	0.00031	7	27925	34	675	74492	0.00044	7	18698
5	1063	10812	0.00037	6	23067	35	203	74695	0.00046	6	18197
6	266	11078	0.00045	6	18810	36	1883	76578	0.00046	6	18123
7	1030	12108	0.00050	5	17065	37	527	77105	0.00047	6	17741
8	4075	16183	0.00043	6	19486	38	530	77635	0.00048	6	17380
9	1935	18118	0.00044	6	19038	39	1835	79470	0.00048	6	17322
10	262	18380	0.00049	6	17128	40	2994	82464	0.00047	6	17514
11	1166	19546	0.00051	6	16393	41	5816	88280	0.00045	6	18281
12	107	19653	0.00056	5	14984	42	1475	89755	0.00046	6	18133
13	887	20540	0.00058	5	14355	43	1649	91404	0.00046	6	18026
14	1303	21843	0.00060	5	14091	44	1458	92862	0.00046	6	17888
15	3021	24864	0.00056	5	14778	45	839	93701	0.00047	6	17639
16	1616	26480	0.00057	5	14690	46	631	94332	0.00048	6	17364
17	5739	32219	0.00050	6	16757	47	937	95269	0.00048	6	17155
18	10498	42717	0.00040	7	20911	48	1861	97130	0.00048	6	17118
19	2099	44816	0.00040	7	20720	49	1095	98225	0.00049	6	16950
20	5051	49867	0.00038	7	21740	50	2009	100234	0.00049	6	16768
21	501	50368	0.00040	7	20861	51	2992	103226	0.00048	6	16923
22	2221	52589	0.00040	7	20743	52	3810	107036	0.00048	7	17204
23	2162	54751	0.00040	7	20615	53	296	107332	0.00048	6	16919
24	914	55665	0.00041	7	20047	54	980	108312	0.00049	6	16752
25	2351	58016	0.00041	7	20023	55	625	108937	0.00050	6	16536
26	414	58430	0.00043	7	19360	56	901	109838	0.00050	6	16370
27	998	59428	0.00044	7	18933	57	10171	120009	0.00047	7	17567
28	920	60348	0.00045	6	18514	58	614	120623	0.00047	7	17347
29	2937	63285	0.00044	7	18721	59	296	120919	0.00048	6	17089
30	3744	67029	0.00043	7	19145	60	1097	122016	0.00048	7	16930

dotted lines are the estimated control limits; the two straight lines are the control limits (after using the adjustment factor) with $p_0 = 0.0005$ and $\alpha = 0.0027$. From the CCC chart shown in Figure 3.4, it is clear that the process is in control and both the control limits and $\bar{p}$ converges to the true values.

In order to see the effectiveness of the chart in detecting process deterioration, the last 30 data in Table 3.8 are replaced with another 30 process observations simulated with $p = 0.005$ as shown in Table 3.9. These 'deteriorated' process observations are plotted in Figure 3.5.
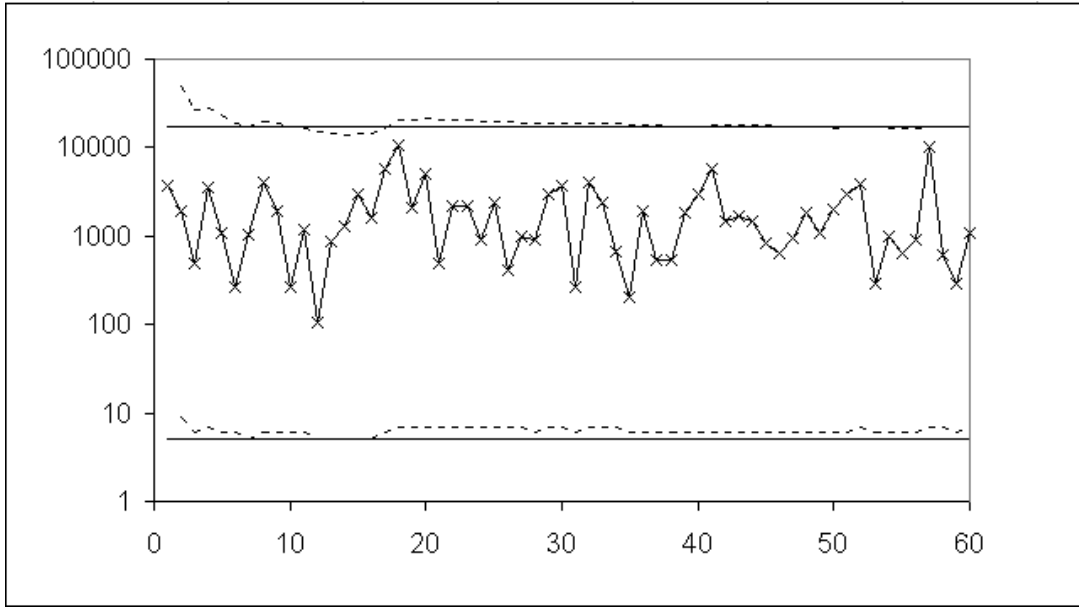
Figure 3.4: CCC chart with estimated control limits, using the simulated data (dotted lines: control limits from proposed scheme; solid straight lines: control limits with known parameters).

From Figure 3.5, the 41st observation is plotted below LCL as well as the estimated LCL, LCL_{ϕ_m}, indicating that the process is out of control; both sets of control limits (known parameter and estimated) detect the process deterioration at the same time.

Table 3.9: The simulated data from geometric distribution for $m = 31$ to 60 with $p = 0.005$.

m	x	$\sum x$	$\bar{p}$	LCL_{ϕ_m}	UCL_{ϕ_m}	m	x	$\sum x$	$\bar{p}$	LCL_{ϕ_m}	UCL_{ϕ_m}
31	143	67172	0.00045	6	18547	46	37	69628	0.00065	5	12815
32	206	67378	0.00046	6	18003	47	829	70457	0.00065	5	12686
33	258	67636	0.00047	6	17507	48	458	70915	0.00066	5	12497
34	8	67644	0.00049	6	16979	49	148	71063	0.00068	5	12262
35	34	67678	0.00050	6	16487	50	831	71894	0.00068	5	12026
36	394	68072	0.00051	6	16110	51	25	71919	0.00070	5	11789
37	189	68261	0.00053	6	15705	52	315	72234	0.00071	5	11609
38	491	68752	0.00054	6	15391	53	119	72353	0.00072	5	11404
39	116	68868	0.00055	6	15011	54	35	72388	0.00073	5	11194
40	20	68888	0.00057	5	14630	55	9	72397	0.00075	5	10988
41	3	68891	0.00058	5	14265	56	301	72698	0.00076	5	10833
42	218	69109	0.00059	5	13961	57	78	72776	0.00077	5	10651
43	327	69436	0.00060	5	13693	58	347	73123	0.00078	5	10514
44	68	69504	0.00062	5	13388	59	42	73165	0.00079	5	10339
45	87	69591	0.00063	5	13100	60	482	73647	0.00080	5	10217
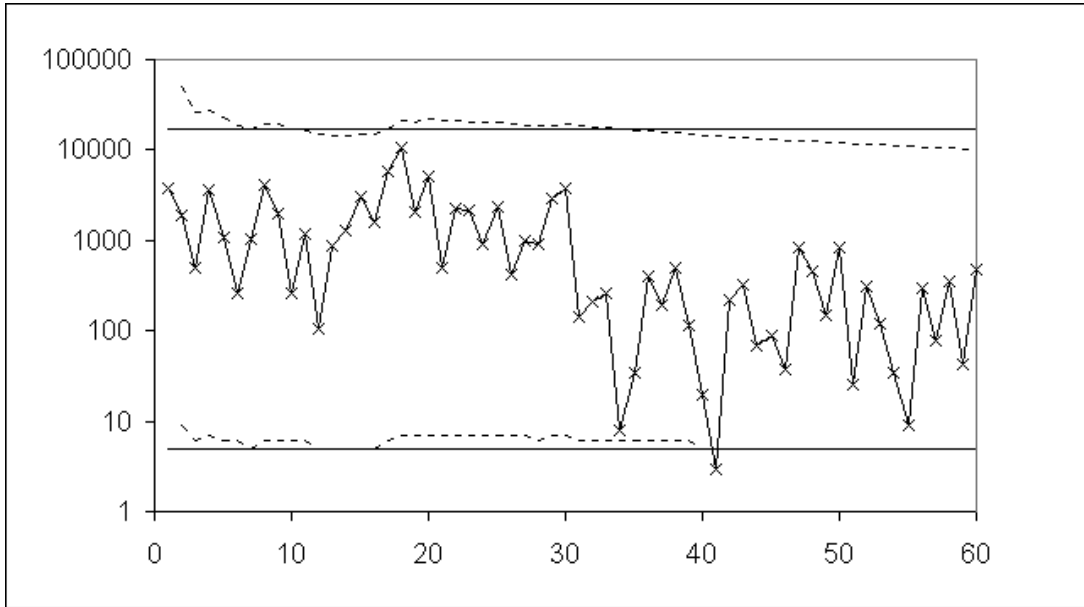
Figure 3.5: CCC chart with estimated control limits, using the out-of-control simulated data from Table 3.9.

3.7   Conclusion

In this Chapter, we propose a CCC scheme in which the estimate as well as the control limits are sequentially updated according to the number of nonconforming items observed, m. The performance of the chart in terms of its false alarm rate and the run length properties is investigated. The strength of the proposed scheme is that the behaviour of ARL is identical to other known-parameter Shewhart chart in that the in-control ARL is tuned to 370 (or other preferred values) and decreases monotonically whenever there is a change in process parameter. Numerical results suggest that the performance of the chart is comparable with that of the known value CCC chart.

Chapter 4

Establishing CCC Charts

Current work on CCC chart (see Chapter 2), including the scheme presented in previous chapter, has yet to provide a systematic treatment for establishing the chart particularly when the parameter is estimated. Though Yang *et al.* [115] studied the effects of parameter estimation on the CCC chart and previous chapter has proposed a sequential estimation scheme, which performs well even when compared to the known value CCC chart, a systematic framework for establishing the CCC chart under different ways of estimating p has not been presented. For example, to implement the CCC chart using the scheme presented in Chapter 3, one must know when to stop updating the estimate of p so that the control limits are not affected by data from drifted processes. If p is estimated using Yang *et al.*'s [115] scheme, the initial sample size must also be specified.

In this chapter, the results from previous chapter and by Yang *et al.* [115] are extended, so that engineers are able to construct the CCC chart under different sampling and estimation conditions. Some procedures for constructing the CCC chart when the process fraction nonconforming is given, when it is estimated

sequentially, and when it is estimated with a fixed sample size are proposed.

In the following, the statistical properties for some of the recent studies on CCC charts are revisited. This is followed by guidelines for establishing CCC charts for schemes presented in previous chapter as well as the scheme proposed by Yang *et al.* [115]. Numerical examples and simulation studies for designing CCC charts are presented for both cases when process fraction nonconforming, *p*, is given or unknown to illustrate the applicability of the proposed guidelines.

4.1 Recent Studies on CCC Chart - Revisited

Here, some of the recent studies on CCC chart such as the adjustment factor proposed by Xie *et al.* [105] which discussed in Section 2.3.1.3, the effects on parameter estimation studied by Yang *et al.* [115] and the control scheme presented in previous chapter are revisited.

4.1.1 Adjustment Factor, γ

In CCC charts, the control limits are determined based on the probability limits from the geometric model given in Equation (2.1). For a given probability of type I error, α, the two-sided control limits are given by Equations (3.20) and (3.21),

$$
\begin{aligned}
UCL &= \frac{\ln \alpha/2}{\ln(1 - p_0)} \\
LCL &= \frac{\ln(1 - \alpha/2)}{\ln(1 - p_0)} + 1
\end{aligned}
$$

where p_0 is the in-control fraction nonconforming (see Section 2.2.1). The resulting ARL initially increases when the process starts to deteriorate (*p* increases) and

decreases after attaining a maximum point at $p > p_0$. It renders the CCC chart rather insensitive in detecting increase in p and may lead to the misinterpretation that the process is well in control, or has been improved (see discussions Section 2.3.1.3).

Xie *et al.* [105] showed that, for a given p_0 and the initial type I error rate ϕ, adjustment factor, γ_ϕ, shown in Equation (2.11) is

$$\gamma_\phi = \frac{\ln\left[\frac{\ln(1-\phi/2)}{\ln(\phi/2)}\right]}{\ln\left[\frac{(\phi/2)}{(1-\phi/2)}\right]}$$

can be applied on the control limits; i.e.,

$$UCL_{\gamma_\phi} = \frac{\ln \phi/2}{\ln(1-p_0)}\gamma_\phi \tag{4.1}$$

$$LCL_{\gamma_\phi} = \left(\frac{\ln(1-\phi/2)}{\ln(1-p_0)}\right)\gamma_\phi + 1 \tag{4.2}$$

so that the ARL is maximized at $p = p_0$. It should be noted that the above control limits do not have a direct probability interpretation; i.e., they do not always give the same probability content within the control limits. Notably, even though the control limits are shifted by the same factor of γ_ϕ, the type I risk of the chart is no longer given by the initial value ϕ. Moreover, the false alarm probabilities beyond both sides of the control limits are no longer the same. The adjusted control limits with equal probabilities are considered by Zhang *et al.* [119]. However, their proposed procedure involves several iterations and only considers known p.

The actual type I risk α_0 needs to be re-computed by summing up the tail probabilities $\alpha_u = P\{X > UCL_{\gamma_\phi}\}$ and $\alpha_l = P\{X < LCL_{\gamma_\phi}\}$, where X is the number of conforming items between two adjacent nonconforming items. From

Equations (4.1) and (4.2), we have

$$\alpha_u = (1 - p_0)^{\frac{\ln(\phi/2)\gamma_\phi}{\ln(1-p_0)}} \quad \text{and} \quad \alpha_l = 1 - (1 - p_0)^{\frac{\ln(1-\phi/2)\gamma_\phi}{\ln(1-p_0)}}.$$

which by using some algebraic manipulations, can be simplified as

$$\alpha_u = (\phi/2)^{\gamma_\phi} \quad \text{and} \quad \alpha_l = 1 - (1 - \phi/2)^{\gamma_\phi} \tag{4.3}$$

respectively. It follows that

$$\alpha_0 = \alpha_u + \alpha_l = (\phi/2)^{\gamma_\phi} - (1 - \phi/2)^{\gamma_\phi} + 1. \tag{4.4}$$

As a result, the actual type I risk, α_0 is a non-linear function of ϕ and despite apparent relation between ϕ and p_0 in Equations (4.1) and (4.2), they are in fact independent of each other.

4.1.2 CCC Scheme with Estimated Parameter

In most circumstances, p_0 is not likely to be known and needs to be estimated. A sequential estimation scheme is presented in previous chapter, while the conventional binomial estimator of p used for the CCC scheme is considered by Yang *et al.* [115].

4.1.2.1 Sequential Estimation Scheme

The scheme presented in previous chapter use the unbiased estimator of p given in Equation (3.2)

$$\bar{p} = \frac{m - 1}{N_m - 1}$$

which the number of nonconforming items to be observed, m, is fixed *a priori* and the total number of samples to be inspected, N_m, is a random variable.

In the proposed scheme in Chapter 3, $\bar{p}$ is updated sequentially and the control limits are revised so that not only the in-control ARL of the chart can be kept to the desired value, but it is also the peak of the ARL curve. The control limits are given in Equations (3.20) and (3.21) as:

$$
\begin{aligned}
UCL_{\phi_m} &= \frac{\ln(\phi_m/2)}{\ln(1-(m-1)/(N_m-1))} \times \gamma_{\phi_m} \\
LCL_{\phi_m} &= \left(\frac{\ln(1-\phi_m/2)}{\ln(1-(m-1)/(N_m-1))}\right)\gamma_{\phi_m} + 1
\end{aligned}
$$

where ϕ_m can be obtained by solving Equation (3.18):

$$
\sum_{n=m}^{\infty} \left((1-\bar{p})^{\frac{\ln(\phi_m/2)\gamma_{\phi_m}}{\ln(1-\bar{p})}} - (1-\bar{p})^{\frac{\ln(1-\phi_m/2)\gamma_{\phi_m}}{\ln(1-\bar{p})}} + 1\right)^{-1} \binom{n-1}{m-1} \bar{p}^m (1-\bar{p})^{n-m} = \tau
$$

with $\bar{p}$ given by Equation (3.2) and γ_{ϕ_m} given by Equation (2.11).

Using similar steps proceeding Equation (4.4), it can be further prove that ϕ_m is independent of $\bar{p}$. In addition, in Chapter 3, by using an example of $ARL_0 = 370$, it has been shown that as m increases, the sensitivity of the chart improves and approaches that with known process parameter. For convenience, we use an index, ρ, which is a factor reflecting the shift in process parameter; i.e., $p = \rho p_0$. If $\rho = 1$, then the process is statistically in-control; otherwise, when $\rho > 1$, the process is deteriorating, while $\rho < 1$ indicates that the process is improving.

Using the Equation (3.22) given in previous chapter, Figure 4.1 depicts the ARL curves of the CCC scheme under sequential estimation, using $m = 5, 10, 30$ and 50, for $\tau = 370$ and $p_0 = 500$ppm.
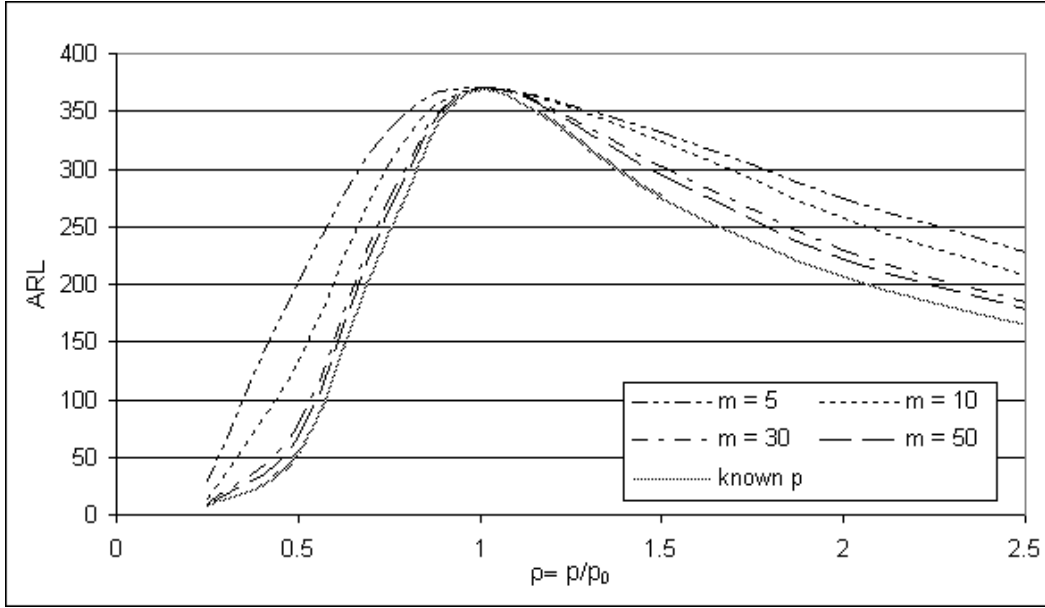
Figure 4.1: ARL under sequential estimation with $m = 5, 10, 30$ and 50, given $\tau = 370$ and p_0 (500ppm).

4.1.2.2 Conventional Estimation Scheme

On the other hand, Yang *et al.* [115] considered using the conventional estimator of p, given in Equation (3.1):

$$\hat{p} = \frac{D_n}{n}$$

where n is the initial sample size that is fixed *a priori* and D_n is the number of nonconforming items among n items sampled.

Yang *et al.* [115] investigated the sample size effect and presented the exact false alarm probability equation when p_0 needs to be estimated using the conventional estimator. By using the exact false alarm probability equation given by Yang *et al.* [115], a similar adjustment scheme proposed in Chapter 3 for sequential estimation can also be applied so that the τ is maximum point of the ARL curve. With the

adjustment, the equation becomes

$$\sum_{d=0}^{n} \left((1-\hat{p})^{\frac{\ln(\phi_n/2)\gamma_{\phi_n}}{\ln(1-\hat{p})}} - (1-\hat{p})^{\frac{\ln(1-\phi_n/2)\gamma_{\phi_n}}{\ln(1-\hat{p})}} + 1 \right)^{-1} \binom{n}{d} \hat{p}^d (1-\hat{p})^{n-d} = \tau \quad (4.5)$$

and the control limits become

$$UCL_{\phi_n} \quad = \quad \frac{\ln(\phi_n/2)}{\ln(1-(D_n/n))} \times \gamma_{\phi_n} \quad (4.6)$$

$$LCL_{\phi_n} \quad = \quad \left(\frac{\ln(1-\phi_n/2)}{\ln(1-(D_n/n))} \right) \gamma_{\phi_n} + 1 \quad (4.7)$$

where ϕ_n could be obtained from solving Equation (4.5), with $\hat{p}$ given in Equation (3.1), and γ_{ϕ_n} from Equation (2.11), after specifying τ.
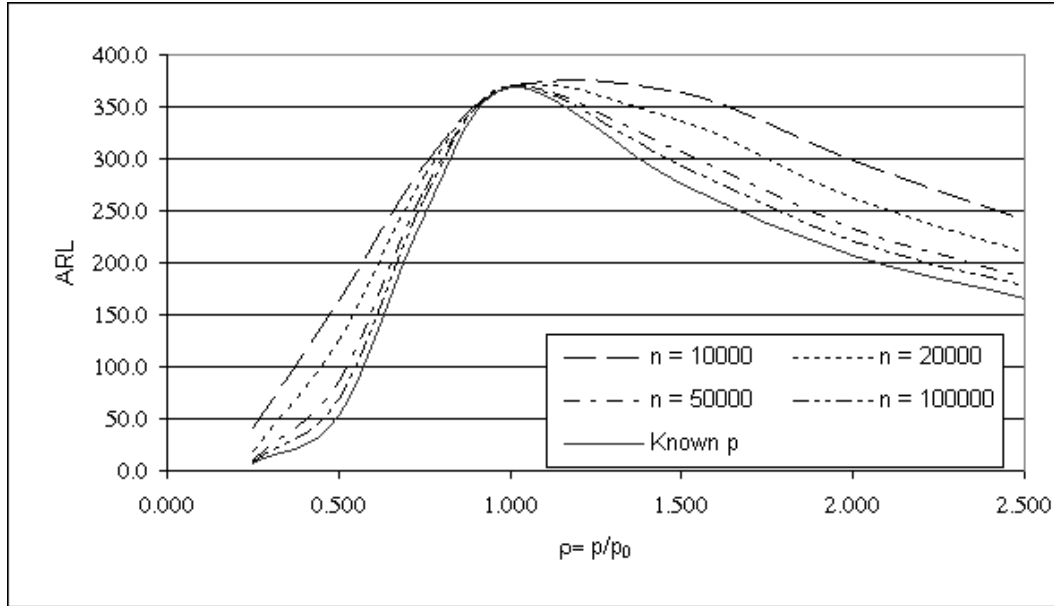
Figure 4.2: ARL for known p (500ppm), $n = 10000, 20000, 50000,$ and 100000, using conventional estimator with τ set at 370 and $\hat{p} = 0.0005$.

From the study of Yang *et al.* [115], the larger the sample size used in estimating p_0, the closer the chart performs to the one with known parameter. Thus, it is expected that the performance of the scheme proposed here approaches the one with known p_0, as the sample size used to estimate p_0 increases. For illustration, Figure

70

4.2 shows the ARL curves for known p_0, $n = 10000, 20000, 50000,$ and 100000, using the proposed scheme, with τ set at 370 and $\hat{p} = 0.0005$, for the case where the conventional estimator is used.

4.2   Constructing CCC Chart

When monitoring a process with given p_0, the control limits can easily be computed from Equations (4.1) and (4.2).

The ARL_0 of the CCC chart is the average number of points plotted within the control limits while the process is indeed in statistical control, which is the reciprocal of α_0, and independent of p_0 (from the derivation of Equation (4.4)). After specifying the preferred ARL_0 of the control scheme, the parameter ϕ can be obtained by solving

$$\frac{1}{\left((\phi/2)^{\gamma_\phi} - (1 - \phi/2)^{\gamma_\phi} + 1\right)} = \tau. \tag{4.8}$$

where γ_ϕ is a function of ϕ given by Equation (2.11). The corresponding control limits can then be easily computed. Table 4.1 gives the values of ϕ and the respective γ_ϕ with different ARL_0 when p_0 is given. These values of ϕ and γ_ϕ can be substituted into Equations (4.1) and (4.2) to determine the control limits for the CCC chart.

Table 4.1: The values of ϕ and respective adjustment factor γ_ϕ, with different ARL_0.

τ	ϕ	γ_ϕ
200	0.00675	1.30603
370	0.00373	1.29269
500	0.00278	1.28653
750	0.00188	1.27864
1000	0.00142	1.27327

4.2.1 Establishing CCC Chart with Sequential Estimator

In an industrial setting where inspections are carried out sequentially, parameter estimation as well as process monitoring can be started once there are two nonconforming items observed ($m = 2$). Control limits can be calculated from Equations (3.20) and (3.21) with ϕ_m based on the required ARL_0 from Equation (3.18). The adjustment factor, γ_{ϕ_m} can be obtained from Equation (2.11).

Table 4.2 gives the values of ϕ_m and the respective adjustment factor γ_{ϕ_m}, for different values of m ranging from 2 to 100 and $\tau(= 200, 370, 500, 750, 1000)$. The last row of the table ($m = \infty$) is the value where p_0 is given, which is ϕ from Table 4.1. Similar to the case when p_0 is given, it has been noted in Section 3.5 that when p is estimated sequentially, it has no effect on ϕ_m, and ϕ_m converges to that of the known value chart as m increases.

To start using the CCC chart without undue delay, it is recommended that p_0 be estimated using $m = 2$ and be sequentially updated as long as the process is deemed to be in statistical control. Two associated problems are that the ARL performance in detecting process shift is poor for small m, and that excessive updating increases the risk of including data from drifted processes. To mitigate these problems, we

Table 4.2: The values of ϕ_m and γ_ϕ for different m and preferred τ for CCC scheme with sequential sampling plan.

ARL	200		370		500		750		1000	
m	ϕ_m	γ_{ϕ_m}	ϕ_m	γ_{ϕ_m}	ϕ_m	γ_{ϕ_m}	ϕ_m	γ_{ϕ_m}	ϕ_m	γ_{ϕ_m}
2	0.00363	1.2921	0.00196	1.2795	0.00145	1.2737	0.00097	1.2663	0.00073	1.2613
3	0.00424	1.2955	0.00229	1.2826	0.00169	1.2767	0.00113	1.2691	0.00085	1.2640
4	0.00459	1.2972	0.00248	1.2842	0.00183	1.2782	0.00122	1.2705	0.00092	1.2654
5	0.00483	1.2984	0.00261	1.2852	0.00193	1.2792	0.00129	1.2715	0.00097	1.2663
6	0.00501	1.2992	0.00271	1.2860	0.00201	1.2800	0.00134	1.2722	0.00100	1.2669
7	0.00516	1.2998	0.00279	1.2866	0.00207	1.2805	0.00138	1.2728	0.00103	1.2675
8	0.00528	1.3004	0.00286	1.2871	0.00212	1.2810	0.00141	1.2732	0.00106	1.2679
9	0.00538	1.3008	0.00292	1.2875	0.00216	1.2814	0.00144	1.2736	0.00108	1.2683
10	0.00547	1.3012	0.00297	1.2879	0.00220	1.2818	0.00147	1.2739	0.00110	1.2686
20	0.00595	1.3031	0.00325	1.2897	0.00241	1.2836	0.00161	1.2757	0.00121	1.2704
30	0.00617	1.3039	0.00337	1.2906	0.00251	1.2844	0.00168	1.2765	0.00127	1.2712
50	0.00638	1.3047	0.00349	1.2913	0.00260	1.2852	0.00175	1.2773	0.00132	1.2719
70	0.00647	1.3050	0.00355	1.2917	0.00265	1.2855	0.00178	1.2776	0.00134	1.2723
100	0.00655	1.3053	0.00360	1.2920	0.00269	1.2858	0.00181	1.2779	0.00136	1.2725
∞	0.00675	1.3060	0.00373	1.2927	0.00278	1.2865	0.00188	1.2786	0.00142	1.2733

propose a two-prong approach. First, a target ARL performance for a given change in p is specified, so that the updating is terminated at a particular m; and more stringent criteria are used to decide whether updating should be suspended, which will be discussed in the following.

4.2.1.1 Termination of Sequential Updating

For a given change in p, which can be indexed by $\rho = p/p_0$, define R_s as the ratio between a desired ARL, ARL_m, and the ARL with known parameter ARL_∞. In other words,

$$R_s = \frac{ARL_m}{ARL_\infty} \tag{4.9}$$

where the values of ARL_m can be calculated from Equation (3.22) with respective values of ρ and m, and ARL_∞ is the out-of-control ARL with respect to ρ for a

given p_0, given by

$$ARL_\infty = \frac{1}{\left((1 - \rho p_0)^{UCL} + 1 - (1 - \rho p_0)^{LCL-1}\right)} \qquad (4.10)$$

The choice of R_s reflects the user's desirability of having a CCC chart that performs close to the ideal case. When the ratio $R_s \to 1$, the performance of the scheme is comparable with that of a known parameter CCC chart.

For a given ρ and ARL_0, Table 4.3 gives the corresponding m required, m^*, in achieving the desired R_s. For example, if the user would like to establish a CCC chart with ARL_0 set at 200, and the required ARL performance at $\rho \geq 2$ is given by $R_s = 1.150$, then, from Table 4.3, one should keep updating the estimate of p and the control limits up to $m = 19$, as long as the following suspension rule is not violated.

4.2.1.2 Suspension of Sequential Update

The updating must be done judiciously to avoid using the contaminated data from drifted processes, which will affect the sensitivity of the control scheme. To mitigate this problem, we impose a more stringent criterion than the usual out-of-control rule for the suspension of sequential estimation.

Two decision lines correspond to the 5th and 95th percentile points are used to create a warning zone. Figure 4.3 shows the warning zones of the CCC chart (the unshaded areas in the chart). The center line of the graph is the 50th percentile of the cumulative distribution function (CDF) and is given by

$$CL = \frac{\ln 0.5}{\ln(1 - \bar{p})} + 1 = -\frac{0.693}{\ln(1 - \bar{p})} + 1. \qquad (4.11)$$

Table 4.3: The values of m^* for different ρ and ARL_0= 200, 370, 500, 750, and 1000

R_s	$\rho = 0.25$	$\rho = 0.50$	$\rho = 0.75$	$\rho = 1.50$	$\rho = 2.00$	$\rho = 2.50$
	$ARL_0 = 200$					
1.100	50	105	29	25	27	29
1.125	48	84	21	18	23	23
1.150	40	71	17	14	19	19
1.175	30	61	14	6	16	16
1.200	27	61	10	2	13	14
1.225	24	49	9	2	10	11
1.250	22	44	7	2	8	9
	$ARL_0 = 370$					
1.100	55	126	40	29	35	35
1.125	45	104	28	20	26	27
1.150	39	87	22	17	20	20
1.175	33	75	18	10	17	18
1.200	30	66	16	2	15	16
1.225	27	60	14	2	12	13
1.250	25	54	10	2	10	11
	$ARL_0 = 500$					
1.100	58	130	43	30	34	36
1.125	48	110	31	23	27	27
1.150	40	93	25	18	21	22
1.175	35	81	20	14	18	19
1.200	31	72	17	7	16	16
1.225	28	64	15	6	13	14
1.250	26	59	13	6	10	12
	$ARL_0 = 750$					
1.100	63	141	49	35	37	13
1.125	51	123	40	27	30	15
1.150	44	106	30	20	24	17
1.175	38	92	25	17	19	20
1.200	34	81	21	10	17	24
1.225	33	73	18	7	14	30
1.250	28	66	16	7	12	40
	$ARL_0 = 1000$					
1.100	66	145	55	36	39	40
1.125	54	131	44	26	30	30
1.150	46	115	32	21	25	25
1.175	40	99	28	17	20	21
1.200	36	88	23	14	18	18
1.225	32	78	20	8	15	16
1.250	30	71	18	8	14	14

and the two decision lines are given by

$$UDL = \frac{\ln(0.05)}{\ln(1 - \bar{p})} \qquad \text{and} \qquad LDL = \frac{\ln(1 - 0.05)}{\ln(1 - \bar{p})} + 1$$
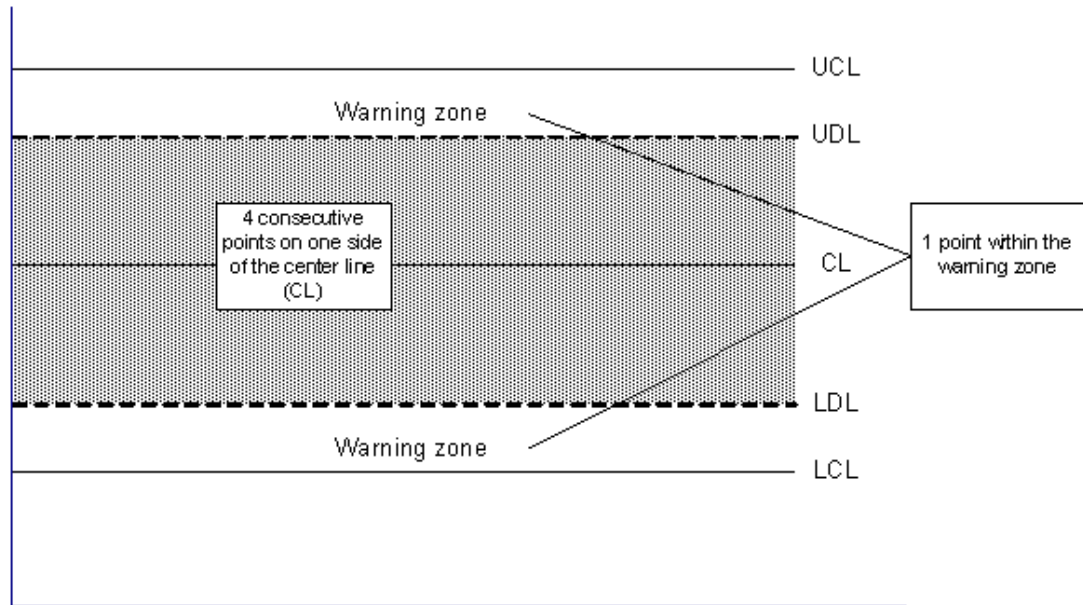
Figure 4.3: Warning zones of the CCC chart.

The updating is suspended after observing any one of the following:

1. One point beyond the shaded area which will occur with probability 0.05 (*alternatively, a points with probability a* $\times$ *0.05*).

2. Four consecutive points plot on one side of center line (CL) which will occur with probability 0.0625 (*alternatively, b consecutive points with probability* $b \times 0.5$).

These rules are simple to implement and provide adequate protection against using contaminated data for updating. The number of points used in the suspension rules can be change accordingly with the probability given above. Following the suspension, process monitoring should be continued without revising the control limits. A new sequential estimate of p is then initiated until the same value of m before suspension occurs. If there is no significant difference ($< 10\%$) between

the two estimates, all data can then be combined to give the estimate of p and

updating is continued until $m = m^*$ provided that the process remains in control.

If another suspension criterion is observed during this period, the same decision

process is repeated.

4.2.2 Establishing CCC Chart with Conventional Estimator

When the conventional estimator of p is used, the control limits of the CCC chart

can be obtained from Equations (4.6) and (4.7) after estimating p_0 from the initial

sample. Similarly, to achieve the desired ARL_0, ϕ_n and γ_n can be obtained from

Equations (4.5) and (2.11) respectively, given the sample size n and $\hat{p}$.

Table 4.4: The values of ϕ_n for different n and $\hat{p}$ with $ARL_0 = 370$ for CCC scheme using Binomial sampling plan.

$n \setminus \hat{p}$	0.0001	0.0002	0.0003	0.0004	0.0005	0.0006	0.0007	0.0008	0.0009	0.0010
10000	0.00148	0.00192	0.00222	0.00242	0.00257	0.00268	0.00277	0.00284	0.00291	0.00296
20000	0.00192	0.00242	0.00268	0.00284	0.00296	0.00305	0.00311	0.00317	0.00321	0.00325
50000	0.00257	0.00296	0.00314	0.00325	0.00333	0.00338	0.00342	0.00345	0.00348	0.00350
100000	0.00296	0.00325	0.00338	0.00345	0.00350	0.00353	0.00356	0.00358	0.00359	0.00360
200000	0.00325	0.00345	0.00353	0.00358	0.00360	0.00362	0.00364	0.00364	0.00366	0.00366
300000	0.00338	0.00353	0.00359	0.00362	0.00364	0.00366	0.00367	0.00367	0.00368	0.00368
400000	0.00345	0.00358	0.00362	0.00365	0.00366	0.00367	0.00368	0.00369	0.00369	0.00369
500000	0.00350	0.00360	0.00364	0.00366	0.00367	0.00368	0.00369	0.00369	0.00370	0.00370
600000	0.00353	0.00362	0.00366	0.00367	0.00368	0.00369	0.00369	0.00370	0.00370	0.00370
700000	0.00356	0.00364	0.00367	0.00368	0.00369	0.00369	0.00370	0.00370	0.00370	0.00371
800000	0.00358	0.00365	0.00367	0.00369	0.00369	0.00370	0.00370	0.00370	0.00371	0.00371
900000	0.00359	0.00366	0.00368	0.00369	0.00370	0.00370	0.00370	0.00371	0.00371	0.00371
1000000	0.00360	0.00366	0.00368	0.00369	0.00370	0.00370	0.00371	0.00371	0.00371	0.00371
2000000	0.00366	0.00369	0.00369	0.00371	0.00371	0.00371	0.00372	0.00372	0.00372	0.00372
∞	0.00373	0.00373	0.00373	0.00373	0.00373	0.00373	0.00373	0.00373	0.00373	0.00373

To facilitate the construction of the CCC chart, Table 4.4 gives the values of

ϕ_n for different n and $\hat{p}$ ranging from 0.0001 to 0.001, with $ARL_0 = 370$, when p_0

is estimated using the conventional estimator. The last row of the table ($n = \infty$)

is the value where p_0 is given, which is ϕ from Table 4.1. As expected, the value

of ϕ_n approaches ϕ as the sample size increases. The values given in this table can

be used as the input for constructing the CCC chart if the desired ARL_0 is 370. Unlike Tables 4.1 and 4.2, these ϕ_n values are dependent on $\hat{p}$.

It also worth noting that in adopting the conventional estimation there can be no nonconforming items in the initial sample. This will lead to a situation where sample size is increased incrementally until some arbitrary number of nonconforming items are observed. In doing so, the resulting estimate of p_0 will be biased (see Girshick [25]). A simple way of avoiding this problem is to ensure that the probability of having at least one nonconforming item is sufficiently large in the initial sample. For example, the sample size for a preliminary guess value of $p_0 = 100$ ppm and a 90% chance of observing at least one non-conforming item can be obtained as the following:

$$n = \frac{\ln(0.1)}{\ln(1 - p_0)} \approx 23,000$$

Nevertheless, Yang *et al.* [115] concluded that the sample size used for estimation should be large enough for better performance of the chart which is evident from Figure 4.2. An updating scheme similar to that of the sequential estimate can be adopted.

Define the ratio of the ARL, R_c as

$$R_c = \frac{ARL_n}{ARL_\infty} \tag{4.12}$$

where ARL_n is the ARL in detecting process shift by a factor of ρ, when a total sample of size n is used for estimating p, and the ARL_∞ is the ARL with known parameter.

Once ARL_0 is specified, for a given $\hat{p}$ (from initial estimate) and a process shift of interest indexed by ρ, the minimum sample size needed, n^* to achieve a certain R_c requirement can be determined. Table 4.5 gives the values of R_c for different ρ and n, with $ARL_0 = 370$ for $\hat{p} = 0.0005$. For example, given the estimated value $\hat{p} = 0.0005$, for ARL_0 specified at 370, and assuming that the required ARL performance at $\rho \leq 0.25$ is given by $R_c = 1.150$, the updating of estimate as well as the control limits is continued until the total number of sample inspected equals to n^*, which is 100,000 for this case, provided that the process remains in control.

Table 4.5: The values of R_c for different ρ, and n, with $ARL_0 = 370$ for $\hat{p} = 0.0005$.

				ρ			
n	0.25	0.50	0.75	1.50	2.00	2.50
10000	5.446	3.021	1.198	1.319	1.433	1.455
20000	2.529	2.323	1.156	1.217	1.26	1.264
50000	1.293	1.584	1.098	1.112	1.122	1.122
100000	1.118	1.279	1.064	1.063	1.067	1.067
1000000	1.011	1.025	1.01	1.008	1.008	1.008

4.3   An Illustrative Example

To illustrate the applicability of the proposed guidelines, numerical examples are presented here. In addition, the simulation studies are carried out to compare the effectiveness of the schemes with those known parameter scheme.

Here, the examples based on data in Table 4.6 taken from Table 1 in Xie *et. al.* [114] are presented. From the table, the first 20 data points are simulated from $p = 500$ ppm, after which the data is from $p = 50$ ppm.

Assuming that p_0 is given, the control limits of the chart can then be calculated

Table 4.6: A Set of Data for a Simulated Process (from Table 1, Xie *et. al.* [114]).

| Nonconforming No.	CCC	Simulation legend	Nonconforming No.	CCC	Simulation legend
1	3706	$p = 500$ ppm	16	753	$p = 500$ ppm
2	9179	$p = 500$ ppm	17	3345	$p = 500$ ppm
3	78	$p = 500$ ppm	18	217	$p = 500$ ppm
4	1442	$p = 500$ ppm	19	3008	$p = 500$ ppm
5	409	$p = 500$ ppm	20	3270	$p = 500$ ppm
6	3812	$p = 500$ ppm	21	5074	Shift, $p = 50$ ppm
7	7302	$p = 500$ ppm	22	3910	$p = 50$ ppm
8	726	$p = 500$ ppm	23	23310	$p = 50$ ppm
9	2971	$p = 500$ ppm	24	11690	$p = 50$ ppm
10	42	$p = 500$ ppm	25	19807	$p = 50$ ppm
11	3134	$p = 500$ ppm	26	14703	$p = 50$ ppm
12	1583	$p = 500$ ppm	27	4084	$p = 50$ ppm
13	3917	$p = 500$ ppm	28	826	$p = 50$ ppm
14	3496	$p = 500$ ppm	29	9484	$p = 50$ ppm
15	2424	$p = 500$ ppm	30	66782	$p = 50$ ppm
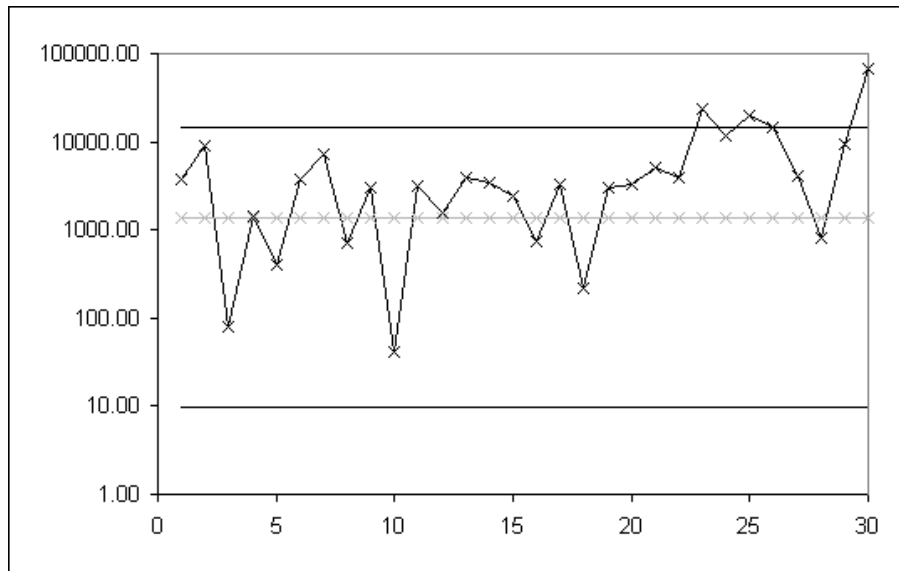
Figure 4.4: CCC chart when p_0 is known ($= 500$ ppm) and in-control ARL $= 200$.

directly, using $\phi = 0.00675$ and $\gamma_\phi = 1.30603$ (from Table 4.1). Figure 4.4 is the

CCC chart plotted, given $p_0 = 500$ ppm. From the chart, it is observed that the

chart signals at the 23rd observation, indicating the decrease in the process fraction

nonconforming, p.

Table 4.7: The values of $\bar{p}$ and the control limits with sequential estimator from Table 4.6.

No.	CCC	$\bar{p}$	LCL_{ϕ_m}	UCL_{ϕ_m}	No.	CCC	$\bar{p}$	LCL_{ϕ_m}	UCL_{ϕ_m}
1	3706	-	-	-	16	753	303 ppm	12	23023
2	9179	78 ppm	31	105092	17	3345	303 ppm	12	23189
3	78	**154** ppm	19	51689	18	217	303 ppm	12	21923
4	1442	154 ppm	19	51689	19	3008	303 ppm	12	21988
5	409	154 ppm	19	51689	20	3270	347 ppm	11	21864
6	3812	268 ppm	12	29410	21	5074	334 ppm	12	22693
7	7302	231 ppm	15	33847	22	3910	**329** ppm	13	23024
8	726	263 ppm	13	29651	23	23310	329 ppm	13	23024
9	2971	270 ppm	13	28709	24	11690	329 ppm	13	23024
10	42	**303** ppm	12	25462	25	19807	329 ppm	13	23024
11	3134	303 ppm	12	25462	26	14703	329 ppm	13	23024
12	1583	303 ppm	12	25462	27	4084	329 ppm	13	23024
13	3917	303 ppm	12	25462	28	826	329 ppm	13	23024
14	3496	303 ppm	12	25462	29	9484	329 ppm	13	23024
15	2424	303 ppm	12	25462	30	66782	329 ppm	13	22897

On the other hand, when p_0 is not given, by using the proposed scheme with sequential estimation, the estimation starts after m reaches 2 and the control limits can be obtained accordingly, with the values of ϕ_m and γ_{ϕ_m} given in Table 4.2. With ARL_0 specified at 200 (i.e., $\alpha_0 = 0.005$), $\rho \geq 2.5$, and $R = 1.1250$, m^* is 23 (from Table 4.3). Figure 4.5 gives the flow for constructing the CCC chart with sequential estimation scheme.

Table 4.7 shows the estimated p together with the control limits for sequential estimation. The CCC scheme is depicted in Figure 4.6 where the two dashed lines are the decision lines. From the chart, estimation is suspended at the third point as it is in the warning zone (beyond LDL). However, since there is no significant difference between the new sequential estimate from the subsequent data with $m = 3$ (104 ppm) and the estimate before suspension (154 ppm), all data are combined. Estimation is suspended again at No.10 and for similar reason, the
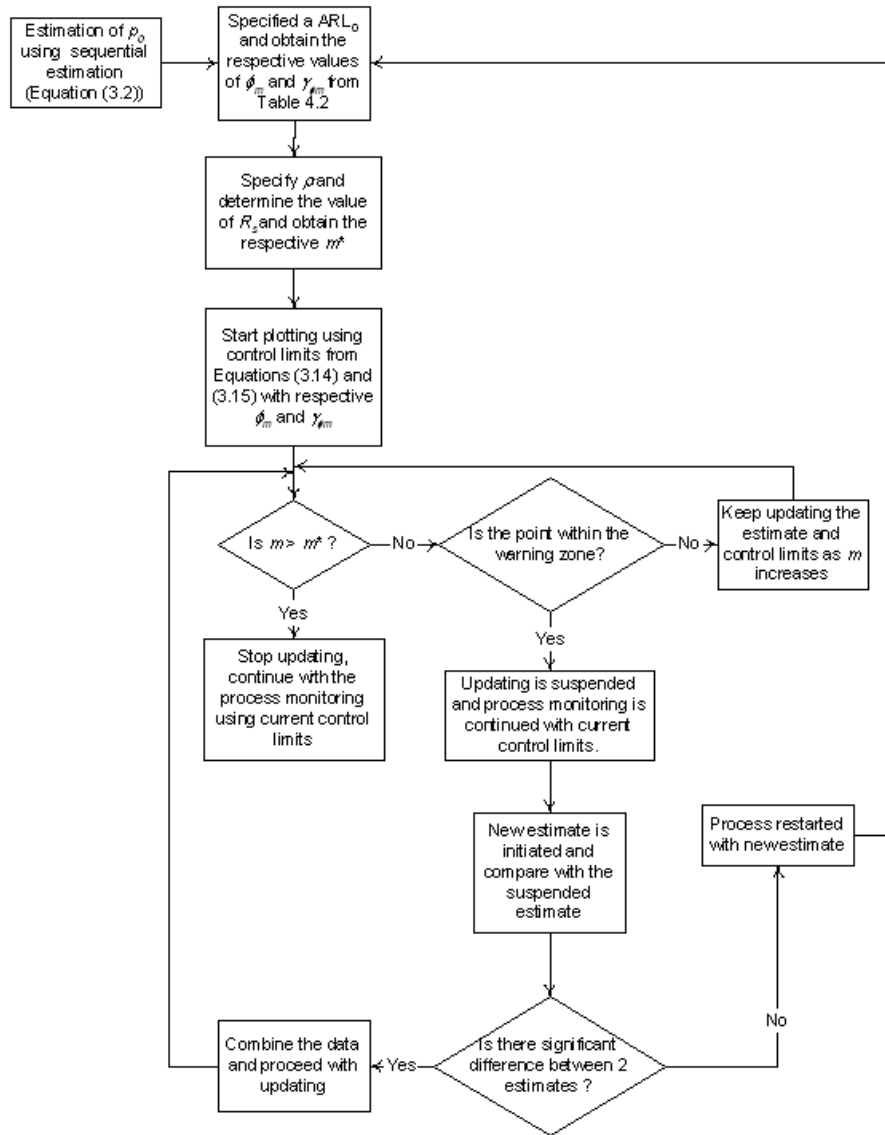
81

Figure 4.5: Flow Chart for Constructing CCC Control Chart with Sequential Estimation.

estimation is resumed at No.20. At No.22, as there are four consecutive points plotted above the center line, estimation is suspended again. The 23rd observation is plotted above the UCL, indicating possible process improvement. Thus, by using the proposed sequential estimation scheme with the guidelines given, the CCC chart with estimated parameter is as effective as that constructed assuming known p in
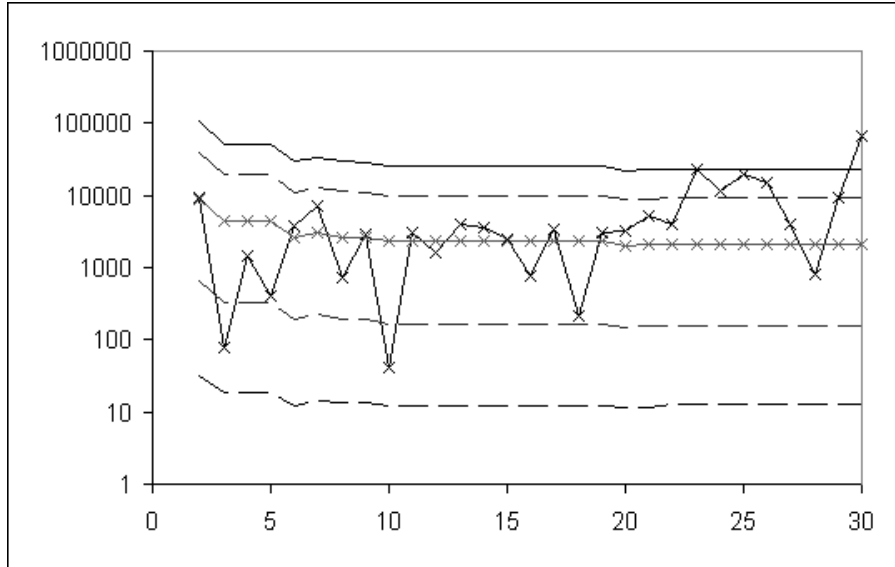
detecting a change in p.

Figure 4.6: CCC chart under sequential estimation scheme simulated from initial $p_0 = 500$ ppm and $ARL_0 = 200$.

If conventional estimate is used, $\hat{p}$ is 300 ppm, for an initial sample size, $n = 20,000$. With ARL_0 specified at 200, $\rho \geq 2.5$, and $R_c = 1.170$, $n^* = 50,000$ (obtained by using Equations (4.5) and (4.12)). Table 4.8 gives the values of the estimates together with the control limits. The estimate is updated once when the sample size collected reaches 50,000, which is 18th observation in Table 4.8, as there is no out of control signal observed between the 7th and 18th plotted points. The flow chart for constructing the CCC chart with conventional estimation is shown in Figure 4.8 in the following section.

This CCC scheme is depicted in Figure 4.7. The 23rd observation is plotted above the UCL, indicating a possible process improvement. Thus, by using this proposed scheme, the CCC chart is also able to detect a change in p.

Table 4.8: The values of $\hat{p}$ and the control limits with conventional estimator from Table 4.6.

| No.	CCC	$\hat{p}$	LCL_{ϕ_n}	UCL_{ϕ_n}	No.	CCC	$\hat{p}$	LCL_{ϕ_n}	UCL_{ϕ_n}
1	3706	-	12	25965	16	753	300 ppm	12	25965
2	9179	-	12	25965	17	3345	300 ppm	12	25965
3	78	-	12	25965	18	217	**360** ppm	12	21081
4	1442	-	12	25965	19	3008	360 ppm	12	21081
5	409	-	12	25965	20	3270	360 ppm	12	21081
6	3812	**300** ppm	12	25965	21	5074	360 ppm	12	21081
7	7302	300 ppm	12	25965	22	3910	360 ppm	12	21081
8	726	300 ppm	12	25965	23	23310	360 ppm	12	21081
9	2971	300 ppm	12	25965	24	11690	360 ppm	12	21081
10	42	300 ppm	12	25965	25	19807	360 ppm	12	21081
11	3134	300 ppm	12	25965	26	14703	360 ppm	12	21081
12	1583	300 ppm	12	25965	27	4084	360 ppm	12	21081
13	3917	300 ppm	12	25965	28	826	360 ppm	12	21081
14	3496	300 ppm	12	25965	29	9484	360 ppm	12	21081
15	2424	300 ppm	12	25965	30	66782	360 ppm	12	21081
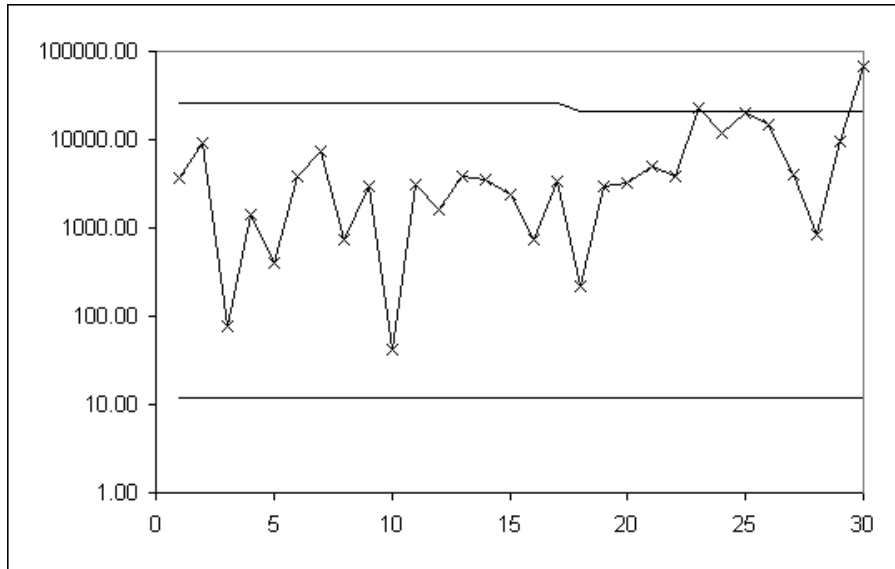
Figure 4.7: CCC chart conventional estimation scheme simulated from $p_0 = 500$ ppm, and in-control ARL = 200.

The simulation studies are carried out, replicating the above numerical examples. 100 sets of simulated data (first 20 data points are from 500 ppm, followed by 10 data points from 50 ppm) are used in three control schemes, known p, sequential estimation, and conventional estimation. Table 4.9 shows the results of

the studies. Signal within 1st and 20th data point is the false alarm as the first 20 data points are simulated from 500 ppm (in-control); whereas nondetection after 30th point shows that the change in p has not been detected yet.

Table 4.9: The simulation studies for the proposed CCC control schemes.

| | | | Scheme | |
		Known p	Sequential	Conventional
Signal at	1st - 20th point	0	1	1
	21st point	45	31	39
	22nd point	29	18	28
	23rd point	13	12	15
	24th point	6	11	6
	25th point	3	8	5
	26th point	2	3	2
	27th point	1	5	2
	28th point	1	1	0
	29th point	0	3	1
Nondetection after	30th point	0	7	1

From the table, the CCC scheme with known p is able to detect the change in p within the range of first changing point and eighth point (21st point to 28th point in scheme). On the other hand, there are some false alarms as well as failures in detection in the schemes with estimated p. For sequential estimation scheme, the scheme produces 1 false alarm out of 100 simulation runs. In addition to that, due to the effects of estimation, there are 7 nondetection out of the total of 100 simulation runs. For the conventional estimation scheme, there is 1 false alarm observed as well as 1 nondetection of the change in p out of the total of 100 simulation runs. Thus, although the sequential estimation scheme is much easier to implement comparing to the conventional estimation, as all the parameters involved in establishing the control scheme is independent on the estimated p, the robustness of the conventional estimation scheme is more satisfactory.

4.4　Conclusion

In this chapter, the basic properties of CCC charts as well as CCC schemes with estimated parameters are revisited. A set of comprehensive guidelines is given for the construction of CCC charts, when p_0 is known and when p_0 is estimated by two different schemes. In addition, the associated parameters for constructing CCC charts with the most commonly used in-control ARLs are given in Tables 4.1 and 4.2. Termination and suspension rules are introduced for the CCC scheme with sequentially estimated parameter to enhance the sensitivity of the CCC scheme. An example together with the simulation studies are presented, illustrates the proposed scheme for constructing CCC charts. In summary, Figure 4.8 gives the flow in constructing CCC charts for high yield process monitoring when p_0 is known and when p_0 is estimated. Before plotting the control chart, the prefered ARL_0 is specified. For the case when p_0 is given, the control limits can be obtained from Equations (4.1) and (4.2) by using the respective ϕ and γ_ϕ. If there is no previous data and p has to be estimated, two estimation method can be used, depending on the nature of the initial data collection and also the availability of the initial production output. If the data available is limited, the sequential estimation scheme can be deployed. On the other hand, both estimation schemes can be used if the initial data set is substantial.
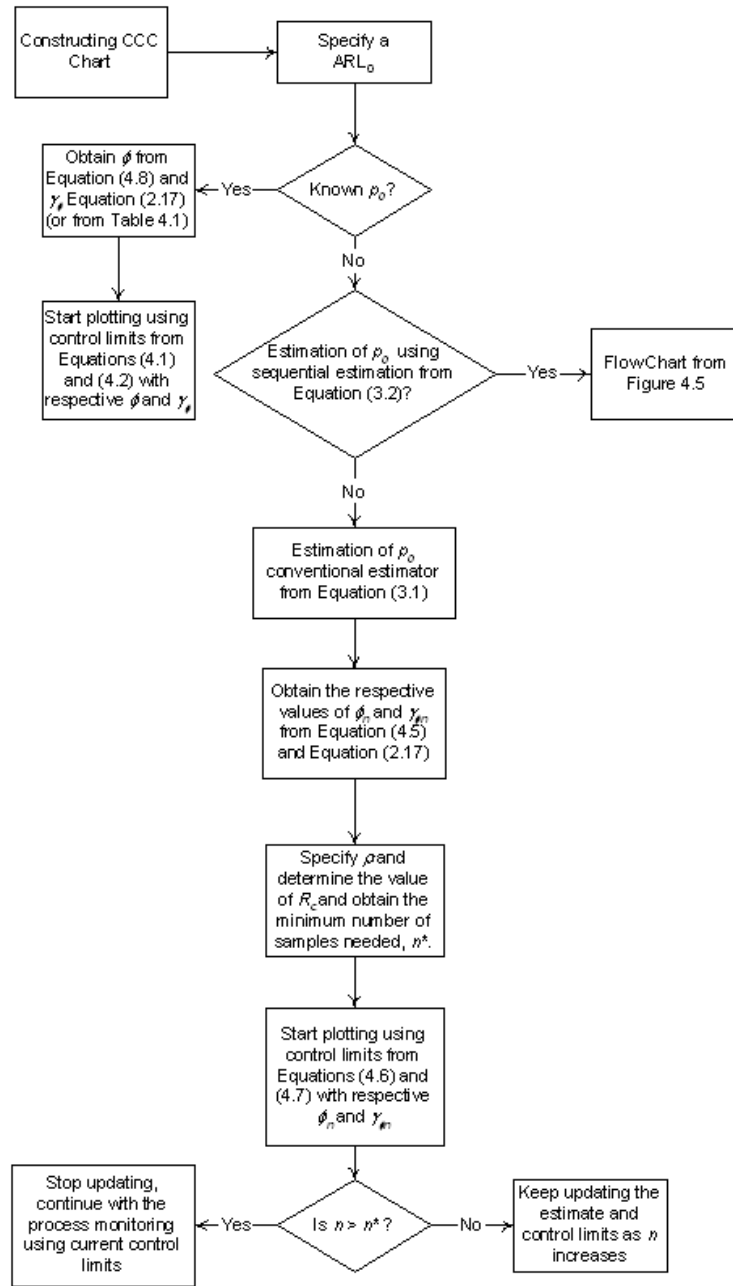
Figure 4.8: Flow Chart for Implementing CCC Control Chart.

PART III

HIGH YIELD PROCESSES WITH SAMPLING INSPECTION

Chapter 5

Control Scheme for High Yield Correlated Production with Sampling Inspection

Besides the Phase I problem, less attention is being paid to the situation where 100% inspection is prohibitively laborious due to large production volume, and sampling inspection from production batches with a pre-determined constant sample size is therefore preferred. This is also common for processes with slower inspection rate than their production rate and/or limited testing facility. This presents a new practical issue as the use of the cumulative conformance count for process monitoring has yet to be investigated under sampling inspection in which the natural ordering of production output is lost. This problem is further intricate by the fact the production outputs are usually correlated under batch processes.

Conventionally, for sampling inspection, the process is monitored using the well-known Shewhart p-chart or np-chart. However, for high yield processes, typical Shewhart attribute charts are inadequate (see discussions in Sections 1.2.1). The problem of these inadequacies of the p-chart and np-chart in detecting the high yield

process with sampling inspection is still remain unsolved as the control scheme based on cumulative conformance count is also not effective in monitoring such process. This will be further discussed in Section 5.2.

This issue is further compounded with the presence of correlation within production batches. In particular, correlation will take a different form within a sample due to loss of ordering (this will be discussed in the following section). The unmitigated presence of correlation under sampling inspection will have an effect on the performance of CCC chart (see Lai *et al.* [50], [51]).

In the following, the effects of correlation within a sample on the performance of the CCC chart are examined, this is followed by the investigations of sampling inspection in high yield processes. The study of the proposed chart based on the Cumulative Chain Conforming Sample (CCCS) is then presented. The proposed scheme extends the idea of chain inspection procedure (see Dogde [22]) to enhance the sensitivity in detecting a process shift. The characteristic of the plotting variable, CCCS, is analyzed using a Markov model from which the performance of the proposed scheme can be analyzed. Subsequently, a numerical example and simulation studies are presented to illustrate the applicability of the proposed chart and its advantage over the existing CCC chart. Finally, a conclusion is given.

5.1 Effects of Correlation

As the production outputs are usually correlated and the ordering of the items within a sample is lost, any pair of the production outputs within the same produc-

tion batch is correlated. A common way to represent such intra-sample correlation is by the notion of exchangeability given by Madsen [55] as follows. Suppose D is the total number of nonconforming items observed within a sample of size n, for a process having p_0 fraction nonconforming with correlation coefficient, ρ. Then the probability of r nonconforming items is

$$
P(D = r) = \begin{cases} \rho(1 - p_0) + (1 - \rho)(1 - p_0)^n & r = 0 \\[2mm] (1 - \rho)\binom{n}{r}p_0^r(1 - p_0)^{n-r} & 1 \le r < n - 1 \\[2mm] \rho p_0 + (1 - \rho)p_0^r & r = n. \end{cases} \tag{5.1}
$$

For a given p_0, the method of moment estimator for ρ is given by (see Madsen [55])

$$
\hat{\rho} = \frac{S^2 - np_0(1 - p_0)}{n(n - 1)p_0(1 - p_0)} \tag{5.2}
$$

where S^2 denotes the sample variance for the observed data (using a divisor of n).

When $\rho = 0$, the probability mass function (pmf) reduces to

$$
P(D = r) = \binom{n}{r}p_0^x(1 - p_0)^{n-r} \tag{5.3}
$$

which is the typical Binomial distribution.

Suppose the first sample of size n from a process with correlation coefficient ρ, is sequentially inspected. The probability of getting a cumulative conformance count less than LCL (signaling probability) is given by

$$P\big(x < LCL\big) = \sum_{r=1}^{n} P(x < LCL, D = r)$$

$$= \sum_{r=1}^{n} P(x < LCL|D = r)P(D = r)$$

$$= \sum_{r=1}^{n} \left(\begin{array}{c} \frac{r}{n} + \left(\frac{n-r}{n} \times \frac{r}{n-1} \right) + \left(\frac{n-r}{n} \times \frac{n-r-1}{n-1} \times \frac{r}{n-2} \right) + \cdots \\[2mm] + \left(\frac{n-r}{n} \times \frac{n-r-1}{n-1} \times \cdots \times \frac{n-r-(LCL-3)}{n-(LCL-3)} \times \frac{r}{n-(LCL-2)} \right) \end{array} \right)$$

$$\times (1 - \rho) \binom{n}{r} p^r \left(1 - p \right)^{n-r}$$

$$= \sum_{r=1}^{n} \left(\sum_{i=1}^{LCL-1} \left(\frac{(n-i)!}{(r-1)!(n-r-i+1)!} \right) (1 - \rho)p^r (1 - p)^{n-r} \right).$$

$$(5.4)$$

When $p = p_0$, the above probability is the false alarm probability, which is presented in Table 5.1 for different values of ρ where the LCL is set with $\alpha/2 = 0.00135$. From the table, the false alarm probability decreases monotonically as ρ increases.

Table 5.1: The false alarm probabilities obtained from Equation (5.4) with different p_0 and ρ

ρ	$p_0 = 50$ ppm	100 ppm	200 ppm	300 ppm	400 ppm	500 ppm
0	0.001399	0.001399	0.001399	0.001499	0.001599	0.001499
0.1	0.001259	0.001259	0.001259	0.001349	0.001439	0.001349
0.5	0.000700	0.000700	0.000700	0.000750	0.000800	0.000750
0.9	0.000140	0.000140	0.000140	0.000150	0.000160	0.000150

The out-of-control signaling probabilities for various values of p and ρ are tabulated in Table 5.4 for a chart designed for $p_0 = 0.0005$, using $\alpha/2 = 0.00135$ and various ρ values. From the table, as expected, for all values of ρ, signaling probabilities increase as the fraction nonconforming increases. However, when there is strong correlation within a sample, the signaling probability is decreased so that

the conventional CCC chart is not effective in detecting process deterioration in the presence of correlation. This is further supported by the one-sided operating characteristic (OC) curves for $p_0 = 100$ ppm with different values of ρ in Figure 5.1. This clearly demonstrates the need to check against correlation to avoid having a false sense of security.

Table 5.2: The one-sided signaling probabilities for CCC with $p_0 = 0.0001$, using $\alpha/2 = 0.00135$.

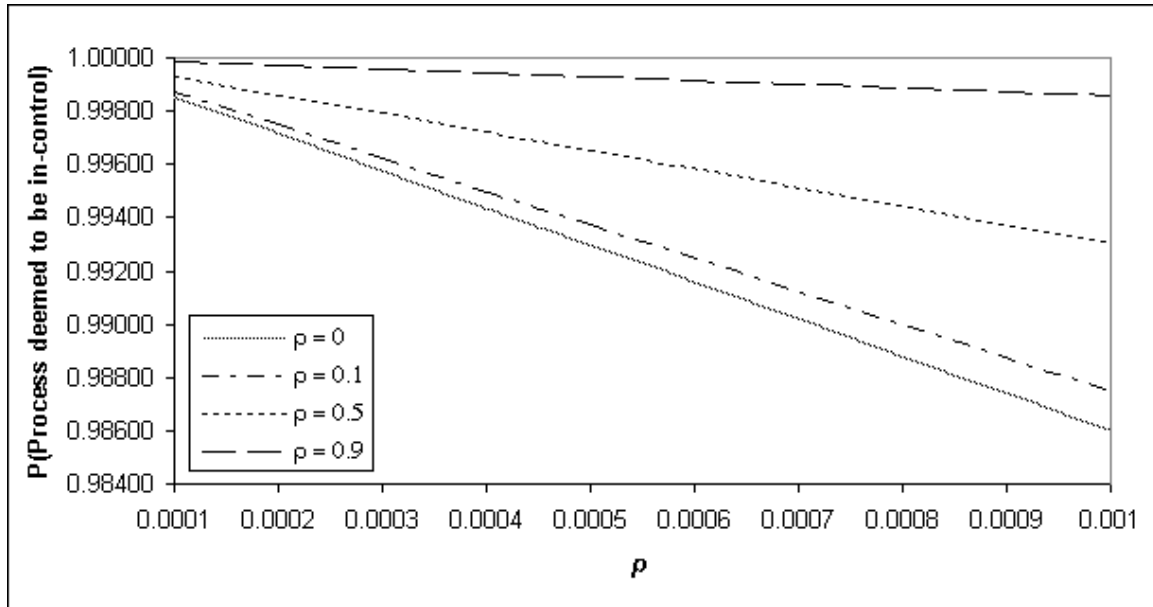| ρ	$p =$**0.0001**	0.0002	0.0003	0.0004	0.0005	0.001
0	**0.001399**	0.002796	0.004192	0.005585	0.006977	0.013909
0.1	0.001259	0.002517	0.003773	0.005027	0.006280	0.012518
0.5	0.000700	0.001398	0.002096	0.002793	0.003489	0.006955
0.9	0.000140	0.000280	0.000419	0.000559	0.000698	0.001391

Figure 5.1: OC Curve with $p_0 = 0.0001$ and $\alpha/2 = 0.00135$ with different values of ρ.

5.2 Sampling Inspection in High Yield Processes

For sampling inspection, the conventional way to monitor the process is to use the well-known Shewhart p-chart or np-chart. However, Goh [28] has shown that, for high yield processes, these typical Shewhart attribute charts are in fact, inadequate. As the control limits of these charts which obtained from significantly low p will result in high false alarm rates and inability to detect process improvement (see discussions in Section 1.2.1).

On the other hand, the CCC control scheme is tracking only the total number of conforming items produced before a nonconforming item is detected. Implicitly, for CCC control scheme, the inspection process is assumed to be carried out sequentially, i.e., items are inspected one at a time and the CCC before a nonconforming item surfaces follows a geometric distribution. Thus, given p_0, the in-control process fraction nonconforming, and the type I error, α, the LCL of the CCC chart can be obtained from Equation (2.6):

$$LCL = \frac{\ln(1 - \alpha/2)}{\ln(1 - p_0)} + 1$$

which is typically much less than the usual sample size when the inspection is carried out sample by sample. For example, if α used is 0.0027 for a process with $p_0 = 500$ ppm, the LCL is

$$LCL = \frac{\ln(1 - 0.0027/2)}{\ln(1 - 0.0005)} + 1$$

$$= 3.7 \approx 4.$$

In addition, the CCC chart is no longer effective as the 'exact cumulative order-

ing' of an item within a sample is indeterminable, i.e., when a nonconforming item is detected within a sample of size n, the order of the nonconforming item could be in the range of (1,n). For example, if the sample size for each inspection, n is 500, and there have been two conforming samples and a nonconforming item is found in the third sample; the possible cumulative count would be from 1001 to 1500, as the order of the nonconforming items from each sample is uniform over (1,500). These provide the motivations of our studies. In this chapter, we will propose a control scheme not only able to monitor the high yield processes with sampling inspection, but also consider the corelation within samples.

5.3 A Chain Inspection Scheme for High Yield Processes Under Sampling Inspection

To address the problems of sampling inspection and the effect of correlation which have stated above, we introduce the concept of cumulative conforming sample. The resulting control scheme categorizes samples as conforming or nonconforming by the total number of nonconforming items in a sample and those of previous i samples by adopting the idea of chain inspection scheme in acceptance sample introduced by Dodge [22].

Chain-sampling plans (or chain inspection plans), which was introduced by Dodge [22], make use of the cumulative results of several preceding lots in acceptance sampling practices. The general procedure for the Chain-sampling plans is as follows:

1. For each lot, select the sample of size n and observe the number of defectives.

2. If the sample has zero defectives, accept the lot; if the sample has two or more defectives, reject the lot; and if the sample has one defectiveaccept the lot provided there have been no defectives in the previous i lots.

(see Montgomery [61] and Schilling [76] for the details of Chain-sampling plans)

5.4 The Proposed Scheme: Cumulative Chain Conforming Sample (CCCS)

Here, we consider a special case of a chain inspection procedure in which a sample with zero nonconforming item is passed and a sample with 2 or more nonconforming items is deemed to be nonconforming. But when a single nonconforming item is found in a sample, information from the previous i samples will be used for decision making. This leads to the following definition:

Definition 2 Chain Conforming Sample

A sample is categorized as chain conforming sample when it contains:

1. zero nonconforming items, or

2. one nonconforming item and there were no nonconforming items in the previous i samples.

The proposed control chart plots the cumulative number of chain conforming samples before a non-chain conforming sample surfaces. Figure 5.2 gives an illustration of how samples are classified until a point is plotted under the proposed control scheme. In essence, whenever a non-chain conforming sample is detected, the Cumulative Chain Conforming Sample (CCCS) is plotted on a control chart

with the above control limits. Similar to the traditional CCC chart, when a point is plotted above the UCL of the chart, it indicates process improvement. On the other hand, if a point is plotted below the LCL of the chart, the process is deemed to be out-of-control with an increase in p. To characterize the distribution of CCCS, the model underlying the plotting procedure is needed.
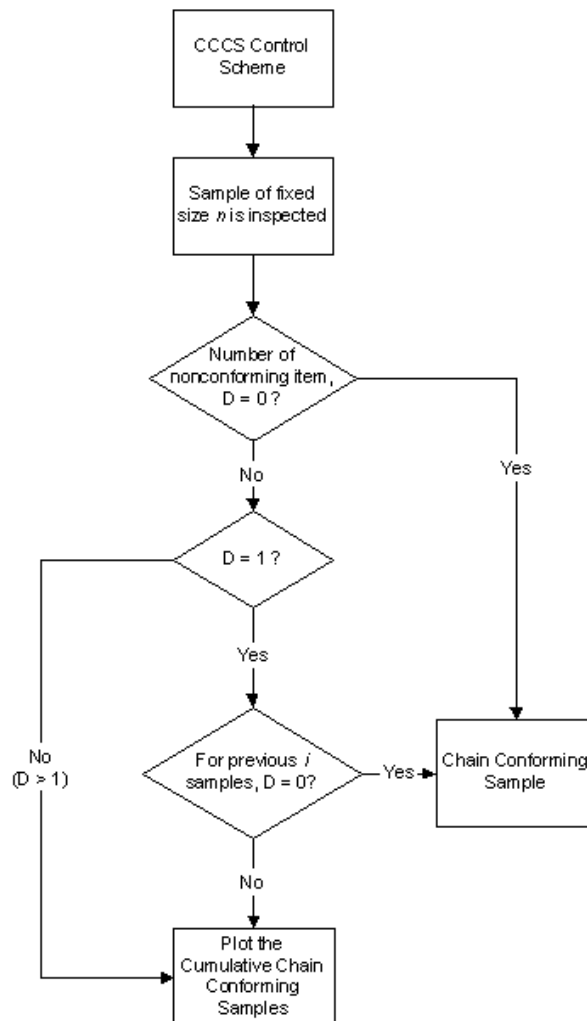

Figure 5.2: The decision rules for chain inspection procedure.

5.4.1 Distribution of CCCS

Let p_{jk} be the probability that there are j nonconforming items in the previous i samples and k nonconforming items in the current inspection sample. We also denote by p_{0+0} the probability of having more than zero nonconforming item(s) in the previous i samples and zero nonconforming item in the current sample. As a result, the probability of observing zero nonconforming item in a sample of size n, regardless of the outcome of previous i samples is given by,

$$p_{00} + p_{0+0} = [P(D=0)]^i P(D=0) + \left(1 - [P(D=0)]^i\right)P(D=0)$$

$$= P(D=0).$$

Similarly, the probability of observing a nonconforming item in current sample and zero nonconforming item in the previous i samples is

$$P_{01} = [P(D=0)]^i P(D=1)$$

From the above definition, the probability of observing a Chain Conforming Sample (CCS) can be obtained by summing up the above probabilities as

$$P\big(\text{Chain Conforming Sample}\big) = P(D=0) + [P(D=0)]^i P(D=1). \quad (5.5)$$

In the same way, the probability of obtaining a Non-chain Conforming Sample (NCCS) is the sum of the following:

i. $p_{01+} = [P(D=0)]^i P(D>1)$

ii. $p_{0+1} = \left(1 - [P(D=0)]^i\right)P(D=1)$

iii. $p_{0+1+} = \left(1 - [P(D=0)]^i\right)P(D>1)$

It follows that

$$P\big(\text{Non-chain Conforming Sample}\big) = 1 - \{P(D=0) + [P(D=0)]^i P(D=1)\}.$$

$$(5.6)$$

Thus, the probability of obtaining an NCCS given that the preceding sample is a CCS, $P\big(NCCS|CCS\big)$, is given by

$$P\big(NCCS|CCS\big) = \left(\frac{\begin{array}{c}\{p_{00} \times P(D>1)\} + \{p_{01} \times P(D=1)\} + \{p_{01} \times P(D>1)\} + \{p_{0+0} \times \frac{1}{i}P(D>1)\} \\ +\{p_{0+0} \times \frac{i-1}{i}P(D=1)\} + \{p_{0+0} \times \frac{i-1}{i}P(D>1)\}\end{array}}{P(D=0) + [P(D=0)]^i P(D=1)} \right)$$

and the probability of observing a CCS given that the preceding sample is an NCCS, is given by

$$P(CCS|NCCS) = \left(\frac{\{p_{01+} \times P(D=0)\} + \{p_{0+1} \times P(D=0)\} + \{p_{0+1+} \times P(D=0)\}}{1 - \{P(D=0) + [P(D=0)]^i P(D=1)\}} \right).$$

The evolution of the outcomes of the inspection can then be modeled by a Markov Chain with states CCS and NCCS. The transition matrix of the Markov Chain is given by

$$\mathbf{P} = \begin{bmatrix} 1 - P(NCCS|CCS) & P(NCCS|CCS) \\ P(CCS|NCCS) & 1 - P(CCS|NCCS) \end{bmatrix} \qquad (5.7)$$

As a result, the limiting probability in state NCCS (long run fraction of NCCS) is given by

$$p_{nccs} = \frac{P(NCCS|CCS)}{P(NCCS|CCS) + P(CCS|NCCS)} \qquad (5.8)$$

and the serial correlation of the samples is given by

$$r = 1 - (P(NCCS|CCS) + P(CCS|NCCS)) \qquad (5.9)$$

The Cumulative Chain Conforming Sample (CCCS) is the number of visits to state CCS in the above Markov Chain which begins with an NCCS and ends with an NCCS; i.e., the recurrence time to state NCCS. Thus, we have

$$P(CCCS = 0) = 1 - P(CCS|NCCS) = r + p_{nccs}(1 - r)$$

$$P(CCCS = y) = P(CCS|NCCS)\,(1 - P(NCCS|CCS))^{y-1}\,P(NCCS|CCS)$$

$$= p_{nccs}(1 - p_{nccs})(1 - r)^2\,(1 - p_{nccs}(1 - r))^{y-1}, \qquad y \geq 1. \tag{5.10}$$

The distribution function of CCCS is found as

$$P(CCCS < y) = 1 - (1 - P_{nccs})(1 - r)\,(1 - p_{nccs}(1 - r))^{y-1}. \tag{5.11}$$

Note that when the serial correlation r is zero $(i = 0)$, the above distribution function reduces to the geometric distribution.

5.4.2 The Control Limits

From the distribution function of CCCS given in Equation (5.11), the control limits for the proposed scheme are obtained as

$$UCL \quad = \quad \frac{\ln(\alpha/2) - \ln[(1 - p_{nccs})(1 - r)]}{\ln[1 - p_{nccs}(1 - r)]} + 1 \tag{5.12}$$

$$LCL \quad = \quad \frac{\ln(1 - \alpha/2) - \ln[(1 - p_{nccs})(1 - r)]}{\ln[1 - p_{nccs}(1 - r)]} + 1 \tag{5.13}$$

where α is the type I risk (false alarm probability). Table 5.3 gives the control limits for $p_{nccs} = 0.000197$ and $r = 0.00483$ ($p_0 = 100$ ppm, $n =, \rho = 0.5$ and $i = 5$).

From Table 5.3, when the value of r is greater than $\alpha/2$, there is no solution for the LCL, because, from Equation (5.11), $P(CCCS = 0) = r + p_{nccs}(1 - r) > \alpha/2$.

Table 5.3: Lower and upper control limits for $p_{nccs} = 0.000197$ and $r = 0.00483$.

α	LCL	UCL
0.0010	-	38645
0.0027	-	33592
0.0050	-	30457
0.0100	1	26931
0.0150	14	24868
0.0200	27	23404
0.0250	39	22269
0.0500	104	18743

5.4.3 Average Run Length and Average Time to Signal

The average run length (ARL) is the average number of points plotted within the control limits before an out of control signal is plotted. As the plotted points are the recurrence times, of the Markov Chain in Equation (5.7), the signaling probability is given by

$$P(E) = P(CCCS < LCL) + P(CCCS > UCL).$$

Since successive values of CCCS are independent, the ARL is given by the reciprocal of $P(E)$. In particular, the ARL for a two-sided scheme is

$$ARL = 1/P(E)$$

where

$$
\begin{aligned}
P(E) =& 1 - (1 - p_{nccs})(1 - r)\left(1 - p_{nccs}(1 - r)\right)^{LCL-1} \\
&+ 1 - \left[1 - (1 - p_{nccs})(1 - r)\left(1 - p_{nccs}(1 - r)\right)^{UCL-1}\right] \\
=& 1 - (1 - p_{nccs})(1 - r)\left(1 - p_{nccs}(1 - r)\right)^{LCL-1} \\
&+ (1 - p_{nccs})(1 - r)\left(1 - p_{nccs}(1 - r)\right)^{UCL-1}.
\end{aligned}
\tag{5.14}
$$

Table 5.4 gives the signaling probability for $p_0 = 0.0001$, $n = 100$, $\alpha = 0.02$, and $i = 5$ for different values of ρ. From the table, for all values of ρ, the signaling

probability increases as the fraction of nonconforming, p, changes from p_0 to any other values.

Table 5.4: The signaling probability for $p_0 = 0.0001$, $n = 100$, $\alpha = 0.02$, and $i = 5$ for different values of ρ.

ρ	p = 0.00001	0.00005	**0.0001**	0.0005	0.001	0.005	0.01
0	0.95333	0.31238	**0.02000**	0.04979	0.09841	0.41572	0.66129
0.1	0.94461	0.30505	**0.02000**	0.06477	0.15133	0.70326	0.91761
0.5	0.85906	0.23698	**0.02000**	0.10888	0.30166	0.97917	0.99975
0.9	0.65898	0.11711	**0.02000**	0.06505	0.15839	0.82843	0.98553

The performance of the control scheme can also be expressed in terms of its average time to signal (ATS) (see Montgomery [61]). Due to the difference of the inspection schemes for the conventional CCC chart and the proposed CCCS chart, the ATS, which is the average number of items inspected before a signaling event, is better for comparison than is the ARL or $P(E)$. For a constant sample size, n, the ATS of the proposed scheme is given by

$$
\begin{aligned}
ATS_{CCCS} &= \frac{n}{p_{nccs}} \times ARL_{CCCS} \\
&= \frac{n}{p_{nccs} \times \alpha};
\end{aligned}
\tag{5.15}
$$

whereas the ATS for the CCC scheme with sequential inspection is given by

$$
\begin{aligned}
ATS_{CCC} &= \frac{ARL_{CCC}}{p} \\
&= \frac{1}{p \times \alpha_{CCC}}.
\end{aligned}
\tag{5.16}
$$

From the above equations, the probability of a type I error, α, is adjusted so that the resulting ATS is equivalent to that of the conventional CCC chart. To achieve this, the value of α used in the proposed scheme is set to be

$$
\alpha = \frac{n \times p_0 \times \alpha_{CCC}}{p_{nccs}},
\tag{5.17}
$$

where α_{CCC} is the type I risk used in conventional CCC charts.

Table 5.5 gives the one-sided ATS of CCC and CCCS charts with $p_0 = 0.0005$, $n = 100$, $i = 5$, $\alpha_{CCC} = 0.0027$ and the corresponding α for CCCS from Equation (5.17), for different values of ρ. The values shown in the parenthesis are the out-of-control ATS values expressed as a percentage of the in-control ATS. Table 5.5 shows the superior performance of the proposed CCCS chart in this way. Keeping constant α_{CCC}, and the in-control ATS of the CCCS chart, the out-of-control ATS of the CCC chart always exceeds that of the CCCS chat, the ratio of ATS values increases with correlation. This is because, for the CCC chart with a designated α_{CCC}, the false alarm probability decreases as ρ increases (see column 1 of Table 5.4). In addition, as p increases, the ATS for CCCS decreases drastically compared to that of the CCC chart. For $\rho= 0.1$ and 0.5, the ATS curves for the CCCS and CCC control charts are plotted in Figure 5.3. It is clear from Figure 5.3 that the proposed CCCS control chart is more effective in detecting a process shift and its performance is not affected by the presence of correlation.

Table 5.5: The one-sided ATS of CCC and CCCS charts with $p_0 = 0.0001$, $n = 100$, $\alpha_{CCC} = 0.0027$, and i = 5, for different values of ρ.

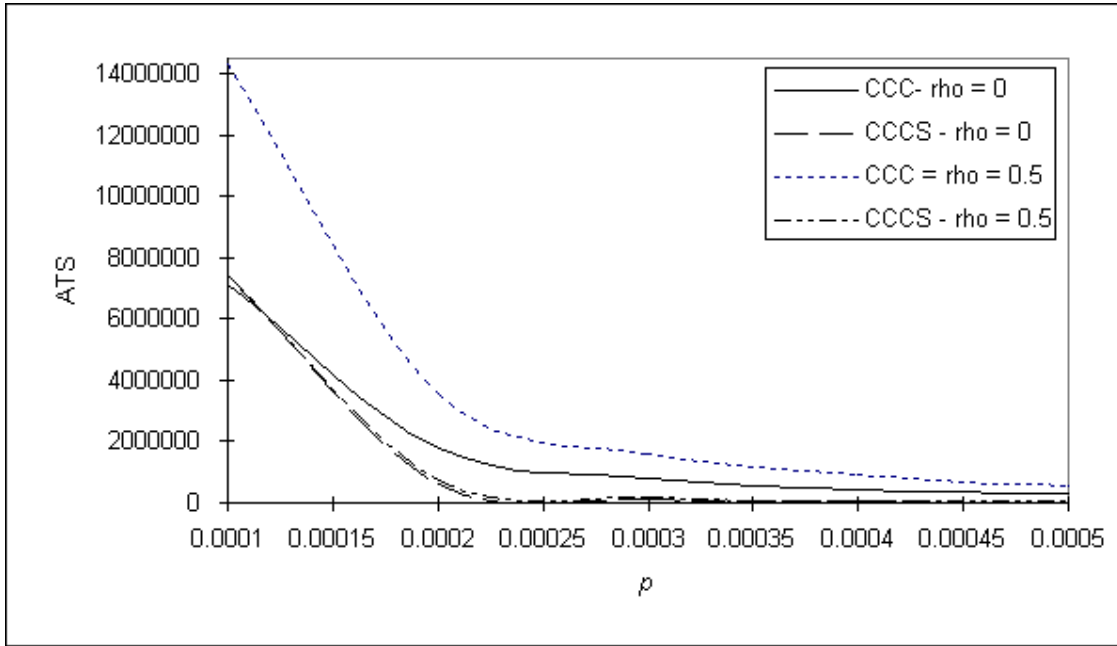| p	$\rho = 0$		$\rho = 0.1$		$\rho = 0.5$		$\rho = 0.9$	
	CCC	CCCS	CCC	CCCS	CCC	CCCS	CCC	CCCS
0.0001	7147503	7407407	7941676	7407407	14295006	7407407	71475030	7407407
0.0002	1788039	631682	1986705	611946	3576077	707777	17880387	1665765
	(25.02%)	(8.53%)	(25.02%)	(8.26%)	(25.02%)	(9.55%)	(25.02%)	(22.49%)
0.0003	795200	151613	883555	145581	1590399	184181	7951995	686543
	(11.13%)	(2.05%)	(11.13%)	(1.97%)	(11.13%)	(2.49%)	(11.13%)	(9.27%)
0.0004	447591	56644	497322	54478	895181	74989	4475907	367207
	(6.26%)	(0.76%)	(6.26%)	(0.74%)	(6.26%)	(1.01%)	(6.26%)	(4.96%)
0.0005	286644	27145	318493	26308	573288	39449	2866438	228097
	(4.01%)	(0.37%)	(4.01%)	(0.36%)	(4.01%)	(0.53%)	(4.01%)	(3.08%)
0.001	71894	3633	79882	3786	143788	8117	718938	59206
	(1.01%)	(0.05%)	(1.01%)	(0.05%)	(1.01%)	(0.11%)	(1.01%)	(0.80%)

Figure 5.3: The ATS curves of CCC and CCCS charts with $p_0 = 0.0001$, $n = 100$, $\alpha_{CCC} = 0.0027$, $i = 5$ for $\rho = 0$ and 0.5.

5.4.4 Selection of i

The role of the parameter i, the number of previous samples to be reviewed when a nonconforming item is found in the current sample, is to augment information from previous samples so that the performance of the chart improves. This is particularly so when intra-sample correlation, which reduces the amount of information in a sample, exists.

However, it is impractical to use information that is too remote, as the marginal benefits derived are diminishing with increasing i. To illustrate, Figure 5.4 gives the ARL curves for CCCS charts with $p_0 = 0.0001$, $\rho = 0.9$, $\alpha = 0.01$, and $i = 0$, 3, 5, 10, and 20. From the figure, the performances of CCCS charts improve as i increases. However, there is only a slight improvement of sensitivity of the chart

104

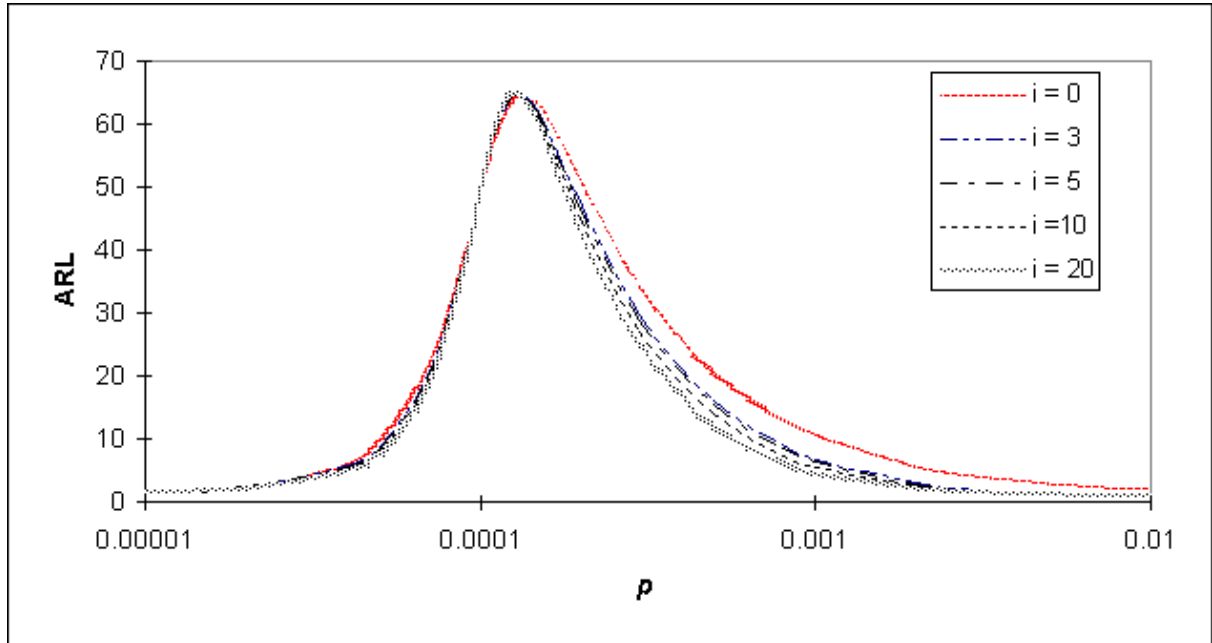as i increases from $i = 5$ onwards. Hence, using i between 3 to 5 is appropriate.

Figure 5.4: The ARL curves for CCCS charts with $p_0 = 0.0001$, $n = 100$, $\alpha = 0.01$, $\rho = 0.9$ and $i = 0, 3, 5, 10$ and 20.

5.4.5 Effects of Sample Size

One of the main motivations of this paper is to address the issue of sampling inspection in which the natural sequence of production within an inspection sample is lost. In addition, the effect of correlation, which renders conventional CCC chart ineffective in detecting process deterioration, is evaluated and addressed appropriately under the proposed scheme.

Here, we investigate the performance of the proposed scheme under different sample sizes and correlation coefficients, ρ. For illustration, the out-of-control ARL for some settings are plotted. Figure 5.5 depicts the out-of-control ARL for p increases from 100 ppm to 500 ppm for different values of ρ and n. From the

figure, it can be seen that when there is no correlation, the ideal group size for detecting a shift of this size is one to obtain the minimum ARL. This is intuitively clear as the sample size should be as small as possible so that changes in p can be detected promptly. When the correlation is weak, $(0 < \rho \leq 0.1)$, the sample size for inspection should be small (< 50) to achieve the minimum out-of-control ARL. For ρ ranging from 0.1 to 0.7, the group size used should range from 100 to 250 as the effectiveness of the scheme deteriorates as sample size increases beyond 250. This further reaffirms the intuition of having smaller sample size in order to detect an out-of-control situation promptly. However, for $\rho > 0.7$, a larger sample size can be used. Thus, an appropriate group size for monitoring high yield process with weakly correlated output is about 100; while that for monitoring strongly correlated output can be much higher.
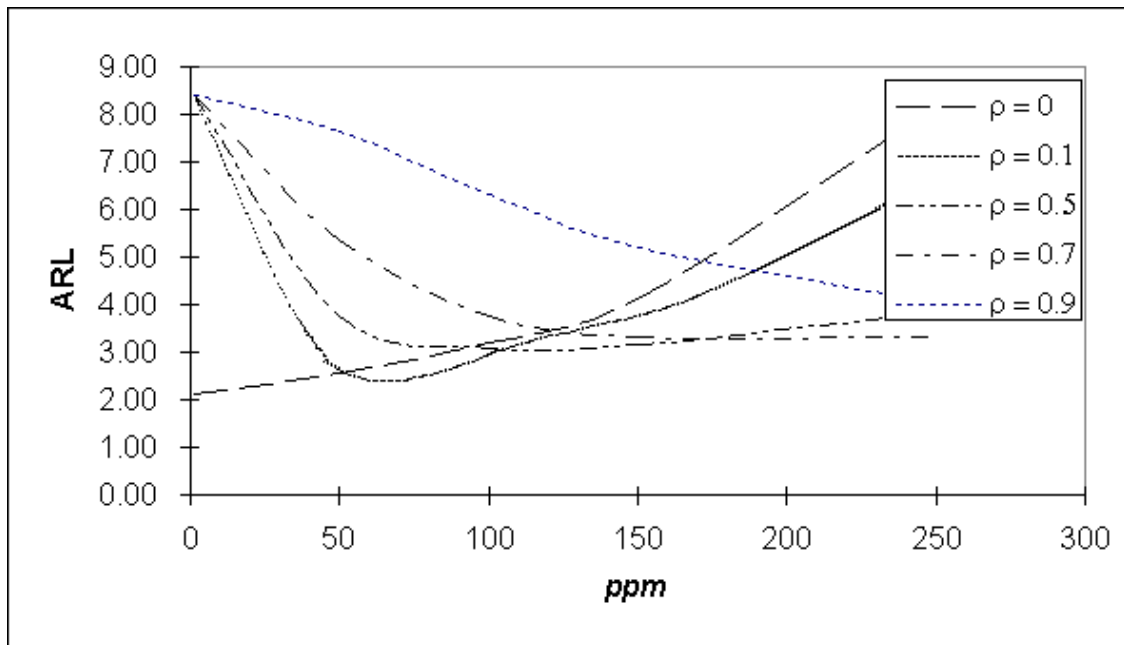

Figure 5.5: The out-of-control ARL for CCCS charts when $p_0 = 0.0001$, $p = 0.0005$, $i = 5$, and $\alpha = 0.05$, with different ρ and n.

106

5.5 Numerical Example

Here we give an example to illustrate the use of proposed CCCS chart and demonstrate its effectiveness through a simulation study.

A set of 5000 samples each with $n = 100$, $\rho = 0.5$, $p = p_0 = 100$ ppm is simulated. Subsequently 500 samples is also simulated with $p = 500$ ppm under the same setting. By using $i = 5$, values of CCCSs are obtained from the simulated data and tabulated in Table 5.6. From the table, the first 3 entries are from the in-control process, the 4th entry is a result of a mixture of $p = 100$ ppm and 500 ppm, and the 5th entry is obtained from out-of-control process ($p = 500$ ppm).

Table 5.6: Values of CCCS plotted with $i = 5$ from the simulated data.

Plotting point	1	2	3	4	5
Values of CCCS	2966	568	579	1370	**5**

For comparison with the conventional CCC chart, the value of α used in the proposed scheme is obtained from Equation (5.17). For the above simulation setting, the value of α is 0.137 for α_{CCC}. Thus, from Equations (5.12) and (5.12), the control limits of the proposed scheme are

$$UCL \quad = \quad 13625$$

$$LCL \quad = \quad 336.$$

The CCCS control chart is plotted with the data in Table 5.6 and the above control limits in Figure 5.6, and in which the shift in p is detected at the fifth observation.

For comparison, the simulated data is used to construct the conventional CCC chart with $\alpha = 0.0027$. When there is/are nonconforming item(s) within a sample,
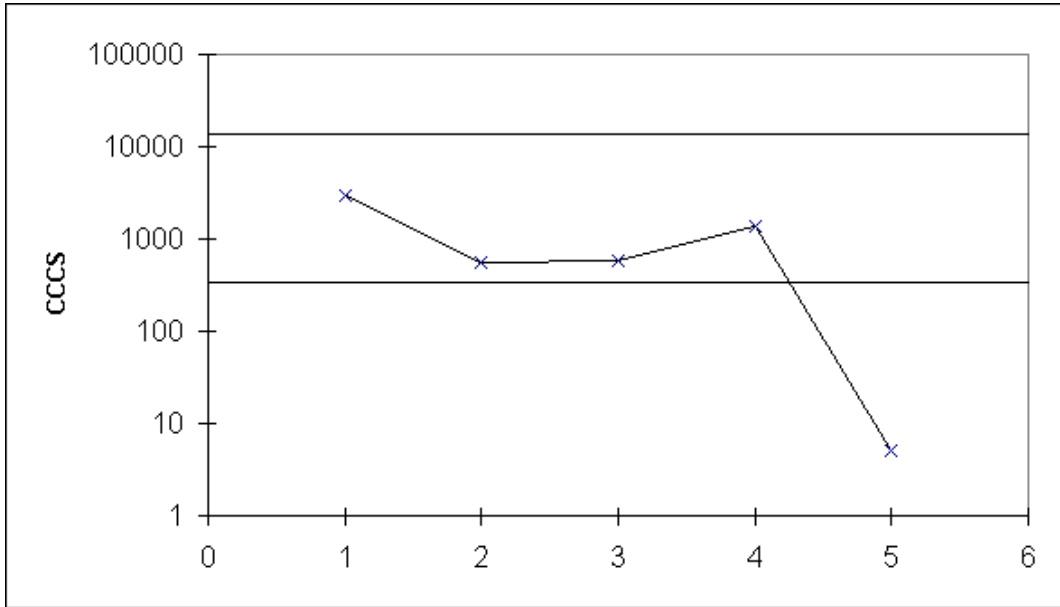
Figure 5.6: The CCCS Chart with $\alpha = 0.137$, using the simulated data from Table 5.6

the 'location' of the item(s) will be distributed evenly within the sample, each nonconforming item found in the data is treated as a plotting point in CCC chart and is tabulated in Table 5.7. The first 15 entries are from $p_0 = 100$ ppm, followed by the mixture of p_0 and $p = 500$ ppm for the 16th entry, and all entries after the 17th are from $p = 500$ ppm. With the control limits set at 15 and 66073, the conventional CCC chart is shown in Figure 5.7.

Table 5.7: The CCCs with $\alpha = 0.0027$, from the simulated data.

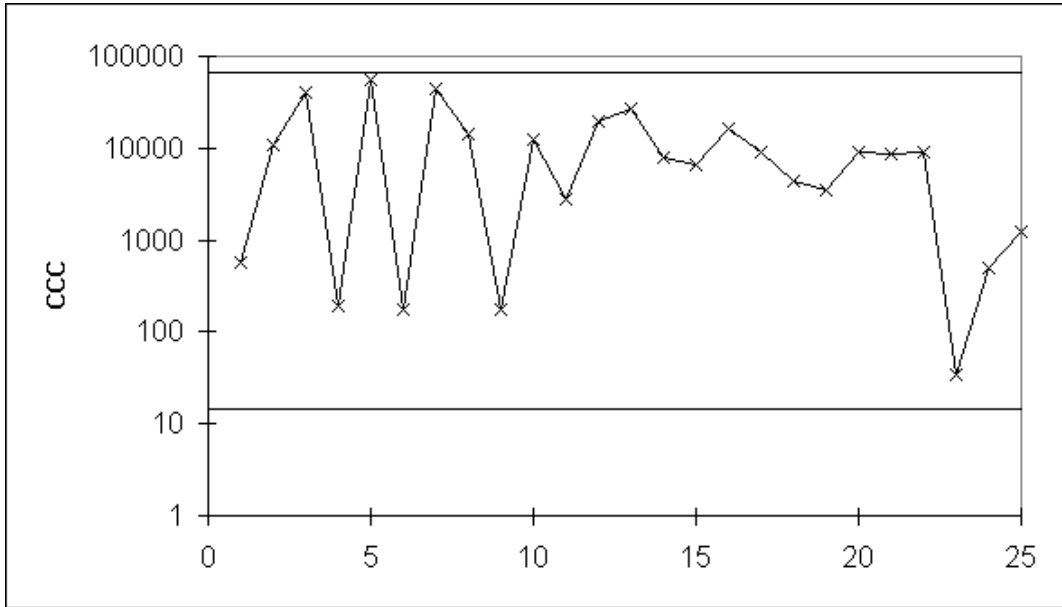| No	CCC	No	CCC
1	582	13	27128
2	10982	14	7924
3	39580	15	6663
4	192	16	**16682**
5	56620	17	9239
6	177	18	4469
7	43577	19	3460
8	14206	20	9154
9	178	21	8482
10	12264	22	8930
11	2798	23	34
12	19739	24	499

Figure 5.7: The CCC Chart with $\alpha = 0.0027$ from Table 5.7

From the chart, there is no out-of-control signal, even though later entries are from $p = 500$ ppm.

To establish the superiority of the proposed CCCS scheme over that of the CCC chart, further simulation runs were carried out with 100 replicates of the above setting (first 5000 samples with $p = p_0 = 100$ ppm, followed by 500 samples with $p = 500$ ppm). Table 5.8 shows the results of the simulation. "Number of out-of-control detected" gives the number of runs in which the control scheme gave an out-of-control signal within the 500 samples when p shifted from 100 ppm to 500 ppm. "Number of false alarm at LCL (UCL)" gives the number of runs in which false alarms occurred below LCL (or above UCL) during the first 5000 samples.

It is clear from the comparison in Table 5.8 that the conventional CCC chart is not effective in monitoring high yield processes under sampling inspection in that it is not able to detect the out-of-control situation promptly and that it pro-

Table 5.8: Comparison of the simulation results for the CCCS and CCC.

	CCCS	CCC
Number of out-of-control detected	**41**	**2**
Number of false alarm at LCL	10	0
Number of false alarm at UCL	0	63
Number "in-control after 5500 groups	49	35
Total	100	100

duces significantly more false alarms at UCL, misleading users that the process has improved. On the other hand, the proposed CCCS scheme is more effective in detecting process shift and tends to err on the conservative end. The non-detection situations are common to both as, for high yield processes, there are insufficient number of nonconforming items produced to trigger an out-of-control signal within the next 500 samples.

5.6 Conclusion

In this chapter, we propose a control scheme, the CCCS chart for monitoring high yield high volume production/process under sampling inspection with consideration of correlation within each sample. Circumstances that lead to sampling inspection include slower inspection rate than production rate, economy of scale in sampling inspections, and strong correlation in the output characteristic. The performance of the chart in terms of its run length properties is investigated. To achieve better sensitivity in detecting a process shift, the recommended sample size is about 100. Numerical results reveal that the performance of the chart is much better than the existing CCC charting scheme under the stated condition.

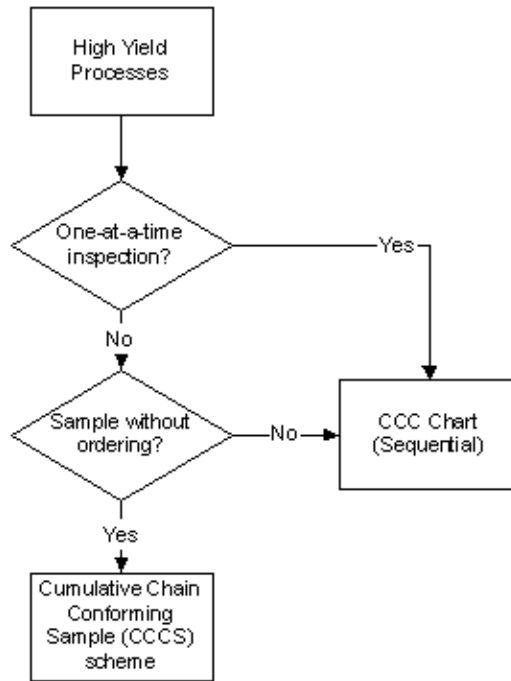In summary, a basic guideline for monitoring high yield processes under sam-

Figure 5.8: The Basic Guideline for Monitoring High Yield Production with sampling Inspection

pling inspection can be summarized in Figure 5.8.

PART IV

STUDIES OF HIGH PERFORMANCE SYSTEMS

Chapter 6

High Performance Systems

6.1   Introduction

Due to the rapid advances in technology, development of highly sophisticated products, intense global competition, and increasing consumer expectations, it is inevitable for today's manufacturers to face strong pressure to design, develop, and manufacture products of high quality and reliability in ever-shorter times while improving productivity at low or minimum cost. Besides having very low defects per million opportunities (dpmo) quality level, some of the products are also required to be highly reliable. The products involve not only those used in mission-critical systems, but also some domestic products. Customers expect purchased product to be reliable and safe. The purchased products should, with high probability, be able to perform their intended function under encountered operating conditions, for a certain period of time. These products are also expected to have not only highly reliable life expectancy, but also well-maintained, degradation-free performance. In the near future, most likely there will be more and more products having such criteria in the market.

Systems/products with high performance criteria stated above can be achieved by significant level of building-in redundancies, such that their intended functions will not be compromised even if there are nonconformities within each item. In addition to being highly reliable, these systems usually have a very high quality level. Here, we define such systems as *high performance systems* (HPmS). HPmS can be as simple as an electronic component such as memory (see Huang *et al.* [42]) or as complicated as a computer hard disk drive.

The system performance level is well-maintained with the significant level of build-in redundancies. Redundancy is a technique whereby the system is provided with redundant (replicate) resources, more than what is required to maintain the overall reliability of the system (see Blischke and Murthy [2], and Elsayed [23]). Redundancy can ensure that if a failure occurs there are enough extra resources available to maintain satisfactory system operation.

The redundant resources within the system are usually the key elements that would lead to performance deficiency or system failure if the key component fails. Such key elements could be the components or subsystems of the HPmS. System failure occurs only when some or all of the replicates fail.

By having a highly significant level of redundancies (far beyond the minimum required), any element-level-failure that occurs within the system would not affect the overall performance. Thus, the performance of the HPmS is expected to be non-degrading, unless the amount of element-level-failure is more than the critical threshold. By possessing a degradation-free period, the systems are also expected

114

to have a certain age of failure-free life - the age of a system below which no failure
should occur.

6.2   Reliability Tests

Among the most important information sources for reliability improvement/assurance
programs are reliability tests. Testing can be treated as the application of some
form of stimulation to a system so that the resulting performance can be measured
and compared to design requirements. Reliability tests can be categorized into two
groups: upstream tests and downstream tests (see Meeker and Hamada [59]).
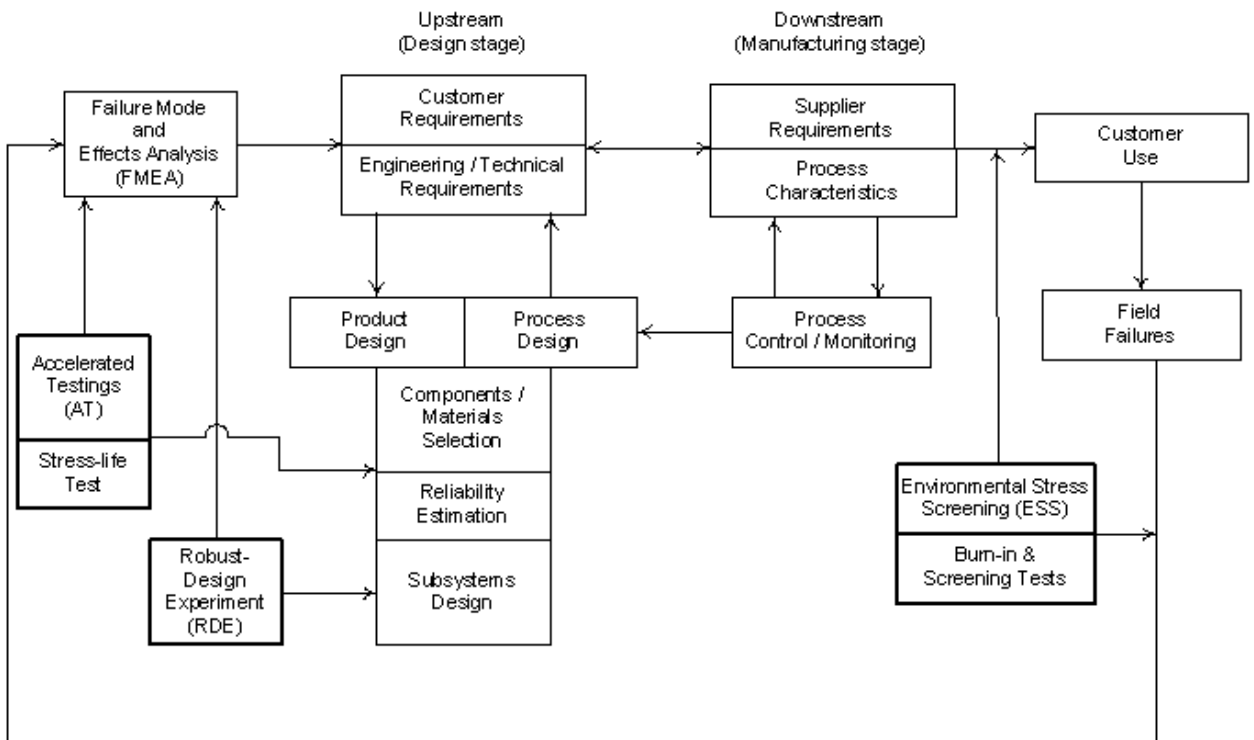

Figure 6.1: Reliability Tests in a System/Product Development Cycle.

Figure 6.1 shows an example of the role of reliability tests in the system/product
development cycle. The arrows between processes represent information sources

and information flow paths.

6.2.1 Upstream Tests

Upstream tests, also known as developmental tests, are those tests used in the early stages of the system design cycle. These tests focus on discovering unanticipated failure modes and improving interactions and interfaces among system components/elements and subsystems; they also estimate system reliability. Examples of upstream tests are accelerated tests (AT), which include the accelerated life test (ALT) and the accelerated degradation test (ADT); robust-design experiments (RDE); and stress-life tests.

6.2.1.1 Accelerated Tests

Accelerated tests (AT) consist of a variety of test methods for shortening the life of systems or hastening the degradation of their performance (see Nelson [65]). The aim is to quickly obtain data, which can be used in design-for-reliability processes to assess or demonstrate component and subsystem reliability, certify components, detect and identify failure modes, and compare different manufacturers. This data yield desired information on system life or performance under normal use, if modeled and analyzed properly. Besides eliminating potential reliability problems early in the system design stage, such testing saves much time and money.

In ALT, units are subjected to a more severe environment than the normal operating environment –for example, higher levels of accelerating variables such as elevated use rate, temperature, and voltage – so that failures can be induced in

116

short periods of time. Inferences about the reliability of units at normal conditions can then be made from the results obtained under the ALT conditions.

However, for most of the highly reliable systems, determining the reliability information via life testing is difficult because no failures are likely to occur during the test, even if the technique of censoring and/or testing at accelerated level is used (see Yu and Tseng [117]). Thus, for some highly reliable systems degradation over time can be related to reliability, ADT is used for reliability assessment instead of life testing (see Meeker *et al.* [58]).

6.2.1.2 Robust Design Experiments

Robust design is an experimental strategy in making a quality characteristic robust to various noise factors and thus enhance the overall system reliability. Empirically, robust design experiments identify the important ones, and find levels of system-design factors that yield quality and reliability improvements.

By using robust design experiments, the optimal combinations of system-design factors can be obtained. In particular, it is possible to minimize the variation and maximize system quality and reliability and thus improve the interactions and interfaces among system components/elements and subsystems within the system.

6.2.1.3 Stress-life Tests

Besides using ALT to identify failure modes, the alternative way of identifying failure modes is the stress-life test. The purpose of such test is to identify and eliminate potential reliability problems early in the system design stage. The idea is to stress and test the prototype of early production units aggressively to force

failures.

6.2.2 Downstream Tests

Downstream tests, on the other hand, are normally executed during manufacturing. The purpose of such a tests is to eliminate manufacturing defects and early part failures. The testing requirements can change over the period of production. Usually, for a new system, in the early stages of production, considerable testing is required to establish the process characteristics and the effect of process parameters on the reliability of the system. As the system matures, the testing requirements are reduced. Examples of such tests are environment stress screening (ESS), burn-in tests, and screening test. In addition, these tests are also used to verify or demonstrate final output reliability or used as a screen to remove defective ones before shipping.

Both ESS and burn-in tests have the same goal, which is to reduce the occurrence of early failures. While ESS exposes the units to excessive environmental extremes outside specification limits over a time interval from several minutes to a few hours, burn-in subjects a unit to stress levels within specifications over a time interval from several hours to a few days.

On the other hand, screening tests expose the units to normal usage conditions over a short period of time, usually at the end of production, to ensure there are no dead-on-delivery occurences. Tang and Tang [87] give a detailed review of the downstream tests mentioned here.

6.3 Quality and Reliability Issues for High Performance Systems

With highly redundant elements built into a system, the performance of the system can be restored to the required level of performance instantly, whenever an element-level-failure occurs during the operation. The performance of HPmS would degrade only when the cumulative number of element-level-failures reaches a critical threshold. In other words, the degradation of the system performance would only be observed when the total number of element-level-failures exceeds the above mentioned critical threshold. The system would then be treated as failure-prone system, as depicted in Figure 6.2.
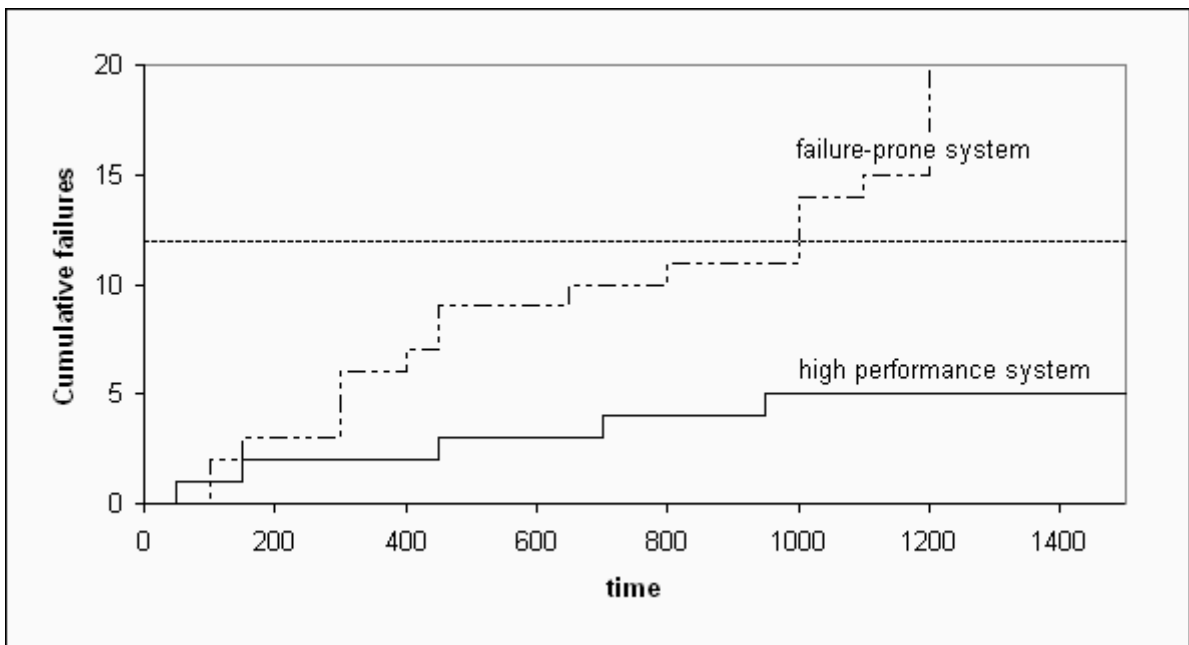

Figure 6.2: Cumulative element-level-failures for HPmS

Rapid technological changes have significantly reduced the life cycles of many systems (or products) and hence amplified the need for new and efficient methods

for reliability assessment. For HPmS, a few or even no failures are expected at ALT conditions, even there might not be significant degradation of performance at ADT conditions. Thus, information prior to the degradation will be the area of interest in future reliability studies. Due to the high-performance capability, besides there is a smaller likelihood of getting meaningful failure data from accelerated life testing (ALT), there would also be difficulties for HPmS in producing degradation data from accelerated degradation test (ADT). As stated in a previous section, a highly significant level of redundancy not only could increase the reliability of the product, but also might mask the element-level-failure occurences within the product. Thus, there would be difficulties in predicting the reliability of high performance products from existing test plans. Alternative tests for assessing the reliability of the system are indeed needed. Similar to the degradation models, if the performance measurement or the failure rate of the key element of the HPmS can be related to the system reliability, such information can be used as a surrogate to the ALT and ADT.

In order to ensure a certain guaranteed top performance age of the HPmS, i.e., to maintain the performance of the HPmS at the required level for a specific period of usage time, the failure rate of the key redundant elements within the HPmS should be stringently kept within the specifications. In addition, manufacturers may be expected to demonstrate to customers that their products have a specified reliability. Thus, those systems with infant mortality behavior or having higher failure rate should be identified at the earliest possible stage in the system design

/ product-development cycle (upstream), as there can be serious economic and noneconomic consequences when a failure mode is discovered first in downstream tests or in service. However, some downstream reliability tests / quality screening tests are still required at some critical stages of production, or after some stress-testings, so as to ensure high quality and field reliability of the system. In addition, the out-of-box audit (OOBA) should be used at the end of the production.

After going through stringent production process monitoring, the final output of the HPmS should have almost 100% yield on system performance, and the occurences of the defects/errors should be uncommon and sporadic. This is again, due to the high performance capability of the system, even for those relatively weak, failure-prone ones could also perform satisfactory under operating conditions. This would make it relatively difficult for planning screening tests if the tests to be carried out are based on measuring on system performance. Other measurements such as number of element-level-failures should be taken into account when planning for any downstream reliability tests/quality screening tests for such systems.

In addition, from the aspect of process monitoring, it is not easy or not possible to detect the number of element-level-failures or the degradation in performance for some of these products. Thus, the quality characteristics needed for process monitoring are not easy to obtain, especially for final products. This is because most of the statistical methodologies for monitoring the characteristics of a process, such as control charts, require quality characteristics that can be measured and expressed on a continuous scale (variable control charts) or at least a quantitative

scale (attribute control charts).

6.4   Conclusion

In this chapter, the term High Performance Systems (HPmS) is coined for systems with built-in redundancies. In addition, reliability tests and reliability improvement programs are summarized. The quality and reliability issues related to HPmS are discussed. As the name implies, the performance level of the system is well-maintained, because any element-level-failure that occurs within the system does not affect the overall performance. Thus, the performance of high performance products is expected to be nondegrading, unless the amount of element-level-failure is more than the critical threshold. Due to the nondegrading performance, the usual reliability assessments cannot be applied on such a system easily. Thus, further research on the planning of the corresponding reliability (stress) tests and the optimality of the decision variables of HPmS tests is much needed.

Chapter 7

Screening Scheme for High Performance Systems

In this chapter, an inspection scheme for high performance systems (HPmS)(as discussed in Section 1.3 and Chapter 6); i.e. outputs from near-to-zero defect processes with built-in redundancies, is investigated. These high performance systems not only have a very high quality level, but are also highly reliable under normal usage. Under normal production, most of these products are conforming with occasional nonconformities within each item. The high performance system (HPmS) is considered to be failure-prone when the number of nonconformities exceeds a critical threshold. Here, we propose a decision rule for detecting these failure-prone systems under a screening scheme. The screening test can be applied either at the end of the production or after some stress-testing, or both; so as to minimize field failures. The decision rule is derived from a model based on modified binomial distribution that is used for fitting real life data from the test. The performance of the test can be evaluated by plotting the corresponding operating-characteristic (OC) curve.

The screening test can be applied at some critical stages of production, or after some stress-testings so as to ensure high quality level and field reliability of the system, as well as used as the out-of-box audit (OOBA - inspection before the shipment, stimulating the costumer receipt) at the end of the production. The objective is to realize the economic benefits of not having "dead-on-delivery", lower warranty claims and field repairs, and the profits of repeat business from satisfied customers. Here, a decision rule for the screening test is introduced to dispose of nonconforming or potentially nonconforming systems and failure-prone systems. It may also be used as a process control rule for monitoring the process if the screening test can be done quickly.

In the following, we present a model for defects occurrence for HPmS. Then the reliability screening scheme and its associated decision rules are presented. A numerical example will be given as illustration.

7.1   A Model for Occurrence of Defects

Here, the production outputs for HPmS are modeled by two subpopulations, one major population with proportion of ω, which is defect-free, and the other population, with proportion of $1 - \omega$ is not defect-free (NDF). If k units of measurement of a HPmS are tested, there would be k opportunities of nonconforming in the test. Such test is carried out to examine the occurrence rate of the nonconformities within a system, the probability of obtaining x nonconformities in each system is

thus given by

$$
P(X = x)
\begin{cases}
\omega + (1 - \omega)(1 - p)^k & x = 0 \\[2mm]
(1 - \omega)\binom{k}{x}p^x(1 - p)^{k-x} & x > 0
\end{cases}
\tag{7.1}
$$

This modified binomial distribution shown in Equation (7.1) is referred to as one of the **Zero-Modified Distributions** and named as *binomial-with-added-zeros* distribution by Johnson *et al.* [44]. The mean and variance for the model (see Johnson *et al.* [44]) are given by

$$
\mu \quad = \quad (1 - \omega)kp
\tag{7.2}
$$

$$
\sigma^2 \quad = \quad (1 - \omega)kp\{1 - p + \omega kp\}
\tag{7.3}
$$

An example of such testing is the read-write error testing of the computer hard disk drives (HDD). The opportunities of nonconforming, k, for such test is interpreted as the total number of bits tested during the test. The parameter, p, is the fraction of error bits within each drive and is expected to be very small.

In the context of reliability screening, this model can be interpreted as having $(1-\omega)$ weak subpopulation which will precipitate an expected fraction of nonconformities within each product after some stress screenings. For example, if a time censored test is planned and products are screened at the end of the test. The fraction of nonconformities, p under exponential assumption is given by

$$
p = 1 - e^{-\lambda At}
\tag{7.4}
$$

where λ is the average failure rate (AFR) of each defect opportunity and A is the

acceleration factor of the stress-test. Other models such as Weibull and lognormal can also be used if it is deemed more appropriate (see Tobias and Trindade [92]).

The planning of this type of stress-test will be dealt with in future research. Here, we focus on decision rule and the model.

7.2   Screening Scheme

From Equation (7.1), it is clear that the two critical aspects that need to be monitored are the proportion of the NDF populations as well as the fraction of non-conformities within each item in the NDF; the respective parameters are ω and p. The frequency of observing the NDF ones is normally not frequent as the overall quality of the product should always be well-maintained at a substantially high level. Thus, the proportion of the NDF population, $1 - \omega$ is expected to be small and usually ranging between 1% to 10%. With the appropriate rational subgroup size and inspection scheme, this minor population can be well-monitored using the idea of Shewhart p or np chart (the p is referred to $1 - \omega$ in this case, which is the subpopulation of NDF), which will be discussed in the later section.

On the other hand, among the NDF ones, the fraction of nonconformities within each item, p, should be as small as possible, so that the performance of the NDF ones conforms to the requirement. This is another parameter of interest. The screening scheme introduced here is different from the existing process monitoring schemes for high yield processes, such as the Cumulative Counts of Conforming (CCC) chart discussed in previous chapters, which considers only conforming and

nonconforming items. Here, we consider cases where the classification of non-conforming products are done based on observing the number of nonconformities/errors occurs within a system/product. Moreover, NDF ones are generally more failure-prone especially when the number of nonconformities is approaching the threshold.

Besides for reliability screening purpose, the proposed scheme can be used for discriminating the failure-prone ones among the NDF populations.

7.2.1 The Decision Rules

The screening scheme presenting here is mainly focused on the fraction of nonconformities, which will affect the reliability and performance of the NDF population if the value of p is larger than expected. Suppose that at the end of the production, in order to ensure the performance of the system/product conforms to the requirements, the reliability screening is carried out. For illustration, the example of the read-write error testing of the HDD is used here.

After taking into the consideration of the testing cost and cycle time constraint, the number of bits used, k, in the test is normally set by the product designer. If there are read errors (nonconformities) found in the test and the number of errors (nonconformities) found exceeds a critical value x_α, the HDD fails the test and labeled as failure-prone. The rate of observing one nonconformity of the failure-prone drive is considered much higher than the specification. The critical threshold, x_α is determined by obtaining the exact probability limits, which will be discussed in the following. When there are nonconformities found in the product and the

number of nonconformities are less than x_α, with a confidence level of $1 - \alpha$, the product will not be categorized as failure-prone.

Failure analysis (FA) should be carried out on each of the failure-prone product to identify the root cause of the nonconformities for continuous improvement; this will provide the start of a closed loop FA and corrective action program for all nonconformities found in the test. If no problem is found (NPF) during FA, for products with high processing cost, it is recommended that a re-test be carried out. If the NPF item passes the test, then it could resume to the production and shipped. This would reduce the wastage of scraping a conforming item. From the production point of view, the rate of NPF product should be as low as possible. Figure 7.1 presents a simple decision making procedure for the screening scheme.

7.2.2   The Critical Value, x_α

The critical x_α can be defined as the maximum number of nonconformities allowable during the test. If the number of nonconformities exceeds x_α, it is very likely the fraction of nonconformities of the product is higher than the specifications, i.e., the reliability of the product could not meet the requirements. After deciding the value of k used in the test, the critical value x_α can then be obtained by using the exact probability limits. Let α be the type I error for the screening test,

$$P(X \geq x_\alpha) = \alpha \tag{7.5}$$

Estimate the product parameters (p, ω) from previous data

Determine the testing parameter, k

Calculate x_α base on desired NPF rate

Implement the scheme in production

Re-test — Yes

Is the product tested pass the test? — No — FA — NPF? — No — Further investigation is needed for continuous product improvement
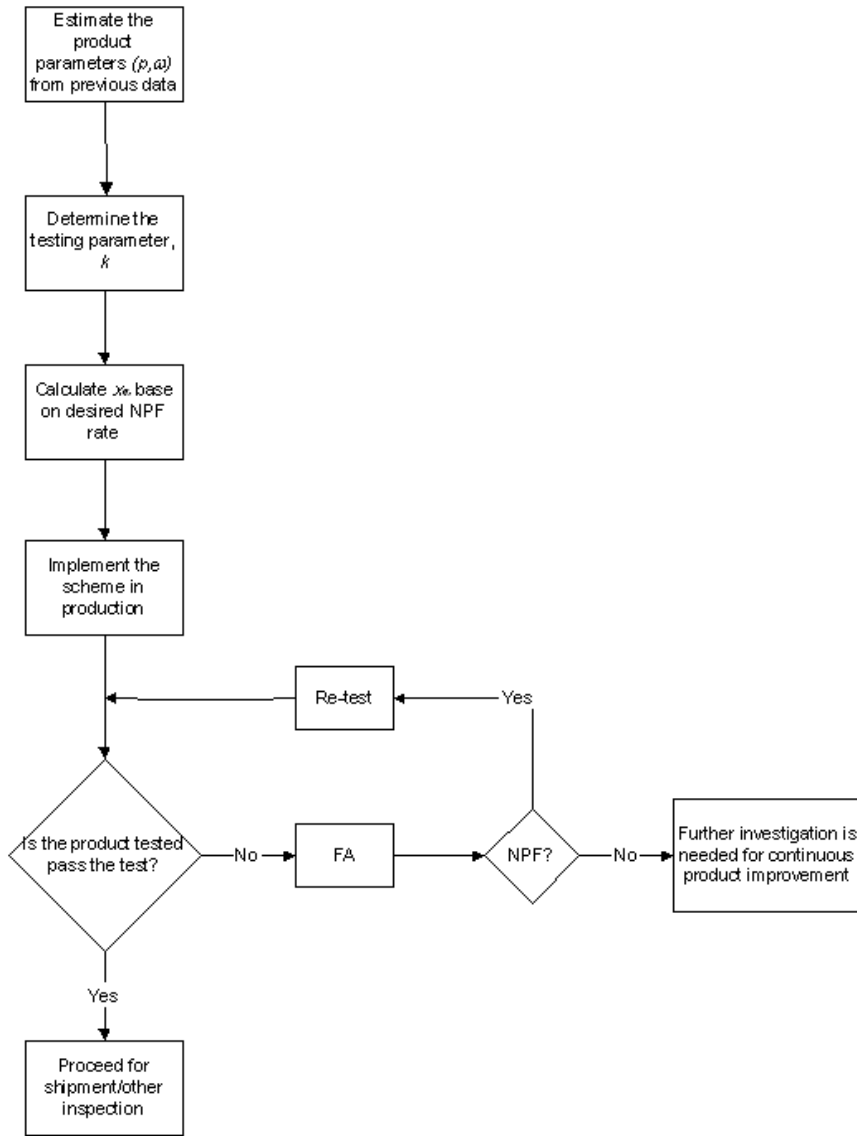
Yes

Proceed for shipment/other inspection

Figure 7.1: The Decision Rules of the Screening Scheme.

the critical value x_α, can thus be obtained by solving the equation as closely as possible

$$
\begin{aligned}
P(X \geq x_\alpha) &= 1 - P(X < x_\alpha) \\
&= 1 - \sum_{x=0}^{x_\alpha - 1} \binom{k}{x} p^x (1-p)^{k-x} \\
&= \alpha
\end{aligned}
\tag{7.6}
$$

The reciprocal of α is the NPF rate, which means that if $\alpha = 0.001$, there will only be one NPF product in 1000 failed products in this screening scheme, on average.

Due to discontinuity in discrete data, for a specific α value the x_α value is the largest integer value so that the exact α value is less than the desired level. Figure 7.2 shows some x_α values with different combinations of p and k with the desired α value closed to 0.001. From the graph, it is clear that the x_α value increases as p increases for the same α and k. Figure 7.3 is the x_α values with different combinations of α and k for $p = 10$ ppm.

As for the case of the HDDs, k is usually in the order of 100 millions (100^6) bits and above; and the fraction of nonconformities, p is in the order of parts-per-million (ppm) or even smaller.

7.2.3 Numerical Example

Here, a numerical example is presented to illustrate the usage of the proposed screening scheme. Consider a screening test of HDD production, using the opportunities of nonconforming $k = 10^9$ and desired α is preferred to be close to 0.005, having the fraction of error bits within each drive is $p = 0.01$ppm. The value of p here is very low because in the case of HDD, which is a highly reliable data storage device, the fraction of error bits found at the end of the production is very low as
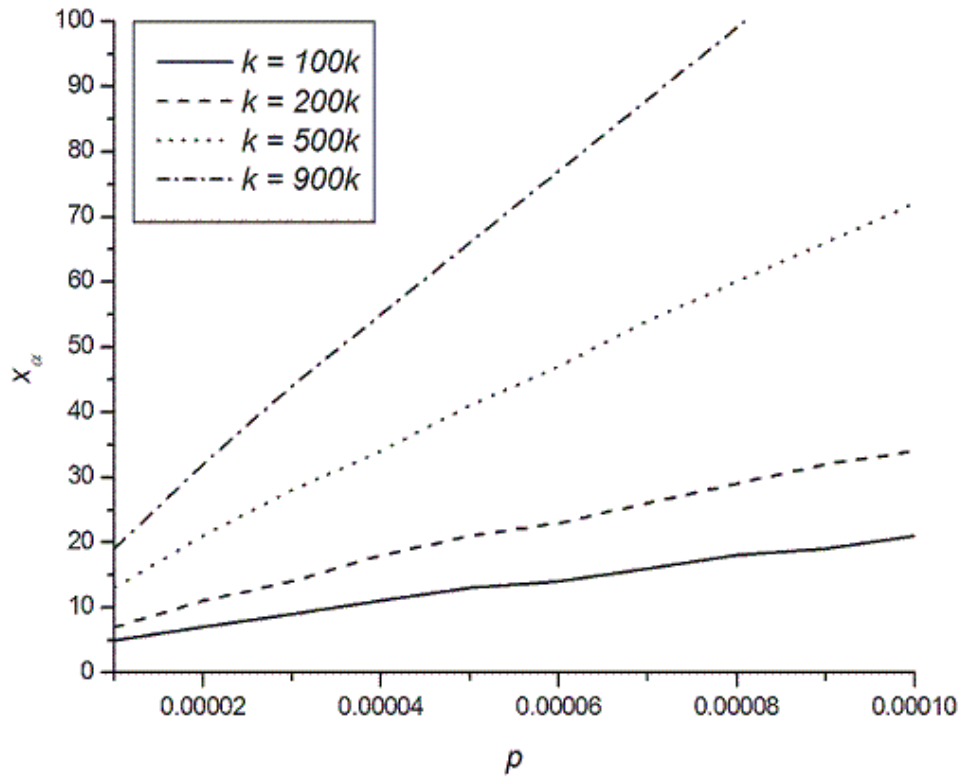
Figure 7.2: x_α values for different combinations of p and k with $\alpha \approx 0.001$.

most of the error ones have already been picked up during the numerous online testings. The suitable critical value x_α is 19, which provides the exact α value of 0.00345, is the closest to the desired α (α for $x = 18$ is 0.00719 whereas for $x = 20$ is 0.00159).

Thus, a product fails the test if the number of nonconformities found in the test is more than 19. The NPF rate for this test is

$$
\begin{aligned}
\text{NPF rate} &= \frac{1}{\alpha} \\
&= \frac{1}{0.00345} \\
&\approx 290,
\end{aligned}
\tag{7.7}
$$

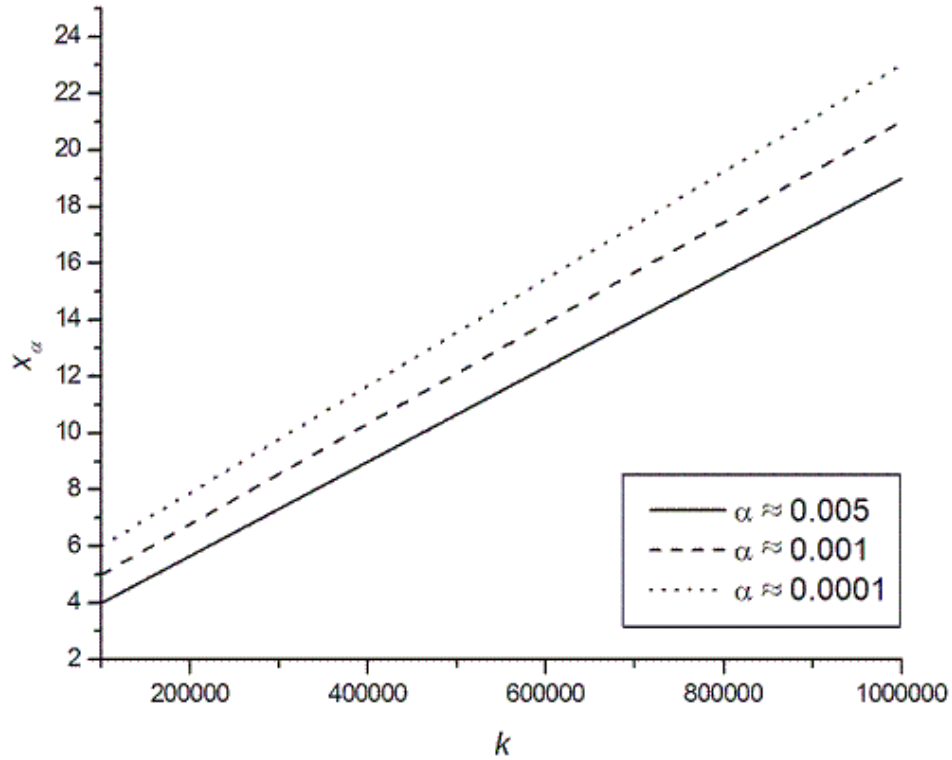which means that the chance of getting a NPF drive is once every 290 fail drives.

131

Figure 7.3: x_α values for different combinations of α and k with $p = 10$ ppm.

Since HDD is usually produced in large volume, α is typically very small.

Table 7.1 shows some of the exact α values for $p = 0.01$ ppm with different values of defect opportunities, k and 3 different desired levels of α. As discussed before, due to the discontinuity behavior of the discrete data, some of the x_α values are the same for different desired α level. Figure 7.4 is the α curves with different values of k with $p = 0.01$ ppm. From the curves, it is clear that the α value decreases as x_α increases for the same values of p and k.

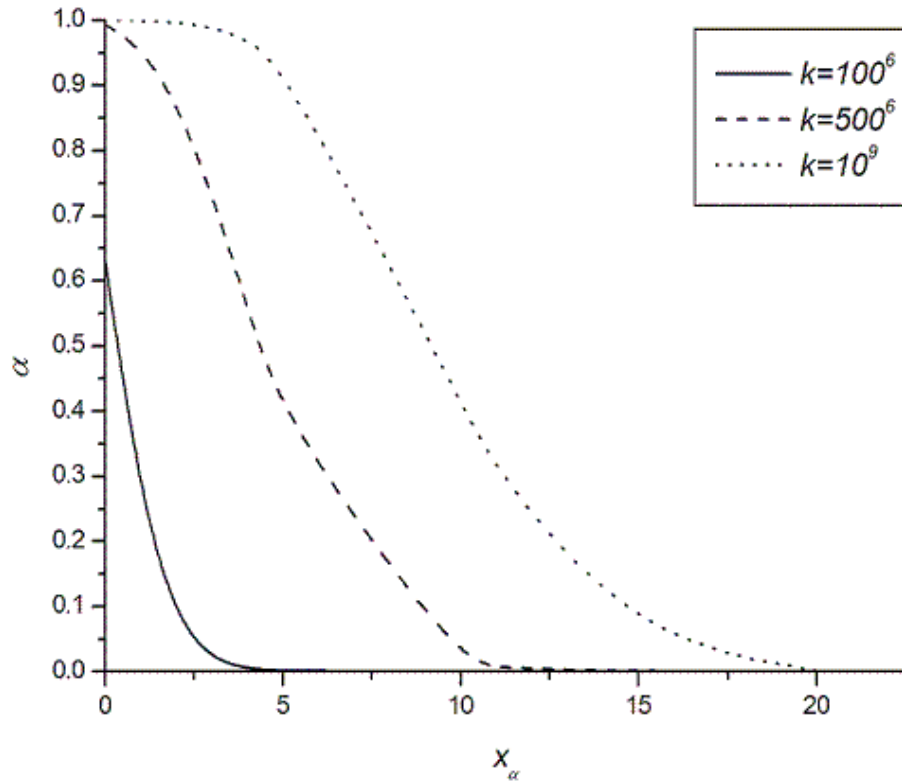The operating characteristic (OC) curve of the test is calculated from Equation

132

Figure 7.4: α values for different values of x_α with $k = 100^6, 500^6$, and 10^9; $p = 0.01$ppm.

Table 7.1: The exact α values for $p = 0.01$ ppm with different combinations of k and desired α.

	desired	$\alpha = 0.001$	desired	$\alpha = 0.005$	desired	$\alpha = 0.01$
k	x_α	exact α	x_α	exact α	x_α	exact α
100000000	5	0.0006	4	0.0037	4	0.0037
200000000	8	0.0002	6	0.0045	6	0.0045
300000000	10	0.0003	8	0.0038	8	0.0038
400000000	11	0.0009	10	0.0028	9	0.0081
500000000	13	0.0007	12	0.0020	11	0.0055
600000000	15	0.0005	13	0.0036	12	0.0088
700000000	16	0.0010	15	0.0024	14	0.0057
800000000	18	0.0007	16	0.0037	15	0.0082
900000000	20	0.0004	18	0.0024	17	0.0053
1000000000	21	0.0007	19	0.0035	18	0.0072

(7.5). The OC curve is plotted in Figure 7.5. From the graph, it is clear that the test can detect the increase in p effectively, i.e., the probability of getting a failure-prone product increased when p increased from the intended value (0.01 ppm).
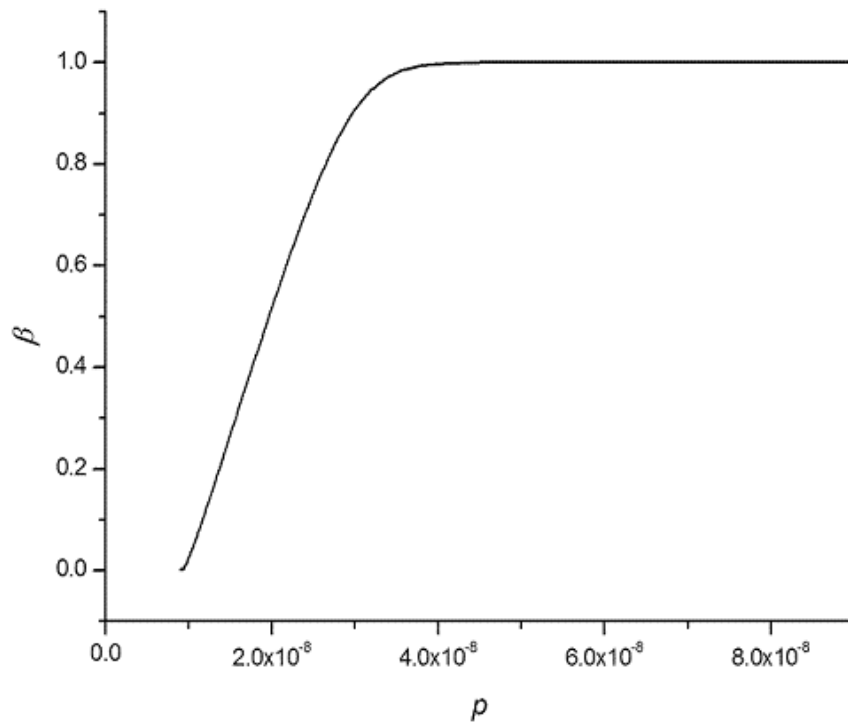

Figure 7.5: The OC curve for the screening test with $p = 0.01$ppm and desired $\alpha = 0.005$.

7.3　Monitoring the Subpopulations

As given in Equation (7.1) from Section 7.1, the production outputs for high performance product consist of two subpopulations. Besides screening the failure-prone ones among the NDF population, the proportion of the two subpopulations, ω is another parameter which would affect the overall product quality. As stated in previous section, by using appropriate rational subgroup size and inspection scheme, the minor population (NDF) can be well-monitored.

From Equation (7.1), the probability of observing a defect-free product is

$$P(X = 0) = \omega + (1 - \omega)(1 - p)^k.$$

Thus, the probability of observing a non defect-free item is given by

$$
\begin{aligned}
P_k &= 1 - P(X = 0) \\
&= 1 - \left(\omega + (1 - \omega)(1 - p)^k \right)
\end{aligned}
\tag{7.8}
$$

Let $\mathbf{N}$ be number of items produced in a production batch. Within the production batch, the probability of observing y number of non defect-free products is given by

$$P(Y = y) = \binom{\mathbf{N}}{P_k} P_k{}^y (1 - P_k)^{\mathbf{N}-y} \tag{7.9}$$

which is the Binomial distribution with parameters $\mathbf{N}$ and P_k.

For high performance product production, the NDF population can be monitored by using a modified Shewhart np-chart using the parameters $\mathbf{N}$ and P_k.

7.4 Conclusion

In this chapter, a modified binomial distribution is used in describing the two subpopulations of the HPmS. The screening scheme introduced here focuses on detecting the failure-prone ones within the minor population of non defect-free (NDF) product. The NDF product with unacceptable failure rate can be detected effectively by implementing the screening scheme in the inspection procedure. Unlike the process monitoring scheme which monitoring the process performance, the proposed screening scheme operates within a system/product, isolating the failure-prone ones from the defect-free subpopulation among the HPmS. A numerical example is given and it shows that the scheme is effective in detecting failure-prone items.

For future research, the frequency of observing a NDF product should be considered in the scheme, as producing too many NDF products will also affect the overall quality level of the product. In addition, planning of the corresponding stress test and the optimality of the decision variables of the screening test (k, and α) can also be investigated.

Chapter 8

Conclusions

Due to the increasing effort of process improvement and rapidly improving technology, more and more industrial processes have been improved to high yield processes, where the process quality level is very high. The fraction of nonconforming items, p for such process is usually on the order of parts-per-million (ppm). On the other hand, the intense global competition and high expectation of consumers have made today's manufacturer inevitable to face strong pressure to design, develop, and manufacture products of high quality and reliability in ever-shorter times while improving productivity at low or minimum cost. The products involved are not only for those mission-critical products, but also for some domestic products. These products have not only highly reliable life expectancy, but also well-maintained, degradation-free performance.

In this dissertation, we explored the area of Statistical Process Control (SPC) techniques for high yield processes, and some topics in high reliability systems. It comprises a thorough study of Cumulative Conformance Count (CCC) chart, guidelines in establishing the CCC chart, a control scheme for high yield correlated

production with sampling inspection, and the studies of high performance systems. The contributions in the high yield process monitoring and high performance systems are summarized in the following sections.

8.1 Contributions In High Yield Process Monitoring

The Cumulative Conformance Count (CCC) chart has been used for monitoring processes with low ppm. However, previous work has yet to address the problems of establishing the chart when the parameter is either given or estimated. In Chapter 3, we examined a sequential sampling scheme for CCC chart that arises naturally in practice and investigate the performance of the chart constructed using an unbiased estimator of the fraction nonconforming, p. In particular, the false alarm rate and its intended target as well as deriving the mean and standard deviation of the run length are examined; and compare the performance with that established under a conventional binomial sampling scheme. A scheme is proposed for constructing the CCC chart in which the estimated p can be updated and the control limits are revised so that not only the in-control average run length (ARL) of the chart is always a constant but it is also the largest which is not the case for conventional CCC chart even when the p is known.

Current work on CCC charts has yet to provide a systematic treatment for establishing the chart particularly when the parameter is estimated. In Chapter 4, results from Chapter 3 and recent studies by Yang *et al.* [115] are extended so that engineers are able to construct the CCC chart under different sampling

and estimation conditions. New insights on the behaviours of CCC chart when the parameter is estimated are given and some procedures for constructing the CCC chart when the process fraction nonconforming is given, when it is estimated sequentially, and when it is estimated with a fixed sample size are presented.

It is shown that the proposed scheme performs well in detecting process changes, even in comparison with the often utopian situation in which the process parameter, p, is given exactly prior to the start of the CCC chart. The proposed steps are implemented using data from a high yield process, which, in some degree, demonstrate the effectiveness of the scheme.

In Chapter 5 (third part of this dissertation), we proposed a chain control scheme, the Cumulative Chain Conforming Sample (CCCS) chart, with adjusted control limits for monitoring high yield high volume production/process under sampling inspection with consideration of correlation within each sample. The performance of the chart in terms of its run length properties is investigated. Numerical results have shown that the performance of the chart is much better than the existing CCC charting scheme under the stated condition.

8.2   Contributions In High Performance Systems

In Chapter 6, the High Performance System (HPmS) is defined and the importance of reliability tests in reliability improvement programs are highlighted. Besides, quality and reliability issues for high performance systems are discussed. This provides insight and promising opportunity for future research on high reliability

systems. As the name implies, the performance level of the system is well maintained, with the significant level of build-in redundancies. The resources provided redundantly in the system are usually the key elements - could be just the component or some sub-assemblies - that would lead to performance deficiency or product failure. System failure occurs only when some or all of the replicates fail. By having highly significant level of redundancies, any element-level-failure occurs within the system would not affect the overall performance. Thus, the performance of the high performance products is expected to be nondegrading, unless the amount of element-level-failure is more than the critical threshold.

Following with the introduction on HPmS, Chapter 7 presents a screening scheme for such systems, with the computer hard disk drive (HDD) as the application example. The scheme introduced focused on detecting the failure-prone ones within the minor population of non defect-free (NDF) product. The NDF product with unacceptable failure rate can be detected effectively by implementing the scheme in the inspection procedure.

Due to the nondegrading performances on the HPmS, the usual reliability assessments could not be applied on such system easily. Thus, further researches in this area are much needed. For example, the frequency of observing a Not Defect-free (NDF) product should be studied and monitored, as producing too many NDF products will affect the overall quality level of the product. In addition, planning of the corresponding reliability (stress) tests and the optimality of the decision variables of the tests on HPmS can also be investigated.

8.3   Future Research Recommendations

The statistical process control for high quality products involves a wide range of research scope. This dissertation covers some important aspects under the umbrella of this topic as summarized above. However, there are some other areas where future research should be carried out.

Chapters 3 and 4 of this dissertation focused merely on the CCC chart, due to time and cost constraints, the in-depth analysis on the extension of the CCC model has not been done. Similar extentions can be done on the CCC-r chart presented by Xie *et. al.* [107], considering the case when p is estimated.

Chapter 5 deals with the high yield process monitoring with sampling inspection, considering the intra-sample correlation. However, it is assumed that the process parameters are known, the future research could focus on the effects of estimated parameters used in the proposed scheme. In addition, some enhancements could be developed to improve the sensitivity of the proposed scheme.

The final part of the thesis is an introductory study of the HPmS. Detailed analysis is needed to strengthen concept of HPmS. As discussed in Chapter 6 (particularly Section 6.3), further investigations on quality and reliability issues of HPmS are much needed.

Bibliography

[1] Bischak, D. P. and Silver, E. A. (2001) 'Estimating the Rate at Which a Process Goes Out of Control in a Statistical Process Control Context,' *International Journal of Production Research*, **39**, 2957-2971.

[2] Blischke, W. R. and Murthy, D. N. P. (2000) *Reliability: Modeling, Prediction, and Optimization* Wiley, New York.

[3] Bourke, P. D. (1991) 'Detecting a Shift in Fraction Non-conforming Using Run-length Control Charts with 100% Inspection,' *Journal of Quality Technology*, **23**, 225-238.

[4] Box, G. and Ramírez, J. (1992) 'Cumulative Score Chart,' *Quallity and Reliability Engineering International*, **8**, 17-27.

[5] Braun, W. J. (1999) 'Run Length Distributions for Estimated Attributes Charts,' *Metrika*, **50**, 121-129.

[6] Calvin, T. W. (1983) 'Quality Control Techniques for "Zero Defects",' *IEEE Transactions on Components, Hybrids, and Manufacturing Technology*, **CHMT-6**, 323-328.

[7] Carlyle, W. M., Montgomery, D. C. and Runger, G. C. (2000) 'Optimization Problems and Methods in Quality Control and Improvement,' *Journal of Quality Technology*, **32**, 1-31.

[8] Chakraborti, S. (2000) 'Run Length, ARL and False Alarm Rate of Shewhart $\bar{X}$ Chart: Exact Derivations by Conditioning,' *Communications In Statistics: Simulation and Computation*, **29**, 61-81.

[9] Champ, C. W. and Jones, L. A. (2004) 'Designing Phase I $\bar{X}$ Charts with Small Sample Sizes,' *Quality and Reliability Engineering International*, **20**, 497-510.

[10] Champ, C. W. and Woodall, W. H. (1987) 'Exact Results for Shewhart Control Charts with Supplementary Run Rules,' *Technometrics*, **29**, 393-399.

[11] Chan, L. Y., Lin, Dennis K. J., Xie, M. and Goh, T. N. (2002) 'Cumulative Probability Control Charts for Geometric and Exponential Process Characteristics,' *International Journal of Production Research*, **40**, 133-150.

[12] Chan, L. Y., Xie, M. and Goh, T. N. (2000) 'Cumulative Quantity Control Charts for Monitoring Production Processes,' *International Journal of Production Research*, **38**, 397-408.

[13] Chang, T.C. and Gan, F.F. (1999) 'Charting Techniques for Monitoring a Random Shock Process,' *Quality and Reliability Engineering International*, **15**, 295-301.

[14] Chang, T.C. and Gan, F.F. (2001) 'Cumulative Sum Charts for High Yield Processes,' *Statistica Sinica*, **11**, 791-805.

[15] Chen, G. (1997) 'The Mean and Standard Deviation of the Run Length Distribution of $\bar{X}$ Charts When Control Limits are Estimated,' *Statistica Sinica*, **7**, 789-798.

[16] Chen, G. (1998) 'The Run Length Distributions of the R, s and s^2 Control Charts When σ is Estimated,' *The Canadian Journal of Statistics*, **26**, 311-322.

[17] Cheong, W. T., and Tang, L. C. (2003) 'Screening Scheme for High Performance Products' *Proceedings of Ninth ISSAT International Conference on Reliability and Quality in Design*, 65-69.

[18] Chou, Y., Polansky, A. M. and Mason, R. L. (1998) 'Transforming Non-normal Data to Normality in Statistical Process Control,' *Journal of Quality Technology*, **30**, 133-141.

[19] Del Castillo, E. (1996) 'Evaluation of Run Length Distribution for $\bar{X}$ Charts with Unknown Variance,' *Journal of Quality Technology*, **28**, 116-122.

[20] Del Castillo, E. (1996) 'Run Length Distributions and Economic Design of $\bar{X}$ Charts with Unknown Process Variance,' *Metrika*, **43**, 189-201.

[21] Deming, W. E. (1986), *Out of the Crisis*, Cambridge, MA: Center for Advanced Engineering Studies.

[22] Dodge, H. F. (1955) 'Chain Sampling Inspection Plan,' *Industrial Quality Control*, **11**, 10-13.

[23] Elsayed, E.A. (1996) *Reliability Engineering*, Addison Wesley Longman, Massachusetts.

[24] Ghosh, B. K., Reynolds, M. R. and Hui, Y. V. (1981) 'Shewhart $\bar{X}$-charts with Estimated Process Variance,' *Communications In Statistics: Theory and Methods*, **18**, 1797-1822.

[25] Girshick, M. A., Mosteller, F. and Savage, L. J. (1946) 'Unbiased Estimates for Certain Binomial Sampling Problems with Applications,' *The Annals of Mathematical Statistics*, **17**, 13-23.

[26] Glushkovsky, E. A. (1994) ' "On-line" G-control Chart for Attribute Data,' *Quality and Reliability Engineering International*, **10**, 217-227.

[27] Goh, T. N. (1987) 'A Charting Technique for Control of Low-Defective Production,' *International Journal of Quality and Reliability Management*, **4**, 53-62.

[28] Goh, T. N. (1987) 'A Control Chart for Very High Yield Processes,' *Quality Assurance*, **13**, 18-22.

[29] Goh, T. N. and Xie, M. (2003) 'Statistical Control of a Six Sigma Process,' *Quality Engineering* **15**, 587-592.

[30] Gollwitzer, S. and Rackwitz, R. (1990) 'On the Reliability of Daniels Systems,' *structural Safety*, **7**, 229-243.

[31] Grigoriu, M. (1989) 'Reliability of Daniels Systems Subject to Gaussian Load Processes,' *Structural Safety*, **6**, 303-309.

[32] Grigoriu, M. (1989) 'Reliability of Daniels Systems Subject to Quasistatic and Dynamic Nonstationary Gaussian Load Processes,' *Probabilistic Engineering Mechanics*, **4**, 128-134.

[33] Grigoriu, M. (1990) 'Applications of Diffusion Models to Reliability Analysis of Daniel Systems,' *Structural Safety*, **7**, 219-228.

[34] Grigoriu, M. (1990) 'Reliability Analysis of Dynamic Daniels Systems with Local Load-sharing Rule,' *Journal of Engineering Mechanics*, **116**, 2625-2642.

[35] Grigoriu, M. (1990) 'Reliability of Degrading Dynamic Systems,' *Structural Safety*, **8**, 345-351.

[36] Hahn, G. J. (1982) 'Statistical Assessment of a Process Change,' *Journal of Quality Technology*, **14**, 1-9.

[37] Haldane, J. B. S. (1945) 'A Labour-saving Method of Sampling,' *Nature*, **155**, No.3924.

[38] Hawkins, D. M. (1987) 'Self-starting Cusum Charts for Location and Scale,' *The Statistician*, **36**, 299-315.

[39] Hawkins, D. M. (1992) 'A Fast Accurate Approximation for Average Run Lengths of CUSUM Control Charts,' *Journal of Quality Technology*, **24**, 37-43.

[40] Hawkins, D. M. (1993) 'Cumulative Sum Control Charting: An Underutilized SPC Tool,' *Quality Engineering*, **5**, 463-477.

[41] Hawkins, D. M. and Olwell, D. H. (1998) *Cumulative Sum Charts and Charting for Quality Improvement*, Springer-Verlag, New York.

[42] Huang, CT., Wu, CF., Li, JF. and Wu, CW. (2003) 'Built-in Redundancy Analysis for Memory Yield Improvement,' *IEEE Transactions on Reliability*, **52**, 386-399.

[43] Hughes, G. F., Murray, J. F., Kreutz-Delgado, K., and Elkan, C. (2002) 'Improved Disk-drive Failure Warnings,' *IEEE Transactions on Reliability*, **5**, 350-357.

[44] Johnson, N. L., Kotz, S., and Kemp, A. W. (1992) *Univariate Discrete Distributions*, 2nd Edition, Wiley, New York.

[45] Jones, L. A., Champ, C. W. and Rigdon, S. E. (2001) 'The Performance of Exponentially Weighted Moving Average Charts with Estimated Parameters,' *Technometrics*, **43**, 156-167.

[46] Kaminsky, F. C., Benneyan, J. C., Davis, R. D., and Burke, R. J. (1992) 'Statistical Control Charts Based on a Geometric Distribution,' *Journal of Quality Technology*, **24**, 63-69.

[47] Kittlitz, R. G. Jr. (1999) 'Transforming the Exponential for SPC Applications,' *Journal of Quality Technology*, **31**, 301-308.

[48] Koren, I. and Koren, Z. (1989) 'On Gracefully Degrading Multiprocessors with Multistage Interconnection Networks,' *IEEE Transactions on Reliability*, **38**, 82-89.

[49] Kuralmani, V., Xie, M. and Goh, T. N. (2002) 'A Conditional Decision Procedure for High Yield Processes,' *IIE Transactions*, **34**, 1021-1030.

[50] Lai, C. D., Govindaraju, K. and Xie, M. (1998) 'Effects of Correlation on Fraction Non-conforming Statistical Process Control Procedures,' *Journal of Applied Statistics*, **25**, 535-543.

[51] Lai, C. D., Xie, M. and Govindaraju, K. (2000) 'Study of a Markov Model for a High-quality Dependent Pocess,' *Journal of Applied Statistics*, **27**, 461-473.

[52] Leemis, L. M. and Beneke, M. (1990) 'Burn-in Models and Methods: A Review,' *IIE Transactions*, **22**, 172-180.

[53] Lucas, J. M. and Crosier, R. B. (1982) 'Fast Initial Response for CUSUM Quality-control Schemes: Give Your CUSUM a Head Start,' *Technometrics*, **24**, 199-205.

[54] Lucas, J. M. (1989) 'Control Scheme for Low Count Levels,' *Journal of Quality Technology*, **21**, 199-201.

[55] Madsen, R. W. (1993) 'Generalized Binomial Distribution,' *Communications In Statistics: Theory And Methods*, **22**, 3065-3086.

[56] McCool, J. I., and Joyner-Motley, T (1998) 'Control Charts Applicable When the Fraction Nonconforming is Small,' *Journal of Quality Technology*, **30**, 240-247.

[57] Meyer, J. P. (1980) 'On Evaluation the Performability of Degradable Computing Systems,' *IEEE Transactions on Computers*, **29**, 720-731.

[58] Meeker, W. Q., Escobar, L. A., and Lu, J. C. (1998) 'Accelerated Degradation Test: Modeling and Analysis,' *Technometrics*, **40**: 89-99.

[59] Meeker, W. Q., and Hamada, M. (1995) 'Statistical Tools for the Rapid Development & Evaluation of High-Reliability Products,' *IEEE Transactions on Reliability*, **44**: 187-198.

[60] Mohamed, A., Leemis, L. M. and Ravindran, A. (1992) 'Optimization Techniques for System Reliability: A Review,' *Reliability Engineering and System Safety*, **35**, 137-146.

[61] Montgomery, D. C (1996) *Introduction to Statistical Quality Control*, 3rd Edition, New York : Wiley.

[62] Naijar, W. A. and Gaudiot, J. (1991) 'Scalability Analysis in Gracefully-degradable Large Systems,' *IEEE Transactions on Reliability*, **40**, 189-197.

[63] Nelson, L. S. (1994) 'A Control Chart for Parts-Per-Million Nonconforming Items,' *Journal of Quality Technology*, **26**, 239-240.

[64] Nelson, L. S. (1999) 'Notes on the Shewhart Control Chart,' *Journal of Quality Technology*, **31**, 124-126.

[65] Nelson, W. (1990) *Accelerated Testing: Statistical Models, Test Plans, and Data Analyses*, Wiley, New York.

[66] O'Connor, P. (2003) 'Testing for Reliability,' *Quality and Reliability Engineering International*, **19**, 73-84.

[67] Ohta, H., Kusukawa, E., and Rahim, A. (2001) 'A CCC-r Chart for High Yield Processes,' *Quality and Reliability Engineering International*, **17**, 439-446.

[68] Phoenix, S. L. (1978) 'Stochastic Strength and Fatigue of Fiber Bundles,' *International Journal of Fracture*, **14**, 327-344.

[69] Phoenix, S. L. (1978) 'The Asymptotic Time to Failure of a Mechanical System of Parallel Members,' *Journal of Applied Mathematics*, **34**, 227-246.

[70] Phoenix, S. L. (1979) 'The Asymptotic Distribution for the Time to Failure of a Fiber Bundle,' *Advances in Applied Probability*, **11**, 153-187.

[71] Quesenberry, C. P. (1993) 'The Effect of Sample Size on Estimated Limits for $\bar{X}$ and X Control Charts,' *Journal of Quality Technology*, **25**, 237-247.

[72] Quesenberry, C. P. (1995) 'Geometric Q Charts for High Quality Processes,' *Journal of Quality Technology* **27**, 304-315.

[73] Raju, C. (1990) 'Designing Chain Sampling Plans (ChSP-1) with Fixed Sample Size,' *The International Journal of Quality and Reliability Management*, **7**, 59-64.

[74] Reibman, A. L. (1990) 'Modeling the Effect of Reliability on Performance,' *IEEE Transactions on Reliability*, **39**, 314-320.

[75] Roes, K. C. B., Does, R. J. M. M. and Jonkers, B. S. (1999) 'Effective Application of Q(R) Charts in Low-volume Manufacturing,' *Quality and Reliebility Engineering International*, **15**, 175-190.

[76] Schilling, E. G. (1982) *Acceptance Sampling in Quality Control*, New York : M. Dekker.

[77] Sentler, L. (1997) 'Reliability of High Performance Fibre Composites,' *Reliability Engineering and System Safety*, **56**, 249-256.

[78] Shankar, G., Mohapatra, B. N. and Joseph, S. (1991) 'Chain Sampling Plan for Three Attribute Classes,' *The International Journal Of Quality and Reliability Management*, **8**, 46-58.

[79] Shewhart, W. A. (1931), *Economic Control of Quality of Manufactured Product*, New York : D. Van Nostrand.

[80] Singh, A. D. and Murugesan, S. (1990) 'Fault-tolerant Systems,' *Computer*, **23**, 15-17.

[81] Smith, R. M., Trivedi, K. S. and Ramesh, A. V. (1988) 'Perfomability Analysis: Measures, an Algorithm, and a Case Study,' *IEEE Transactions on Computers*, **37**, 406-417.

[82] Sun, J. and Zhang, G. X. (2000) 'Control Charts Based on the Number of Consecutive Conforming Items Between Two Successive Nonconforming Items for the Near Zero-nonconformity Processes,' *Total Quality Management*, **11**, 235-250.

[83] Tagaras, G. (1998) 'A Survey of Recent Developments in the Design of Adaptive Control Charts,' *Journal of Quality Technology*, **30**, 212-231.

[84] Tang, L. C. and Cheong, W. T. (2004) 'CCC Chart with Sequentially Estimated Parameter,' *IIE Transactions*, **36**, 841-853.

[85] Tang, L. C. and Cheong, W. T. (2005) 'On Establishing CCC Charts,' *International Journal of Performability Engineering*, **1**.

[86] Tang, L. C. and Cheong, W. T. (to appear) 'A Control Scheme for High Yield Correlated Production under Group Inspection,' *Journal of Quality Technology*.

[87] Tang, K, and Tang, J. (1994) 'Design of Screening Procedures: A Review,' *Journal of Quality Technology*, **26**: 209-226.

[88] Taylor, H. M. (1979) 'The Time to Failure of Fiber Bundles Subjected to Random Loads,' *Advances in Applied Reliability*, **11**, 527-541.

[89] Thomas, D. W. *et al.* (1958) *Statistical Quality Control Handbook*, 2nd Edition, Western Electric Co.

[90] Thomas, P. R. (2000) *Statistical Methods for Quality Improvement*, 2nd Edition, New York : Wiley.

[91] Thorsen, N. (1998) *Fiber Optics and the Telecommunications Explosion*, Prentice Hall PTR, Upper Saddle River, NJ.

[92] Tobias, P. A. and Trindade, D. C. (1995) *Applied Reliability*, 2nd Edition, Van Nostrand Reinhold, New York.

[93] Tseng, S., Tang, J. and Ku, I. (2002) 'Determination of Burn-in Parameters and Residual Life for Highly Reliable Products,' *Naval Research Logistics*, **50**, 1-14.

[94] Vardeman, S. and Ray, D. (1985) 'Average Run Lengths for CUSUM Schemes When Observations are Exponentially Distributed,' *Technometrics*, **27**, 145-150.

[95] Vaughan, T. S. (1994) 'An Alternative Framework for Short-run SPC,' *Production and Inventory Management Journal*, **35**, 48-52.

[96] Wheeler, D. J. (1995) *Advanced topics in statistical process control : the power of Shewhart's charts*, SPC Press, Inc., Tennessee.

[97] Whitmore, G. A. and Schenkelberg, F. (1997) 'Modeling Accelerated Degradation Data Using Wiener Diffusion with a Time Scale Transformation,' *Lifetime Data Analysis*, **3**, 27-45.

[98] Woodall, W. H. (1997) 'Control Charts Based on Attribute Data: Bibliography and Review,' *Journal of Quality Technology*, **29**, 172-183.

[99] Woodall, W. H. and Adams, B. M. (1993) 'The Statistical Design of CUSUM Charts,' *Quality Engineering*, **5**, 559-570.

[100] Woodall, W. H. and Montgomery, D. C. (1999) 'Research Issues and Ideas in Statistical Process Control,' *Journal of Quality Technology*, **31**, 376-386.

[101] Wu, Z., Yeo, S. H. and Fan, H. (2000) 'A Comparative Study of the CRL-type Control Charts,' *Quality and Reliability Engineering International*, **16**, 269-279.

[102] Wu, Z., Zhang, X. and Yeo, S. H. (2001) 'Design of the Sum-of-conforming-run-length Control Charts,' *European Journal of Operational Research*, **132**, 187-196.

[103] Xie, M. and Goh, T. N. (1992) 'Some Procedures for Decision Making in Controlling High Yield Processes,' *Quality and Reliability Engineering International*, **8**, 355-360.

[104] Xie, M. and Goh, T. N. (1997) 'The Use of Probability Limits for Processes Control Based on Geometric Distribution,' *International Journal of Quality and Reliability Management*, **14**, 64-73.

[105] Xie, M., Goh, T. N. and Kuralmani, V. (2000) 'On Optimal Setting of Control Limits for Geometric Chart,' *International Journal of Reliability, Quality and Safety Engineering*, **7**, 17-25.

[106] Xie, M., Goh, T. N. and Kuralmani, V. (2002) *Statistical Models and Control Charts for High-Quality Processes*, Boston: Kluwer Academic Publishers.

[107] Xie, M., Goh, T. N. and Lu, X. S. (1998) 'Computer-aided Statistical Monitoring of Automated Manufacturing Processes,' *Computers and Industrial Engineering*, **35**, 189-192.

[108] Xie, M., Goh, T. N. and Lu, X. S. (1998) 'A Comparative Study of CCC and CUSUM Charts,' *Quality and Reliability Engineering International*, **14**, 339-345.

[109] Xie, M., Goh, T.N., and Ranjan, P. (2002) 'Some Effective Control Chart Procedures for Reliability Monitoring,' *Reliability Engineering and System Safety*, **77**: 143-150.

[110] Xie, M., Goh, T. N. and Tang, X. Y. (2000) 'Data Transformation for Geometrically Distributed Quality Characteristics,' *Quality and Reliability Engineering International*, **16**, 9-15.

[111] Xie, M., Goh, T. N. and Xie, W. (1997) 'A Study of Economy Design of Control Charts for Cumulative Count of Conforming Items,' *Communications in Statistics - Simulation and Computation*, **26**, 1009-1027.

[112] Xie, M., Lu, X. Y., Goh, T. N. and Chan, L. Y. (1999) 'A Quality Monitoring and Decision-making Scheme for Automated Production Processes,' *International Journal of Quality and Reliability Management*, **16**, 148-157.

[113] Xie, M., Tang, X. Y. and Goh, T. N. (2001) 'On Economic Design of Cumulative Count of Conforming Chart,' *International Journal Of Production Economics*, **72** 89-97.

[114] Xie, W., Xie, M. and Goh, T. N. (1995) 'A Shewhart-like Charting Technique for High Yield Processes,' *Quality and Reliability Engineering International*, **11**, 189-196.

[115] Yang, Z., Xie, M., Kuralmani, V. and Tsui, K. L. (2002) 'On the Performance of Geometric Charts with Estimated Control Limits,' *Journal of Quality Technology*, **34**, 448-458.

[116] Yourstone, S. A. and Zimmer, W. J. (1992) 'Non-normality and the Design of Control Charts for Averages,' *Decision Sciences*, **23**, 1099-1113.

[117] Yu, H. F., and Tseng, S. T. (1999) 'Designing a Degradation Experiment,' *Naval Research Logistics*, **46**, 689-706.

[118] Yu, H. F. and Tseng, S. T. (2002) 'Designing A Screening Experiment For Highly Reliable Products,' *Naval Research Logistics*, **49**, 514-526.

[119] Zhang, L., Govindaraju, K., Bebbington, M. and Lai, C. D. (2004) 'On the Statistical Design of geometric Control Charts,' *Quality Technology and Quantitative Management*, **1**, 233-243.

[120] Zhao, W. and Elsayed, E. A. (2004) 'An Accelerated Life Testing Model Involving Performance Degradation,' *Proceedings of Annual Reliability and Maintainability Symposium*, 324-329.

Appendix A

Order Statistics Analysis

Here, the first order statistics of the cumulative conformance count within a sample is investigated. Consider a sample of size n of which r nonconforming items are detected, thus, there would be r sequence of CCCs within that sample. Let $Y_{i:r}$ be the i-th occurrence of the r nonconforming items, i.e. $Y_{1:r}$ is the first occurrence, $Y_{2:r}$ is the second, and so on. Assuming constant rate of occurrence (constant p within each sample), $Y_{1:r}, \ldots, Y_{r:r}$ are the order statistics from discrete uniform distribution $(1, n)$ with the CDF given as $F(y) = \dfrac{y}{n}$. Figure A.1 is the graphical representation of this order statistics.

The pmf of the i-th order statistic $Y_{i:r}$ can be obtained by direct reasoning: for $Y_{i:r}$ to equal y, preceeding $i - 1$ values of $Y_{j:r}, j \leq i - 1$ should be less than y, $r - i$ succeeding $Y_{j:r}; j \geq i + 1, \ldots, r$ should be greater than y. This probability is given by

$$\left(\frac{y}{n}\right)^{i-1}\left(1 - \frac{y}{n}\right)^{r-i}\frac{y}{n}$$

Whereas, as there are

$$\binom{r}{i-1, r-i, 1} = \frac{n!}{(r-i)!(i-1)!}$$

different partitions of the r random variables $Y_{i:r}; i = 1 \ldots, r$ into the three groups.

The conditional pmf of $Y_{i:r}$ given r nonconforming items, is given by

$$F_{Y_{i:r}}(y|r) = \frac{n!}{(r-i)!(i-1)!}\left(\frac{y}{n}\right)^{i-1}\left(1-\frac{y}{n}\right)^{r-i}\frac{y}{n} \tag{A.1}$$

In general, the CDF of $Y_{i:r}$ can be obtained by realizing that

$$F_{i:r}(y|r) = P(Y_{i:r} \leq y|r)$$

$$= P\left(\text{at least } i \text{ of } Y_1, Y_2, \ldots, Y_r \text{ are at most } y | \text{there are } r \text{ } Ys\right)$$

$$= \sum_{k=i}^{r} P\left(\text{exactly } k \text{ of } Y_1, Y_2, \ldots, Y_r \text{ are at most } y | \text{there are } r \text{ } Ys\right) \tag{A.2}$$

$$= \sum_{k=i}^{r}\binom{r}{k}\left(\frac{y}{n}\right)^{k}\left(1-\frac{y}{n}\right)^{r-k}.$$

Note that $Y_{i:r}$ will be less than or equals to y if and only if at least i of the r random
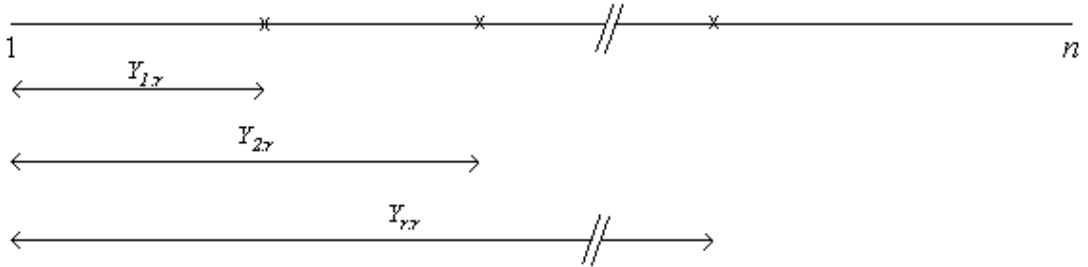
variables are less than or equals to y.

Figure A.1: Graphical Representation of the Order statistics

Thus, the probability for the first occurrence of the nonconforming item from

the r nonconforming items found in a sample of size n, $Y_{1:r} < l$ is given by

$$P(Y_{1:r} < l|r) = \sum_{k=1}^{r}\binom{r}{k}\left(\frac{l-1}{n}\right)^{k}\left(\frac{n-l-1}{n}\right)^{r-k} \tag{A.3}$$

For high yield process with sample inspection, when there are $r(\geq 2)$ noncon-

forming items found within a sample of size n, we have to consider the joint pmf

of $Y_{i:r}$ and $Y_{j:r}$. The joint pmf of $Y_{i:r}$ and $Y_{j:r}$ for $i < j$ is given by

$$
\begin{aligned}
F_{Y_{i:r},Y_{j:r}}(y_i, y_j|r) &= P\big(Y_{i:r} = y_i, Y_{j:r} = y_j|r\big) \\
&= \frac{r!}{(i-1)!(j-i-1)!(r-j)!} \times \left(\frac{y_i}{n}\right)^{i-1} \times \left(\frac{y_j}{n} - \frac{y_i}{n}\right)^{j-i-1} \\
&\quad \times \left(1 - \frac{y_j}{n}\right)^{r-j} \left(\frac{1}{n}\right)^2
\end{aligned}
$$

(A.4)

For $j = i + 1$, the above equation become

$$
F_{Y_{i:r},Y_{i+1:r}}(y_i, y_{i+1}|r) = \frac{r!}{(i-1)!(r-i-1)!} \times \left(\frac{y_i}{n}\right)^{i-1} \times \left(1 - \frac{y_{i+1}}{n}\right)^{r-i-1} \left(\frac{1}{n}\right)^2 \quad \text{(A.5)}
$$

Let $W_i = Y_{i+1:r} - Y_{i:r}$, where $W_0 = Y_{1:r}$, we can write

$$
P(W_{i:r} = w) = \sum_{y \in S} P(Y_{i:r} = y, Y_{i+1:r} = y + w) \tag{A.6}
$$

As the distribution of Y_i is discrete uniform ranging from $S\{1, n\}$, for r noncon-

forming items detected, the maximum of the least consecutive conforming items

would be $\dfrac{n}{r+1}$. Thus, y from the above equation would be ranging from 1 to $\dfrac{n}{r+1}$

and the above probability can thus be written as

$$
\begin{aligned}
P(W_{i:r} = w|r) &= \sum_{y=1}^{n/(r+1)} P(Y_{i:r} = y, Y_{i+1:r} = y + w) \\
&= \sum_{y=1}^{n/(r+1)} \sum_{i=1}^{r-1} \frac{r!}{(i-1)!(r-i-1)!} \left(\frac{y}{n}\right)^{i-1} \left(\frac{n-y-w}{n}\right)^{r-i-1} \left(\frac{1}{n}\right)^2
\end{aligned}
$$

(A.7)

The probability of the first order statistics given r nonconforming items $(Y_{1:r})$

within the first sample of size n is less than the LCL of the chart can be obtained

based on Equation (A.3) as

$$P(Y_{1:r} < LCL|r) = \sum_{k=1}^{r} \binom{r}{k} \left(\frac{LCL-1}{n}\right)^k \left(\frac{n-LCL-1}{n}\right)^{r-k} \tag{A.8}$$

For the rest of the orders statistics for $Y_{i:r}$, the probability that the CCC is smaller than the LCL of the conventional CCC chart given r nonconforming items is given by

$$P(W_{i:r} < LCL|r) = \sum_{l=1}^{LCL-1} \sum_{y=1}^{n/(r+1)} \sum_{i=1}^{r-1} \frac{r!}{(i-1)!(r-i-1)!} \left(\frac{y}{n}\right)^{i-1} \left(\frac{n-y-w}{n}\right)^{r-i-1} \left(\frac{1}{n}\right)^2$$

$$\text{for } i = 2, \ldots, r; \ \ 1 < r \le n \tag{A.9}$$

Thus, the probability for any CCC within the first sample to be smaller than LCL of the CCC chart can be obtained from the above derivations and be written as

$$P(W_{i:r} < LCL)$$

$$= \sum_{r \in n} \sum_{i=1}^{r} P(W_{i:r} < LCL)$$

$$= \sum_{r \in n} \left(\begin{array}{c} \sum_{k=1}^{r} \binom{r}{k} \left(\frac{LCL-1}{n}\right)^k \left(\frac{n-LCL-1}{n}\right)^{r-k} \\ + \sum_{l=1}^{LCL-1} \sum_{y=1}^{n/(r+1)} \sum_{i=2}^{r-1} \frac{r!}{(i-1)!(r-i-1)!} \left(\frac{y}{n}\right)^{i-1} \left(\frac{n-y-l}{n}\right)^{r-i-1} \left(\frac{1}{n}\right)^2 \end{array} \right)$$

$$\times \binom{n}{r} p^r (1-p)^{n-r}. \tag{A.10}$$

To simplify the computation, the number of nonconforming items, r is truncated up to the number such that the probability of observing more than r_u items is

smaller than 10^{-6}.

$$P(d > r) = 1 - P(d \le r_u)$$
$$= 1 - \binom{n}{r_u} p^{r_u} (1-p)^{n-r_u} \quad < 0.000001 \tag{A.11}$$

Table A.1 gives the probabilities for any group of consecutive conformance items (CCI) within the first sample of inspection to be smaller than LCL of the conventional CCC chart with $\alpha/2 = 0.00135$, which obtained from Equation (A.10), for different in-control ppm with sample sizes, n ranging from 100 to 20000. The last row in the table shows the false alarm probabilities for the conventional CCC charts. From the table, it is clear that as sample size increases, the probability deviates from the conventional CCC chart false alarm probability. The inconsistency of the probability become more obvious as p increases from 50 ppm to 500 ppm.

Table A.1: The probabilities for any group of CCI within the first sample of inspection is smaller than LCL of the CCC chart with $\alpha/2 = 0.00135$ for different in-control ppm with sample sizes, n ranging from 100 to 20000

n	ppm= 50	100	200	300	400	500
100	0.001399	0.001399	0.001398	0.001498	0.001598	0.001497
500	0.001399	0.001399	0.001399	0.001499	0.001599	0.001500
1000	0.001399	0.001399	0.001400	0.001502	0.001604	0.001507
5000	0.001401	0.001408	0.001428	0.001558	0.001694	0.001618
10000	0.001408	0.001429	0.001483	0.001647	0.001811	0.001740
20000	0.001429	0.001483	0.001585	0.001775	0.001949	0.001863
	0.001399	**0.001399**	**0.001399**	**0.001499**	**0.001599**	**0.001499**

Hence, if the high yield process is inspected based on samples, a control scheme different from the CCC chart is needed in order to monitor the process effectively. In addition, as mentioned before, when the inspection is carried out in samples, CCC chart could not be implemented at all in monitoring the process. This is due to the observation of the inspection is the number of nonconforming detected,

instead of the exact ordering for every items, which is needed in implementing conventional CCC chart.